

AUS Repository

Lateral Confinement of RC Columns by Internal Structural Steel Strip Bands

Item Type	Thesis
Authors	Towaiq, Ahmad
Download date	2026-03-07 05:55:49
Link to Item	http://hdl.handle.net/11073/8768

LATERAL CONFINEMENT OF RC COLUMNS BY INTERNAL STRUCTURAL
STEEL STRIP BANDS

by

Ahmad Towaiq

A Thesis Presented to the Faculty of the
American University of Sharjah
College of Engineering
in Partial Fulfillment
of the Requirements
for the Degree of

Master of Science in
Civil Engineering

Sharjah, United Arab Emirates

December 2016

© 2016 Ahmad Towaiq. All rights reserved.

Approval Signatures

We, the undersigned, approve the Master's Thesis of Ahmad Towaiq.

Thesis Title: Lateral Confinement of RC Columns by Internal Structural Steel Strip Bands.

Signature

Date of Signature
(dd/mm/yyyy)

Dr. Sami Tabsh
Professor, Department of Civil Engineering
Thesis Advisor

Dr. Adil Al-Tamimi
Professor, Department of Civil Engineering
Thesis Committee Member

Dr. Lotfi Romdhane
Professor, Department of Mechanical Engineering
Thesis Committee Member

Dr. Robert Houghtalen
Head, Department of Civil Engineering

Dr. Mohamed El-Tarhuni
Associate Dean, College of Engineering

Dr. Richard Schoephoerster
Dean, College of Engineering

Dr. Khaled Assaleh
Interim Vice Provost for Research and Graduate Studies

Acknowledgements

I would like to thank Professor Sami Tabsh, my mentor and my Thesis Adviser for his invaluable guidance and support. His devotion and commitment were an inspiration for me throughout my master career. I would also like to thank all the Professors and staff at the Civil Engineering department in the American University of Sharjah for their support. Thanks to the Department of Civil Engineering for the assistantship support, which made it possible for me to undertake the master's program.

Special thanks to Mr. Arshi Faridi and Mr. Mohammad Ansari for their immense support in the laboratory. Thanks to Mr. Ricardo and Mr. Ronaldo from the College of Engineering for their help in the experimental work.

I am very grateful to the following friends for their sincere support: Ahmad Mirghani, Abdulla Sagher, AbuBakr Mohammad, Mohammad Anas, Khalid Mustafa, Faress Hraib, Adel Khurram, Daniyal Ali, Mohammad Shanti, and Kamel.

Dedication

To my mother for her prayers, my father for his trust and Basma and Ghassan,
for their incredible support....

Abstract

The most common type of lateral reinforcement in reinforced concrete (RC) columns is rectilinear steel ties. Ties provide confinement to the concrete core increasing its compressive strength and ductility. Past studies have shown that tied columns fail while the stress in the ties is below the yield strength, which represents inefficient use of the material. Furthermore, ties are labor intensive making them costly and time-consuming to fabricate and install. Additionally, the presence of end hooks to anchor them into the concrete adds up to the material cost. A new method of lateral reinforcement is explored in this study where the concrete column core is confined by Internal Structural Steel Strip Bands (ISSSBs) in lieu of ties. These ISSSBs are cut from structural steel square or rectangular tubes. This method has the potential of improving the structural behavior of RC columns without increasing the amount of lateral steel. There are two main objectives for this study. The first one is to verify the feasibility of the use of ISSSBs as lateral reinforcement in RC columns, while the second is to develop design recommendations for columns transversely reinforced with ISSSBs. To achieve the stated objectives, five variables are considered: (1) aspect ratio of the cross section, (2) spacing of ISSSBs, (3) thickness to width ratio of the ISSSBs, (4) compressive strength of concrete, and (5) area of the column's cross-section. The experimental work involved the construction and testing of 25 short specimens with different configurations under concentric axial compression. On average, the results of the study showed that the use of ISSSBs can cause 5% increase in the strength, 65% increase in initial stiffness, and 20% increase in ductility of the concrete core compared to the use of ties. Moreover, it was found that the lateral confining steel is more effective in moderate and high strength concrete than in low strength concrete. The lateral steel volumetric ratio has little effect on strength but great impact on stiffness and ductility. Findings of the study showed that the strength of ISSSB-confined columns can be predicted by the tied columns equation of the ACI 318M-14.

Search terms: Column, confinement, ductility, strength, transverse reinforcement, reinforced concrete

Table of Contents

Abstract	6
List of Figures	10
List of Tables	13
Chapter 1. Background	15
1.1 Introduction	15
1.2 Problem Statement	17
1.3 Proposed System of Confinement	18
1.4 Objectives of Study	20
1.5 Scope of Study	21
1.6 Thesis Organization.....	22
Chapter 2. Literature Review.....	23
2.1 Introduction	23
2.2 Internal Structural Steel Strip Bands	23
2.3 Characteristics of Confined Concrete	25
2.4 Stress-Strain Relationship of Confined Concrete.....	27
2.5 Confinement of Concrete by External Steel Jacketing.....	30
2.6 Lateral Confinement of Concrete by Welded Wire Reinforcement.....	32
Chapter 3. Experimental Work.....	34
3.1 Introduction	34
3.2 Experimental Program.....	34
3.3 Specimen Naming and Designation	37
3.3.1 Explanation of naming system.....	37
3.4 Laboratory Work and Instrumentation.....	40
3.5 Materials.....	40
3.5.1 Concrete.....	40
3.5.2 Steel reinforcing bars.....	43

3.5.3	Structural steel tubes.....	45
3.6	Specimen Fabrication.....	47
3.7	Data Acquisition.....	51
3.8	Test Setup.....	52
Chapter 4.	Results.....	54
4.1	Introduction.....	54
4.2	Stress-Strain Relationship for the Unconfined Concrete Cylinder.....	54
4.3	Specimens Load-Deflection Relationships.....	54
4.4	Strain in the Confined Concrete Core.....	58
4.5	Stress-Strain Relationship of the Confined Concrete Core.....	66
4.6	Concrete Performance Criteria.....	68
4.7	Results.....	69
Chapter 5.	Discussion and Analysis of Results.....	100
5.1	Introduction.....	100
5.2	Failure of Specimens.....	100
5.3	Stress-Strain Relationships of Confined Concrete.....	102
5.4	Effect of Variables on Confined Concrete.....	103
5.4.1	Effect of concrete strength.....	103
5.4.2	Effect of lateral reinforcement spacing.....	105
5.4.3	Effect of core size.....	106
5.4.4	Effect of core aspect ratio.....	107
5.4.5	Effect of thickness to width ratio of ISSSB.....	108
5.5	Overall Comparison of ISSSB and Tie Confinement.....	109
5.6	Test Results versus ACI 318.....	111
5.7	Effect of lateral steel volumetric ratio.....	113
Chapter 6.	Summary and Conclusions.....	115
6.1	Summary.....	115

6.2	Conclusions	116
	References.....	119
	Vita.....	121

List of Figures

Figure 1: Effect of tie confinement on the column behavior	15
Figure 2: Typical load-deflection behavior of tied and spiral RC columns.....	17
Figure 3: Internal Structural Steel Strip Bands cut from a square steel tube.	19
Figure 4: Steel cage for an RC column made with ISSSBs in lieu of ties.	19
Figure 5: (a) Tie lateral reinforcement (b) ISSSB lateral reinforcement	20
Figure 6: Axial load-strain relationships for the tested confinement schemes [1]	24
Figure 7: Backbone relationships for the tied and ISSSB-confined columns [6].....	24
Figure 8: Effective confined area in a tied column [11]	26
Figure 9: Determination of f_{cc}' in rectangular sections [11]	27
Figure 10: Stress-strain relationships for unconfined and confined concrete [10]	28
Figure 11: Column steel cage using WWF sheets [13].....	28
Figure 12: Predicted vs. experimental results for WWF reinforced specimens [13]...30	
Figure 13: Models for identifying confined and unconfined concrete [16].....	30
Figure 14: External jacketing using steel straps [4].....	31
Figure 15: Columns with uniform and non-uniform steel strip placement [17]	32
Figure 16: Normalized stress-strain for WWR-confined concrete [18].....	33
Figure 17: Values considered for the five design variables	36
Figure 18: Testing of typical concrete cylinder	41
Figure 19: Stress-strain for the weak strength concrete	42
Figure 20: Stress-strain for the medium strength concrete	42
Figure 21: Stress-strain for cylinder for the strong concrete	43
Figure 22: Testing of steel bars.....	43
Figure 23: Stress-strain for 12 mm deformed bar	44
Figure 24: Stress-strain for 10 mm deformed bar	44
Figure 25: Stress-strain for 8 mm deformed bar	45
Figure 26: Stress-strain for 6 mm non-deformed bar.....	45
Figure 27: ISSSBs cut from steel tubes	46
Figure 28: Steel coupon machined from Tube 4.....	46
Figure 29: Stress-strain from tensile testing of Tube1	47
Figure 30: Making formwork in the manufacturing lab	47
Figure 31: Example of completed wood formwork.....	48
Figure 32: Making end hooks on ties using the steel bender	48

Figure 33: Cutting ISSSBs from hollow structural steel	48
Figure 34: Assembling and tack-welding the steel cage.....	48
Figure 35: Top view of one ISSSB-confined specimen steel cage.....	49
Figure 36: Connecting strain gauges to longitudinal bars to a tied specimen	49
Figure 37: Placement of steel cages in formwork.....	49
Figure 38: Concrete mixing	50
Figure 39: Concrete curing	50
Figure 40: Painting specimens	50
Figure 41: Smoothing specimen ends by electric grinding.....	51
Figure 42: Connecting the LVDTs to the specimen	51
Figure 43: Test setup of specimen in the UTM	52
Figure 44: Load-displacement relationships for specimens 1 to 4	55
Figure 45: Load-displacement relationships for specimens 5 to 12	56
Figure 46: Load-displacement relationships for specimens 13 to 21	57
Figure 47: Load-displacement relationships for specimens 21 to 25	58
Figure 48: Individual strains against the number of time steps for S2C.....	59
Figure 49: Average strains against the number of time steps for S2C.....	59
Figure 50: Average strains for specimens 1 to 8.....	60
Figure 51: Average strains for specimens 9 to 16.....	61
Figure 52: Average strains for specimens 17 to 24.....	62
Figure 53: Average strains for specimen 25	63
Figure 54: Modified Stress-strain model for rebars prone to buckling [22]	64
Figure 55: Steel rebar that buckles before reaching yield.....	65
Figure 56: Steel rebar that buckles after reaching yield	66
Figure 57: Steel rebar that does not buckle.....	66
Figure 58: Force against strain in longitudinal rebar in S4A.....	67
Figure 59: Stress in the concrete core vs. strain for specimen S4A.....	68
Figure 60: Stress-strain for S1A-T1A and the corresponding cylinder	72
Figure 61: Stress-strain for S1B-T1B and the corresponding cylinder.....	74
Figure 62: Stress-strain for S2A-T2A and the corresponding cylinder	76
Figure 63: Stress-strain for S2C-T2C and the corresponding cylinder.....	78
Figure 64: Stress-strain for S3A-T3A and the corresponding cylinder	80
Figure 65: Stress-strain for S3C-T3C and the corresponding cylinder.....	82

Figure 66: Stress-strain for S4A-T4A and the corresponding cylinder	84
Figure 67: Stress-strain for S4B-T4B and the corresponding cylinder.....	86
Figure 68: Stress-strain for S5A-T5A and the corresponding cylinder	88
Figure 69: Stress-strain for S2C4B-T2C4B and the corresponding cylinder	90
Figure 70: Stress-strain for S3C4B-T3C4B and the corresponding cylinder	92
Figure 71: Stress-strain for A1 concrete core and the corresponding cylinder.....	93
Figure 72: Stress-strain for A2 concrete core and the corresponding cylinder.....	94
Figure 73: Stress-strain for A3 concrete core and the corresponding cylinder.....	95
Figure 74: Stress-strain in the concrete core of A1, A2, and A3	96
Figure 75: Observed damage of ISSSB and tied specimen (weak concrete).....	101
Figure 76: Observed damage of ISSSB and tied specimen (medium concrete).....	101
Figure 77: Observed damage of ISSSB and tied specimens (strong concrete).....	102
Figure 78: Typical stress-strain for confined vs. unconfined concrete.....	102
Figure 79: Effect of concrete compressive strength	104
Figure 80: Effect of spacing of lateral reinforcement.....	105
Figure 81: Effect of core size.....	106
Figure 82: Effect of aspect ratio, a/b	108
Figure 83: Effect of thickness to width ratio, t/w	109
Figure 84: S_r values for all ISSSB-tie specimen pairs	110
Figure 85: K_r values for all ISSSB-tie specimen pairs	111
Figure 86: D_r values for all ISSSB-tie specimen pairs	111
Figure 87: Experimental/ theoretical strength for specimen pairs	113
Figure 88: Effect of volumetric steel ratio, ρ	114

List of Tables

Table 1: Values considered for the five design variables	35
Table 2: ISSSB details and corresponding tie bar size	37
Table 3: Details of ISSSB-confined specimens	38
Table 4. Details of tie-confined specimens.....	39
Table 5: Details of the ISSSB specimens without tied counterpart.....	39
Table 6: Material properties of fine aggregates	41
Table 7: Material properties of coarse aggregates	41
Table 8: Mix proportions for the considered concrete mixes	41
Table 9: Yield strength of the different steel bars.....	45
Table 10: Dimensions of steel tubes used.....	46
Table 11: Yield strength of the steel tubes used as ISSSBs.....	46
Table 12: f_c' from cylinder testing of the seven concrete batches.....	54
Table 13: Strain at buckling for the ISSSB and tied reinforced specimens.....	63
Table 14: Strain at buckling for the 3 extra ISSSB reinforced specimens.....	64
Table 15: Condition of specimen pair S1A-T1A during testing.....	71
Table 16: Condition of specimen pair S1B-T1B during testing	73
Table 17: Condition of specimen pair S2A-T2A during testing.....	75
Table 18: Condition of specimen pair S2C-T2C during testing	77
Table 19: Condition of specimen pair S3A-T3A during testing.....	79
Table 20: Condition of specimen pair S3C-T3C during testing	81
Table 21: Condition of specimen pair S4A-T4A during testing.....	83
Table 22: Condition of specimen pair S4B-T4B during testing	85
Table 23: Condition of specimen pair S5A-T5A during testing.....	87
Table 24: Condition of specimen pair S2C4B-T2C4B during testing.....	89
Table 25: Condition of specimen pair S3C4B-T3C4B during testing.....	91
Table 26: Condition of specimen A1 during testing.....	93
Table 27: Condition of specimen A2 during testing.....	94
Table 28: Condition of specimen A3 during testing.....	95
Table 29: Strength results for ISSSB specimens	96
Table 30: Strength results for tied specimens	97
Table 31: Stiffness results for ISSSB specimens.....	97
Table 32: Stiffness results for tied specimens.....	97

Table 33: Ductility enhancement factor for ISSSB specimens.....	98
Table 34: Ductility enhancement factor for tied specimens	98
Table 35: Strength enhancement factor for 3 extra ISSSB specimens	98
Table 36: Stiffness enhancement factor for 3 extra ISSSB specimens.....	98
Table 37: Ductility enhancement factor for 3 extra ISSSB specimens.....	99
Table 38: Experimental and theoretical strengths for all specimen pairs	112
Table 39: Experimental/ theoretical strength for specimen pairs	113

Chapter 1. Background

1.1 Introduction

Lateral steel reinforcement serves many purposes in reinforced concrete (RC) members. In beams, it is responsible for helping in carrying shear. In columns, it provides a necessary constructability function and makes it possible to assemble the reinforcing steel cage for the column. It also gives shear resistance when bending moments are applied to the column or where large lateral loads are induced due to high wind or earthquake loads. Most importantly, lateral steel provides confinement to the concrete core and increasing its strength and ductility. Additionally, the effective length of the longitudinal steel bars between the ties is reduced, causing it to have more resistance to buckling when the concrete cover spalls off at high compressive loads. Figure 1 shows typical load-deflection curves for columns without and with ties.

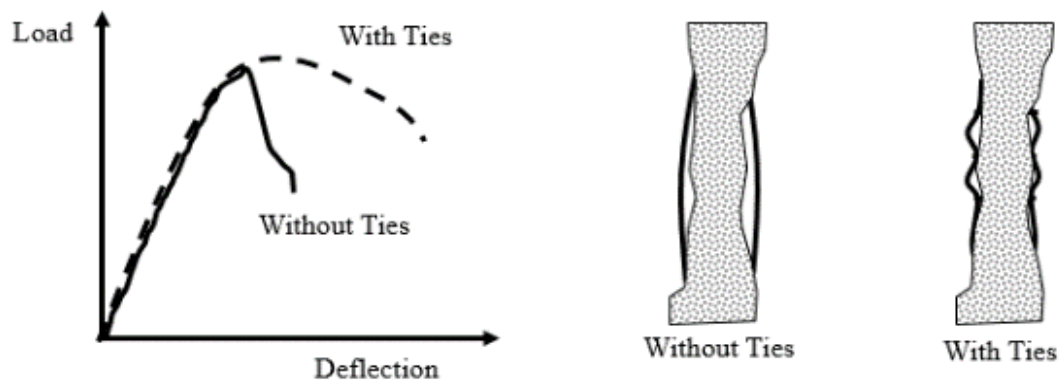


Figure 1: Effect of tie confinement on the column behavior

(a) Load-deflection curves

(b) Buckling of longitudinal steel bars

The most common form of lateral steel reinforcement in RC columns in buildings is the traditional rectilinear ties [1, 2]. Ties provide passive confinement of the concrete core under concentric or eccentric loading. Under the application of load, a column shortens longitudinally and expands laterally due to the Poisson effect. At low load levels, the lateral expansion is not pronounced and the confinement action of the ties is insignificant. The column section remains intact structurally except for minor cracking. When the applied load increases, the lateral expansion increases and eventually the concrete cover spalls off in an abrupt manner causing the column to lose 10-15% of its strength [1]. However, the confinement action provided by the

ties, increases the compressive strength of the concrete core; thus, compensating for the strength loss due to cover spalling. When ties are designed according to the ACI 318M-14 code, the increase in strength due to confinement is assumed to be at least equal to the loss of strength due to the spalling of concrete cover [3]. Henceforth, the provisions for the calculation of the capacity of RC columns are based on the column's gross cross-sectional area including the cover.

The ACI 318M-14 predicts the axial capacity of a reinforced concrete tied column under perfectly concentric loading, P_o (N), using the following equation:

$$P_o = 0.85f'_c(A_g - A_{st}) + f_y A_{st} \quad (1)$$

where f'_c is the compressive strength of the standard concrete cylinder at the age of 28 days (MPa), A_g is the gross sectional area of the column (mm^2), A_{st} is the area of longitudinal steel reinforcement (mm^2), and f_y is the yield strength of the longitudinal steel rebars. To account for accidental eccentricity, the code introduces the reduction factor $\alpha = 0.8$ for tied columns, thus the nominal capacity of the column (P_n) is given by:

$$P_n = 0.8P_o \quad (2)$$

Finally, the design strength of the column is found by incorporating the strength reduction factor $\phi = 0.65$ for tied columns as shown in the equation below:

$$\phi P_n = 0.65P_n \quad (3)$$

The requirements for the steel ties in the ACI 318M-14 code are based on a set of criteria [3]. With regard to the maximum vertical tie spacing along the member, it is the smallest of: (1) 16 times the bar diameter, (2) 48 times the tie diameter, or (3) minimum dimension of column cross-section. As for the minimum size of the tie, the code requires No. 10 ties if longitudinal bars are No. 32 and smaller, and No. 12 ties if longitudinal bars are larger than No. 32 or if bundled bars are used. Other detailing requirements include: (1) every corner and alternate longitudinal bar shall have a lateral tie support with an included angle of not more than 135 degrees (irrespective of the spacing), (2) no longitudinal bar shall be more than 150 mm clear (on each side along the tie) from a laterally supported bar, and (3) ties must be located at no more

than half a tie spacing above the surface of the footing or bottom slab and no more than half a tie spacing below the lowest horizontal reinforcement in slab.

1.2 Problem Statement

Past studies on the subject have revealed that reinforced concrete columns with ties spaced according to the ACI 318M-14 code have low concrete core confinement when compared with corresponding spiral columns. As a result, a typical tied RC column has slightly lower strength than a spiral one. More importantly, tied columns perform poorly with respect to ductility as the longitudinal reinforcement buckles almost immediately after the concrete cover spalls off when the column is subjected to high axial compression [2]. The contrast between the behavior of tied and spiral columns under concentric loading can be observed through a typical axial load-deflection diagram, as shown in Figure 2.

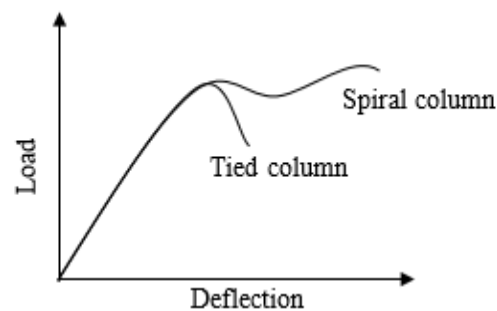


Figure 2: Typical load-deflection behavior of tied and spiral RC columns

In building and bridge structures, it is desirable to increase the aforementioned characteristics of a column, namely strength and ductility. To achieve this goal, an increase in the concrete core confinement must be realized using a combination of the following actions: increasing the size of ties, decreasing the spacing between the ties, or a combination of both. Other techniques include external structural steel jacketing or FRP wrapping [4]. The later techniques are often used as strengthening mechanisms in existing columns, rather than in the construction of new members. All of these actions, however, are quite costly as they require extra material and labor (i.e. more ties, external steel, or FRP wraps). Other problems may arise as well, such as while decreasing the spacing between ties, the flow and placement of concrete could be restricted due to potential congestion of the steel cage inside the column.

A close examination of the use of ties in RC column reveals some

shortcomings of the concept of the tie as lateral reinforcement. Tied columns retain very little post-peak strength since they cannot effectively resist lateral bulging of the concrete beyond that point. This could lead to the collapse of the structure shortly after reaching the peak capacity of the column. Furthermore, previous experimental work shows that the stress level in the ties at the maximum applied axial load is significantly less than the yield stress, which signifies inefficient use of the material [1]. Moreover, the potential for buckling of the longitudinal steel bars remains high in typical tied RC columns and this in turn reduces the load carrying capacity of the column immaturely. The weak confinement associated with rectilinear ties cannot be solved merely by increasing the amount of lateral steel reinforcement since this weakens the bond in the concrete between the column core and the cover. Additionally, increasing the amount of lateral reinforcement comes at a large cost and could lead to congestion in the steel cage, especially that the ties have end hooks to insure their anchorage in the concrete [5].

The inferior confinement provided by ties has led to research for alternatives and supplementary systems. Examples of such systems include Welded Wire Mesh (WWM), Fiber Reinforced Polymers (FRP) wrapping, Expanded Metal Mesh, and Internal Structural Steel Strip Bands (ISSSBs). This study investigates the use of ISSSBs for RC column core confinement as an alternative to ties, which is relatively a new application. As such, the behavior of ISSSB-confined columns is not well documented due to lack of research in this area. The benefits of use of ISSSB as lateral confinement in columns has the potential to be promising; thus, research needs to be conducted in this area to better understand its behavior and assess its practical implementation.

1.3 Proposed System of Confinement

In this study, a new system of lateral reinforcement in columns is put to the test. This system is comprised of Internal Structural Steel Strip Bands (ISSSBs) used in the place of the traditional ties. The steel strip bands are cut from square or rectangular structural steel tubes, depending on the cross-section of the column, and subsequently used to contribute to the RC column steel cage. The ISSSBs can be attached by wires or spot-welded into place (without changing the material

properties). Figure 3 shows square ISSSBs and Figure 4 presents a steel cage for an RC column made with ISSSBs.



Figure 3: Internal Structural Steel Strip Bands cut from a square steel tube.



Figure 4: Steel cage for an RC column made with ISSSBs in lieu of ties.

It is important to recognize that this system is not the same as external steel jacketing, which is often used for strengthening or rehabilitation of existing columns. Rather, the proposed ISSSB system is to be used internally inside the cross-section for the design of new columns. Figure 5 shows schematic diagrams of two RC columns; one is laterally reinforced with ties and the other utilizes the newly proposed ISSSB lateral reinforcement system.

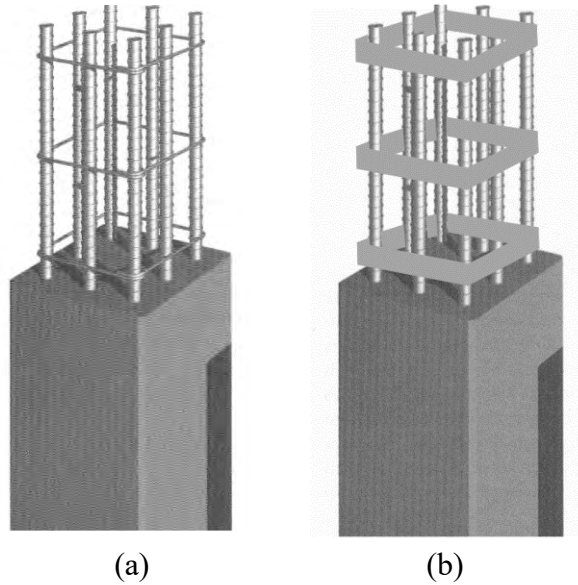


Figure 5: (a) Tie lateral reinforcement (b) ISSSB lateral reinforcement

The basic idea here is not to use more transverse steel than what is normally used in a tied column. Instead, the proposed concept of ISSSB reinforced column is to rearrange the material within the circular cross-section of the tie into a rectangular thin plate with more width; thus, providing more confinement influence area at the location of the lateral reinforcement along the column's length compared to the tie. The ISSSB lateral reinforcement system has the potential to improve the strength and ductility characteristics of RC columns while relieving congestion within the steel reinforcement cage.

Market research in the UAE showed that reinforcing steel bars cost 435-445 US\$/Ton whereas structural steel tubes cost 570-580 US\$/Ton, a difference of about 30%. This difference in cost shall be considered in the overall assessment of the feasibility of ISSSB confinement in comparison with tie confinement using steel bars. However, since nowadays labor is much more expensive than construction material costs, it is expected that the decrease in labor will more than offset the slight increase in material, especially that the ISSSBs have reduced weight compared to the ties since they do not have end hooks.

1.4 Objectives of Study

The main objectives of this study are:

- 1- To investigate the behavior of RC columns confined by ISSSBs under pure axial compression using experimental testing of small-scale models.

- 2- To compare the performance of ISSSB confined columns with that of corresponding tied columns in relation to the strength, stiffness, and ductility of the columns.
- 3- To determine the effect of the aspect ratio of the cross-section, lateral reinforcement spacing, strip band thickness-to-width ratio, concrete compressive strength, and size of the cross-section on the performance of RC columns confined by ISSSBs relative to that of traditional ties.
- 4- To develop design recommendations regarding the use of ISSSB confinement system in RC columns as an alternative to the tie confinement system.

1.5 Scope of Study

This study considers experimental investigation of 25 short column cores that represent about one-third scale. All columns considered were designed in accordance with the ACI 318-14M code criteria for short columns, without the effect of slenderness. Columns were subjected to pure axial compression inside a Universal Testing Machine under displacement-controlled environment at a rate of 0.2 mm/min. The testing program of the column specimens encompassed the following variables:

- 1) Aspect ratio of the cross-section: square and rectangular column cross-sections with dimensions equal to 150 mm x 150 mm and 150 mm x 75 mm.
- 2) Lateral reinforcement spacing: spacing intervals of the ties/ISSSBs: 200, 150, and 100 mm on center.
- 3) Thickness-to-width ratio of the ISSSBs: this applies only to the ISSSBs, not the ties: 0.32, 0.18, and 0.11.
- 4) Concrete compressive strength: different f_c values equal to: 16, 24 and 41 MPa.
- 5) Size of the cross-section: two different core areas were used for the square columns: 200 mm x 200 mm, and 150 mm x 150 mm.

When comparing the performance of an ISSSB reinforced column to that of a tied column, the two columns were configured identically in terms of the cross-section dimensions, spacing of the lateral reinforcement, longitudinal steel area and concrete compressive strength. The cross sectional area of the ties and the corresponding ISSSBs were also made equal. This way, the only difference between two specimens in any comparison was the cross-sectional shape of the lateral

reinforcement (rectangular shape when ISSSB confinement is used and circular shape when tie confinement is used). Although the yield strength was not the same in the ISSSBs and ties, this was not a problem since past studies and observations in the current literature show that the lateral reinforcement did not approach yielding, even at high levels of loads.

1.6 Thesis Organization

Chapter 1 discusses the tie lateral reinforcement system and points its shortcomings, explains the alternative to the ties in the form of the ISSSB concept, outlines the objectives, and spells out the scope of the study. Chapter 2 provides a summary of the state of the art of published literature in the field of concrete confinement in RC columns. Chapter 3 describes the details of the experimental setup, materials characteristics, and testing procedure. Chapter 4 presents the results of the experimental testing and the techniques followed to obtain these results. Chapter 5 summarizes the findings of the study and provides conclusions and recommendations.

Chapter 2. Literature Review

2.1 Introduction

This chapter provides the state-of-the-art literature on lateral confinement in reinforced concrete columns. Firstly, the ISSSB confinement system is previewed. Then there is a discussion of the behavior of laterally confined concrete in terms of the compressive strength, ductility and its stress-strain relationships. Finally, two column reinforcement systems are explored as they are closely related to ISSSB confinement. The first system is external steel jacketing and the second is confinement by internal Welded Wire Reinforcement.

2.2 Internal Structural Steel Strip Bands

Search of the available literature on the subject indicated little published work on lateral confinement of concrete columns by Internal Structural Steel Strip Bands (ISSSBs). Shafqat and Ali [1] investigated the problem of lateral confinement of RC short columns. In their experiment, they compared the performance of tied columns with that of columns laterally reinforced by very thin ISSSBs. Three lateral steel configurations were examined. One column with No. 10 ties (CSB1), one column using 2 mm thick by 26 mm high ISSSBs (CSP1) and another column using 1.2 mm thick by 36 mm high ISSSBs (CSP2). Thus, the area of lateral reinforcement was kept practically constant in all three arrangements. All other variables were kept constant except for the cross-sectional shape of lateral steel reinforcement.

The results showed improved performance of the RC columns that utilized ISSSBs for lateral reinforcement over the tied column. The axial capacity increased by 78% and 16% for CSP1 and CSP2 columns, respectively, in comparison to the CSB1 column. Also, the ductility at ultimate improved following a similar pattern; the tied column failed at normal strain $\varepsilon = 1.15\%$, column CSP1 failed at $\varepsilon = 12.4\%$ and column CSP2 failed at $\varepsilon = 4.9\%$. The aforementioned results are shown graphically in Figure 6.

The results suggest that while ISSSB enhances both the ductility and strength, the use of a very large width-to-thickness ratio of the ISSSB cross-section is not always efficient since the strips become too flexible to resist the bulging of concrete core under high compressive loads.

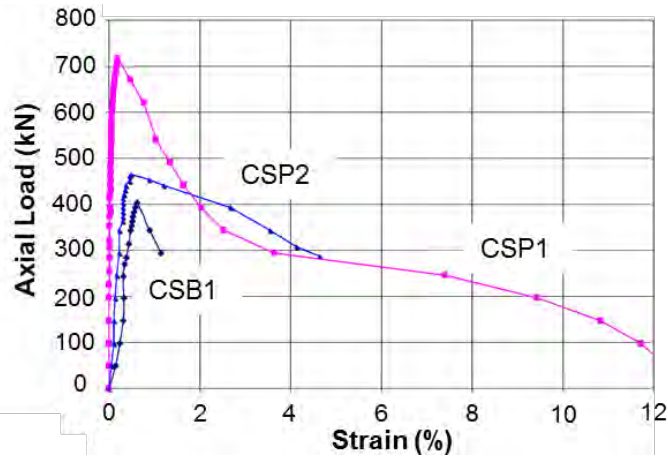


Figure 6: Axial load-strain relationships for the tested confinement schemes [1]

A similar study was conducted by Tahir et al. [6] where the effect of plate strip confinement on RC columns was examined. Two columns were tested under cyclic loading, one with traditional tie reinforcement and the other with ISSSB reinforcement. Both had the same geometry and amount of lateral reinforcement steel. However, the type of reinforcement was not the only variable in this study as the yield strength (f_y) too was varied; the f_y of the ties was 276 MPa while that of steel strips was 242 MPa. The resulting backbone curves in Figure 7 show the improvement in ductility in the order of 25% due to the use of ISSSB confinement, although the strength was reduced by about 15%. This reduction in strength is not in agreement with the results obtained by Shafqat and Ali [1], as was discussed earlier. This could be due to the lower yield strength of the ISSSBs compared to the ties.

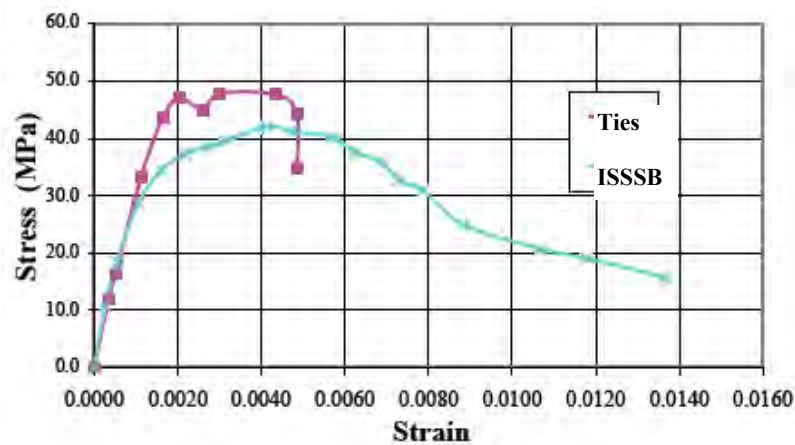


Figure 7: Backbone relationships for the tied and ISSSB-confined columns [6]

The discussion above was based on two published papers. No other literature was found that discusses specifically the topic of lateral confinement of concrete

columns using ISSSBs. There are, however, few studies that touch on the subject but are related to the application of external steel plates or ropes for rehabilitation and strengthening purposes, particularly under seismic loading [7-9]. The rarity of existing literature confirms the need and the significance of conducting research in the area of ISSSBs as an alternative confinement method to conventional ties.

2.3 Characteristics of Confined Concrete

Much research has been done on the calculation of the compressive strength of confined concrete (f'_{cc}). Two well-known methods for the calculation of f'_{cc} are presented herein as proposed by Saatcioglu and Razvi [10] and Mander et al. [11]. The method of Saatcioglu and Razvi [10] is based on the principle that the confining steel cage exerts a uniform lateral pressure on the concrete core. In the case of the lateral pressure being non-uniform, the average lateral pressure can be used and f'_{cc} can be calculated as a function of the compressive strength of unconfined concrete (f'_{co}), the average lateral pressure (f_l), and factors k_1 and k_2 as shown below:

$$f'_{cc} = f'_{co} + k_1 k_2 f_l \quad (4)$$

where the k_1 factor is related to the Poisson's ratio of the concrete and was found by regression analysis of experimental data such as:

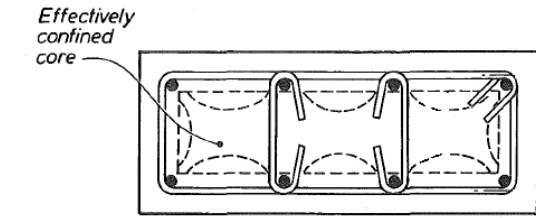
$$k_1 = 6.7 f_l^{-0.17} \quad (5)$$

where the uniform pressure f_l can be obtained from equilibrium of forces and the results of experimental observations.

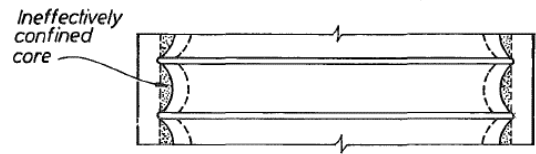
The k_2 factor is introduced to account for the two-way reduction in confining pressure along the ties in the horizontal direction and at the corners along the longitudinal steel in the vertical direction. When the spacing of the ties is small and the longitudinal steel bars are closely spaced and laterally supported, the confining pressure between the ties is close to uniform and k_2 takes a value of 1.0. On the other hand, when the spacing of the ties and/or the longitudinal steel becomes large, the actual lateral pressure becomes far from uniform and the k_2 factor takes a value less than 1.0. The smaller the k_2 value the lower the compressive strength of confined concrete f'_{cc} . The value for k_2 was obtained by regression analysis of experimental

data obtained from testing of tied-columns of various configurations [10].

The method of Mander et al. [11] assumes that the lateral pressure is equal to the average pressure exerted by the ties on the concrete core. Here, the average pressure is assumed to act uniformly over an effective area smaller than the actual area of the concrete core. The smaller area used takes into account the arching effect at the level of the tie from one longitudinal bar to the next and also along the height of the column from one tie to another. Therefore, a reduction factor is applied to the concrete core area by means of the confinement effectiveness factor (k_e). Figure 8 illustrates the arching action and the resulting effectively confined core area by the transverse reinforcement.



(a) Confinement at the tie level (plan)



(b) Confinement between the ties (elevation)

Figure 8: Effective confined area in a tied column [11]

The effective confining pressures can be found at the useful limit (at yield) of the transverse reinforcement using the following equations:

$$f'_{lx} = k_e \rho_x f_y \quad (6)$$

$$f'_{ly} = k_e \rho_y f_x \quad (7)$$

where f'_{lx} and f'_{ly} are the effective confining pressures along the x and y directions, respectively, and ρ_x and ρ_y are the transverse steel ratios in their respective directions.

Assuming a known value for the unconfined concrete compressive strength, f'_{co} , often taken as the cylinder strength, the diagram reported in Figure 9 is used to find the compressive strength of confined concrete f'_{cc} , where f_{l1} and f_{l2} are the

smaller and the larger values of f'_{lx} and f'_{ly} , respectively.

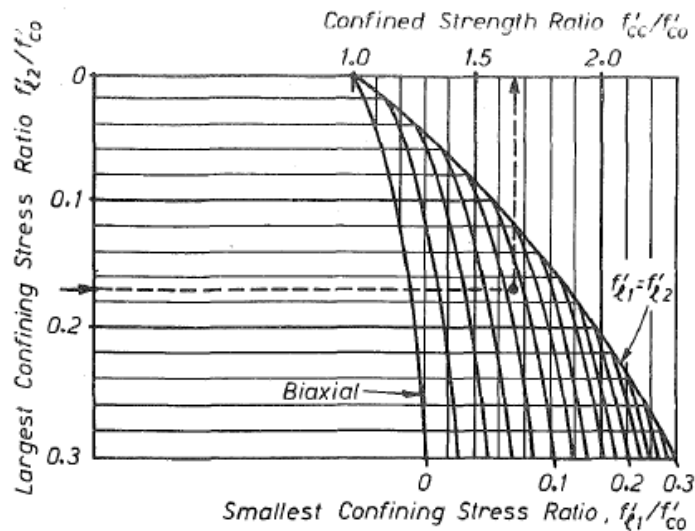


Figure 9: Determination of f'_{cc} in rectangular sections [11]

2.4 Stress-Strain Relationship of Confined Concrete

Plain concrete columns under axial compression have low ductility. They have a small strain corresponding to their ultimate capacity and they also lose most of their strength immediately after attaining their peak capacity. On the other hand, RC columns with confined concrete core due to presence of lateral reinforcement exhibit higher strain at peak load and show slow decay in strength following the peak load. The later phenomenon is demonstrated by a mild descending branch on the stress-strain curve after the peak. Moreover, confinement of the RC column core leads to significant increase in its strength. Published research have indicated that core confinement is improved when: (1) transverse reinforcement is closely spaced; (2) overlapping hoops or cross ties are provided; (3) longitudinal bars are well distributed around the perimeter of the section; and (4) the amount and/or the yield strength of transverse reinforcement are increased [6, 12]. Over the years, many researchers have modeled the stress-strain relationships of unconfined and confined concrete. Figure 10 shows the model developed by Saatcioglu and Razvi [10]. The relationships shown in Figure 10 consist of a parabola for the ascending branch followed immediately by a linear portion for the descending branch. In addition, a constant residual stress is assumed at 20% of the peak stress for the case of confined concrete. Expressions are formulated to give the parabolic portion of the curve, strain at peak stress, and the

strain at 85% strength level beyond the peak [10].

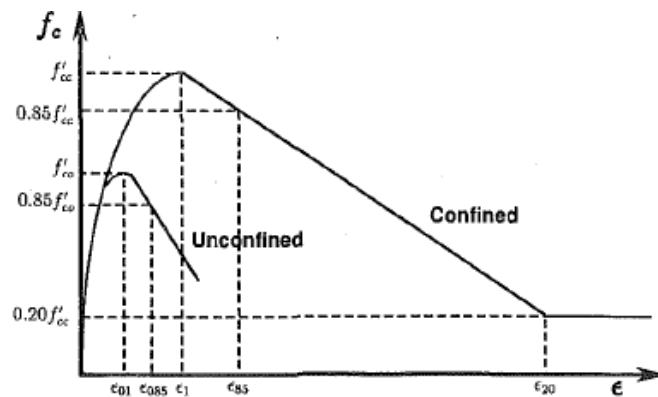
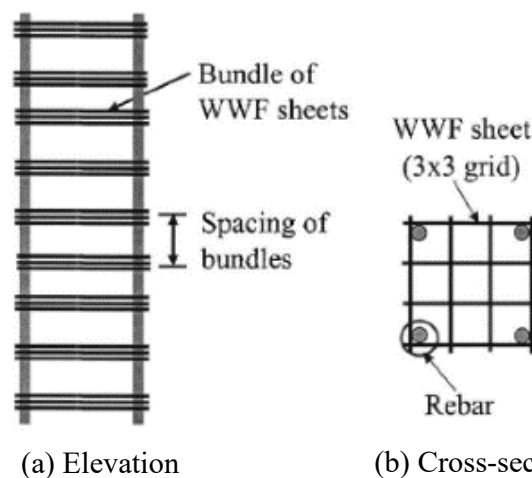


Figure 10: Stress-strain relationships for unconfined and confined concrete [10]

It is observed that both the confined and unconfined concrete have the same initial stiffness (i.e. slope of the ascending branch). On the other hand, the confined concrete shows superior performance in terms of both strength and ductility. This analytical model was compared with a large volume of data in the literature obtained from testing of many tied-columns. The comparison indicates good match between the analytical model and the experimental results from testing.

Another model for stress-strain relationship was proposed by Tabsh for concrete confined using Welded Wire Fabric (WWF) [13]. Ten full-scale columns were transversely reinforced with WWF in place of ties and tested under axial compression. The formed steel cages are illustrated in Figure 11. Two variables were considered: The volumetric ratio of transverse (ρ_s) steel and the number of cells of the WWF layer within the concrete core.



(a) Elevation (b) Cross-section
Figure 11: Column steel cage using WWF sheets [13]

The peak stress, f'_{cc} , and corresponding strain, ϵ'_{cc} , were obtained from

analysis of test results and could be found using the expressions below:

$$f'_{cc} = (7\rho_s + 1)f'_c \quad (8)$$

$$\varepsilon_{cc} = (650,000\rho_s^{3.8})\varepsilon_{c0} \quad (9)$$

where f'_{cc} and ε_{cc} are the peak stress and the corresponding strain of confined concrete, ρ_s is the volumetric ratio of WWF transverse steel, and f'_c and ε_{c0} are the peak stress and the corresponding strain of the unconfined concrete from the cylinder test.

The ascending branch of the stress-strain curve is found using the expression found by Popovics [14]:

$$f_{cc} = \frac{r f'_{cc} \left(\frac{\varepsilon_c}{\varepsilon_{cc}} \right)}{r - 1 + \left(\frac{\varepsilon_c}{\varepsilon_{cc}} \right)^r} \quad (10)$$

where f_c is the stress in the confined concrete at a strain equal to ε_c . This expression is applicable for strains up to ε_{cc} . The parameter r is given by:

$$r = \frac{E_c \varepsilon_{cc}}{E_c \varepsilon_{cc} - f'_{cc}} \quad (11)$$

where E_c is the modulus of elasticity of unconfined concrete.

It was observed from test results that the descending branch is best depicted by a higher order function. This is contrary to many past studies that have attempted to model the descending branch of tied columns with a linear function. Henceforth, the model proposed by Tabsh [13] adopted the expression proposed by Hoshikuma et al. [15] for the descending branch as follows

$$f_{cc} = E_c \varepsilon_{cc} \left[1 - \frac{1}{r} \left(\frac{\varepsilon_c}{\varepsilon_{cc}} \right)^{r-1} \right] \quad (12)$$

where all parameters in the above expression were defined earlier.

The proposed model was compared to experimental results for specimens with various ρ_s and cell numbers. In all cases, the predicted results show a good match with the experimental data as seen in Figure 12.

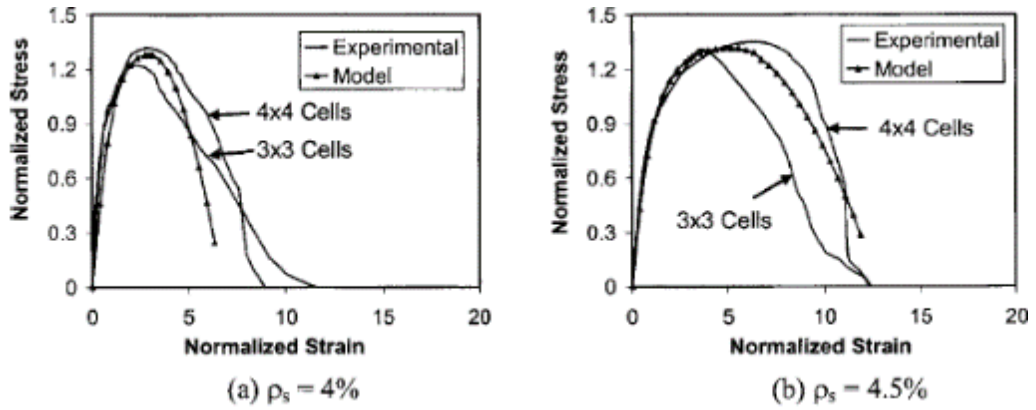


Figure 12: Predicted vs. experimental results for WWF reinforced specimens [13]

2.5 Confinement of Concrete by External Steel Jacketing

Since available literature on concrete confined by ISSSBs is rare, much can be learned on the topic by studying a similar problem involving external steel jacketing of concrete. One such system consists of steel battens welded to steel angles at the four corners of the column. The effect of such a system on concrete is an increase in the effectively confined area of the concrete core. It was observed that the effectively confined core area depends on whether the confinement is by traditional ties only, by steel battens welded to angles only, or by both ties and battens welded to angles [16]. Figure 13 illustrates the effectively confined areas of concrete for the different types of confinement.

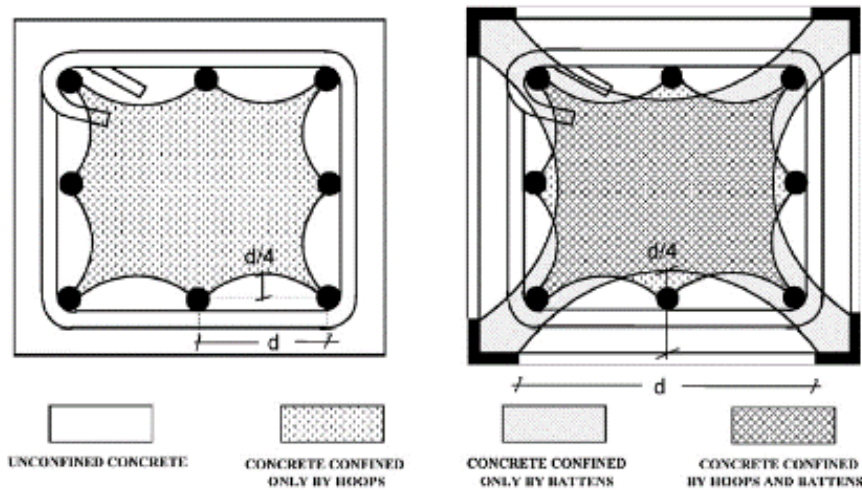


Figure 13: Models for identifying confined and unconfined concrete [16]

Many analytical models were developed to predict the stress-strain relationship of concrete confined externally by steel straps. One of these models is proposed in Badalamenti et al. [4]. This model is of particular interest because it is

developed with the use of steel battens and angles without any ties or longitudinal steel bars, as can be seen in Figure 14.

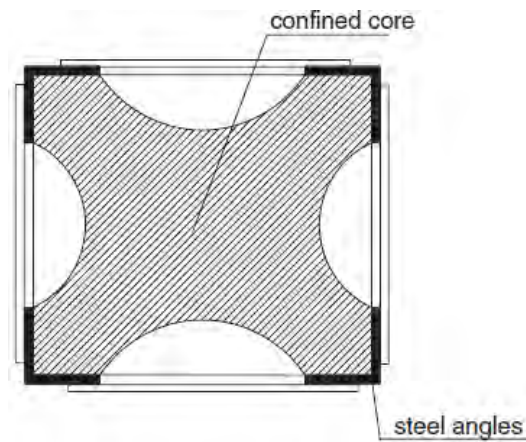


Figure 14: External jacketing using steel straps [4]

The proposed expression for the compressive strength of the confined concrete (f_{cc}) in this case is:

$$f_{cc} = f_{c0} \left[1 + 3.7 \left(\frac{f_1(\varepsilon_{cc})}{f_{c0}} \right)^{0.87} \right] \quad (13)$$

where f_{c0} is the compressive strength of the unconfined concrete, and $f_1(\varepsilon_{cc})$ is the equivalent uniform confining pressure on the concrete core given as a function of the peak strain in the confined concrete, which can be found using the expression:

$$\varepsilon_{cc} = \varepsilon_{c0} \left[1 + 5 \left(\frac{f_{cc}}{f_{c0}} - 1 \right) \right] \quad (14)$$

All other variables in the expression have been defined earlier.

Another study of interest was conducted by Gimenez et al. [17] with the aim of comparing the performance of columns jacketed uniformly with columns employing non-uniform jackets, as shown in Figure 15. The purpose of this study was to evaluate the effect of lateral steel spacing on the ultimate capacity and ductility of the column when steel bands are placed more densely closest to the column ends. It was found that the dense placement of confining steel strips near column ends resulted in appreciable increase in both the axial compressive capacity and the ductility of the column.

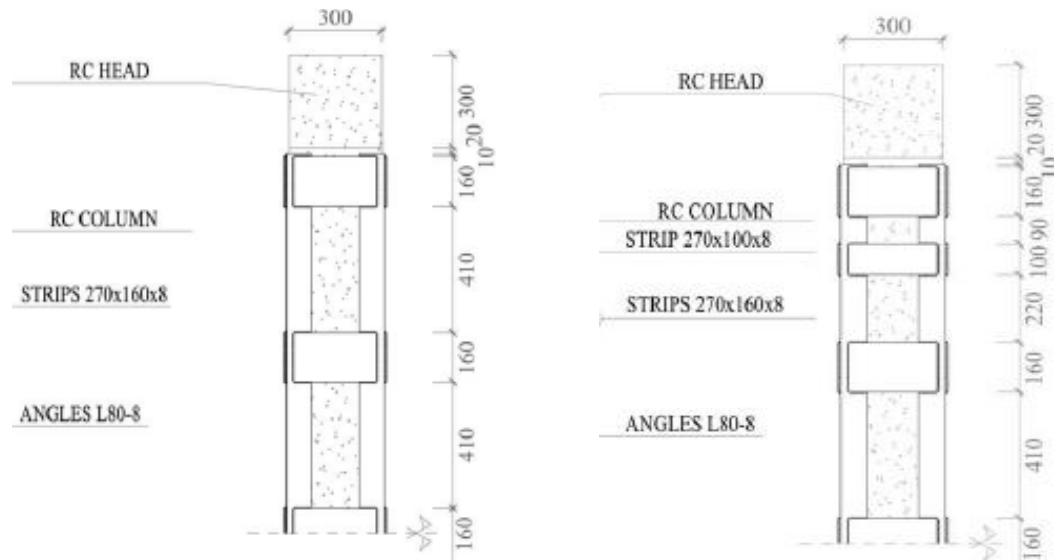


Figure 15: Columns with uniform and non-uniform steel strip placement [17]

2.6 Lateral Confinement of Concrete by Welded Wire Reinforcement

Aikhionbare and Tabsh [18] and Tabsh [13] studied the effectiveness of Welded Wire Reinforcement (WWR) as lateral confinement of high strength concrete in the order of 70 MPa. In this case, ties were replaced by bundles of WWR, as was illustrated in Figure 11. Experimental testing of RC columns using WWR confinement and equivalent tie confinement were conducted and the results from both systems were compared. In order to study the behavior of the confined concrete core only, the contributions to the strength by the longitudinal steel reinforcement and the concrete cover were filtered out.

The stress versus strain diagrams of the concrete cores were plotted after being normalized with respect to the compressive strength and the corresponding strain of the standard concrete cylinder tested at 28 days. The normalized curves show the percentage improvement in the performance of confined concrete in relation to the unconfined concrete. Figure 16 shows a comparison of typical normalized stress-strain plots for the concrete cores of a tied-column and two WWR confined columns with different grid configurations. The study concluded that for the same amount of transverse steel, WWR reinforcement caused the column to attain significantly higher compressive strength and higher ductility than is the case using conventional ties. It was also observed that the ductility of a column improved greatly with an increase in the lateral steel volumetric ratio and decreased spacing of the transverse WWR.

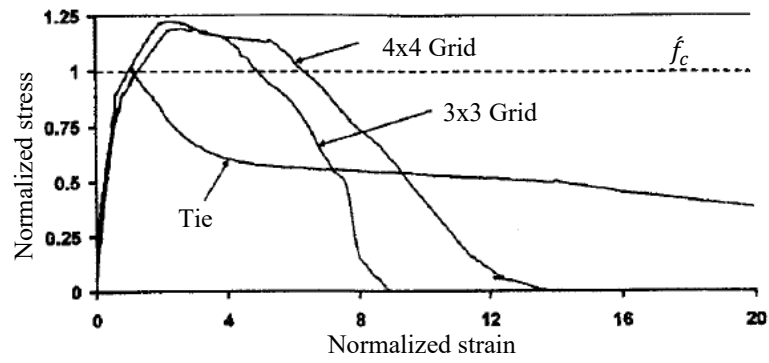


Figure 16: Normalized stress-strain for WWR-confined concrete [18]

Furthermore, the strength of columns was enhanced significantly by using 4x4 WWR sheet grid as opposed to 3x3 WWR sheet grid that has larger cells. The strength was improved to a lesser extent by decreasing the spacing of transverse WWR sheets [18].

Chapter 3. Experimental Work

3.1 Introduction

In this chapter, the experimental program conducted in this study is discussed in detail. The system of labelling of all the specimens is explained. A summary of the laboratory work is provided. Also included are the instrumentation, testing procedure, and method of data acquisition.

3.2 Experimental Program

The experimental program in this research is designed such that the performance of ISSSB confined and tie confined column cores can be directly contrasted and compared. Therefore, the specimens prepared in the lab were categorized in two groups. The first group consists of 11 ISSSB-columns and the second group consists of 11 corresponding tied-columns. Consequently, any specimen in the first group has a matching specimen in the second group with the only difference being the replacement of ISSSBs with ties. Henceforth, any difference in the performance of an ISSSB-column core and its corresponding tied twin can be attributed solely to the use of different lateral reinforcement systems, i.e. ISSSBs versus ties. In addition to the above, three extra ISSSB reinforced specimens with different traverse steel volumetric ratios were tested, without any tied counterparts. All specimens considered were designed as short columns, without the effect of slenderness [3].

The specimens of this study were constructed to represent one-third scale model of typical concrete cores of RC columns used in common structures. The concrete cover was ignored to simplify the problem by focusing solely on the confined concrete core. Otherwise, the contribution of the unconfined concrete cover on the longitudinal reinforced to the stress-strain relationship of the concrete core would have to be considered. Additionally, the columns were proportioned such that they are considered short columns, as per the provisions of the ACI 318-14M; hence, the slenderness effect was ignored. All columns were 900 mm in height except for the columns that have small rectangular cross-sections, which were 470 mm in height to ensure that the slenderness effect is negligible.

Five design variables were considered in the experimental part of the study.

The considered variables are:

- 1- The aspect ratio of the cross section (a/b),
- 2- The spacing of the ties or ISSSBs (s),
- 3- The thickness-to-width ratio of the ISSSBs (t/w),
- 4- The compressive strength of concrete (f'_c), and
- 5- The size of the core.

Table 1 and Figure 17 below show the values considered for each of the variables.

Table 1: Values considered for the five design variables

Parameter	No.	Values considered		
		A	B	C
a/b	1	1, square (std.) 150 mm x 150 mm	2, rectangle 150 mm x 75 mm	NA
s (mm)	2	200 mm	150 mm (std.)	100mm
t/h	3	0.32	0.18 (std.)	0.11
f'_c (MPa)	4	41	24	16 (std.)
Core area	5	150 mm x 150 mm (std.)	200 mm x 200 mm	NA

The thirty specimens with various combinations from the variables are included in the flowchart in Figure 17. It is to be noted that the variable t/w is applicable only to ISSSB-specimens, but not to tied-specimens, since the cross-sectional shape of ties is circular and cannot be varied. One value for each variable was designated as “standard” as noted in both Table 1 and Figure 17. These standard values represent the expected norm and the default value of a variable. To focus on the effect of a particular variable on the performance of the specimens, all other variables were kept constant at their standard values and only the variable of interest was changed by taking one of the values shown in Figure 17. This rule was followed for all but two pairs of specimens, in which two variables were changed at once.

Whenever comparisons were made between an ISSSB-column and an equivalent tied-column, the area of lateral reinforcement was kept constant. For instance, when considering a tied-column with No. 8 mm ties, the cross-sectional area of the ISSSBs in the corresponding column was kept at 50.2 mm², which is equal to the area of No. 8 mm deformed bar.

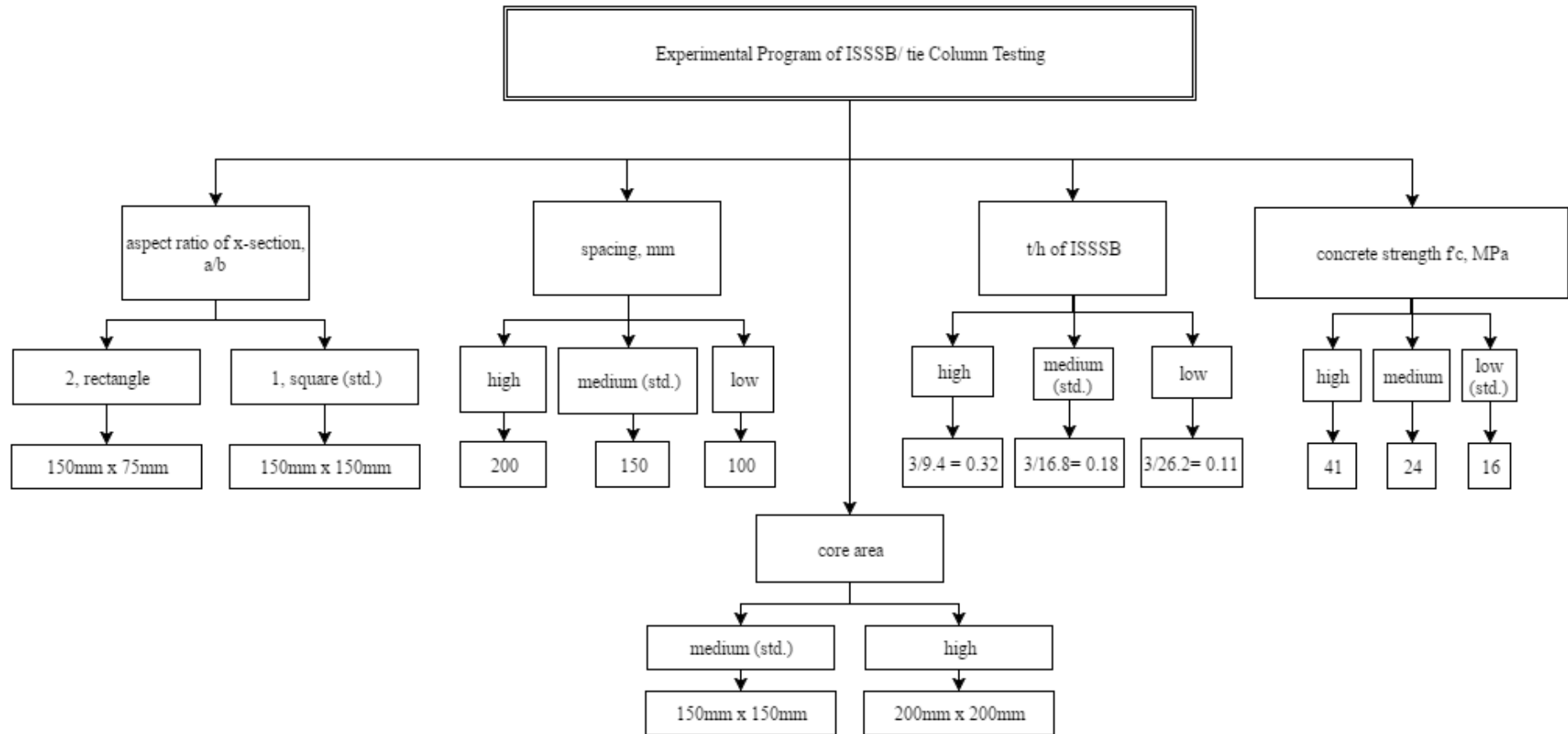


Figure 17: Values considered for the five design variables

The ISSSBs were designed in three different geometries as shown in Table 2 below. Four No.12 deformed bars, one in each corner, were used in all column specimens as longitudinal reinforcement, and their effect on the stress-strain relationship of the concrete core is filtered out from the results.

Table 2: ISSSB details and corresponding tie bar size

Case	Size of tie	Area of equivalent ISSSB (mm ²)	t/w of ISSSB
1	No. 6	28.3	3/9.4 = 0.32
2	No. 8	50.2	3/16.8 = 0.18
3	No. 10	78.5	3/26.2 = 0.11

3.3 Specimen Naming and Designation

3.3.1 Explanation of naming system. Each specimen was given a name consisting of three characters. The first character indicates whether the specimen has ISSSBs or ties. This was denoted using the letter S for (ISSSBs) or T for (ties). The second character is the number tag that indicates the variable of interest in a comparison between two column specimens. These number tags can take the values from 1 to 5, as specified in Table 1. The third character indicates the intensity that the variable of interest takes, as illustrated in Table 1. For example, consider the specimen named S1B. This is a specimen utilizing ISSSBs as lateral reinforcement as indicated by the letter S. The parameter under study is a/b , as indicated by the number 1. Finally, the value of the parameter is 2 as indicated by the letter B; thus the specimen has a 150 mm x 75 mm cross section as shown in Table 1. Similarly, in the limited cases where two variables were of interest in the same specimen at once, the naming of the specimens was expanded. For instance, the specimen S3C4B is an ISSSB-confined column with $t/w = 0.11$ and $f'_c = 24$ MPa, while other variables are kept at their standard values.

Furthermore, the full specification for each of the tested columns is provided in an ordered list containing all the details for each specimen. For example, the specimen T3B is described as 1,150,#8,16,[150x150]. This list follows the same order of variables found in Table 1. Therefore, specimen T3B is a square specimen with ties spaced at 150 mm, tie size is No. 8 mm, f'_c of concrete is 16 MPa, and the core size is 150 mm x 150 mm. On the other hand, the specimen S3B is described as 1,150,0.18,16,[150x150]. It can be seen that the specification for T3B and S3B match

perfectly except that S3B utilizes ISSSBs with $t/w = 0.18$ instead of the No. 8 ties used in specimen T3B. This difference permits the direct comparison between the two different lateral reinforcement systems when comparing the performance of the specimen pair T3B and S3B. The same comparison will be made using all 11 pairs of specimens. A summary of all specimens and their specification is provided in Table 3 and Table 4. The value taken by the variable of interest is indicated in bold for each specimen. Note that specimens S1A and T1A form a comparison of pair, specimens S1B and T1B form another comparison of pair, and so on for the entire set of 22 specimens.

Table 3: Details of ISSSB-confined specimens

Variable	Name	Specimen specification	Variable value				
			a/b	s (mm)	t/w	f'_c	core area
a/b	S1A	1,150,0.18,16,[150x150]	1	std.	std.	std.	std.
	S1B	2,100,0.18,16,[150x75]	2	low	std.	std.	std.
s	S2A	1,200,0.18,16,[150x150]	std.	high	std.	std.	std.
	S2B	1,150,0.18,16,[150x150]	std.	mid	std.	std.	std.
	S2C	1,100,0.18,16,[150x150]	std.	low	std.	std.	std.
t/w	S3A	1,150,0.32,16,[150x150]	std.	std.	high	std.	std.
	S3B	1,150,0.18,16,[150x150]	std.	std.	mid	std.	std.
	S3C	1,150,0.11,16,[150x150]	std.	std.	low	std.	std.
f'_c	S4A	1,150,0.18,41,[150x150]	std.	std.	std.	high	std.
	S4B	1,150,0.18,24,[150x150]	std.	std.	std.	mid	std.
	S4C	1,150,0.18,16,[150x150]	std.	std.	std.	low	std.
$core\ area$	S5A	1,150,0.32,16,[200x200]	std.	std.	high	std.	200x 200
	S5B	1,150,0.18,16,[150x150]	std.	std.	std.	std.	150x 150
s, f'_c	S2C4B	1,100,0.18,24,[150x150]	std.	low	std.	mid	std.
$t/w, f'_c$	S3C4B	1,150,0.11,24,[150x150]	std.	std.	low	mid	std.

For the purpose of arranging the specimens in five categories representing the five design variables, the same standard column shows up under a different label depending on the variable that is being undertaken. These different labels keep the comparisons in perspective and are used to indicate the particular design variable under consideration and the value it takes as was explained in section 3.3.1. The shaded specification cells in Table 3 and Table 4 indicate repeated columns.

Table 4. Details of tie-confined specimens

Variable	Name	Specimen specification	Variable value				
			a/b	s (mm)	t/w	f'_c	core area
a/b	T1A	1,150,#8,16,[150x150]	1	std.	NA	std.	std.
	T1B	2,100,#8,16,[150x75]	2	low	NA	std.	std.
s	T2A	1,200,#8,16,[150x150]	std.	high	NA	std.	std.
	T2B	1,150,#8,16,[150x150]	std.	mid	NA	std.	std.
	T2C	1,100,#8,16,[150x150]	std.	low	NA	std.	std.
t/w (of ISSSB)	T3A	1,150,#6,16,[150x150]	std.	std.	NA	std.	std.
	T3B	1,150,#8,16,[150x150]	std.	std.	NA	std.	std.
	T3C	1,150,#12,16,[150x150]	std.	std.	NA	std.	std.
f'_c	T4A	1,150,#8,41,[150x150]	std.	std.	NA	high	std.
	T4B	1,150,#8,24,[150x150]	std.	std.	NA	mid	std.
	T4C	1,150,#8,16,[150x150]	std.	std.	NA	low	std.
core area	T5A	1,150,#8,16,[200x200]	std.	std.	NA	std.	200x200
	T5B	1,150,#8,16,[150x150]	std.	std.	NA	std.	150x150
s, f'_c	T2C4B	1,100,#8,24,[150x150]	std.	low	NA	mid	std.
$t/w, f'_c$	T3C4B	1,150,#12,24,[150x150]	std.	std.	NA	mid	std.

It could be seen that in both the ISSSB-confined and the tie-confined groups, one of the columns was repeated five times. S1A \equiv S2B \equiv S3B \equiv S4C \equiv S5B and T1A \equiv T2B \equiv T3B \equiv T4C \equiv T5B. Therefore, in the lab only S1A and T1A were actually constructed and tested, and the results obtained were applied to the repeated specimens. Similar to Table 3 and Table 4, details of the 3 extra ISSSB reinforced specimens with different transverse steel volumetric ratios that do not have matching tied specimens are presented in Table 5.

Table 5: Details of the ISSSB specimens without tied counterpart

Name	Specimen specification	Variable Value				
		a/b	s (mm)	t/w	f'_c (MPa)	core area
A1	1,100,0.06,41,[150x150]	1	100	0.06 (3/50)	41	150mm x 150mm
A2	1,150,0.06,41,[150x150]	1	150	0.06 (3/50)	41	150 mm x 150mm
A3	1,80,0.18,41,[150x150]	1	80	0.18 (3/16.8)	41	150 mm x 150 mm

The configurations shown in Table 5 result in lateral steel volumetric ratio, ρ , equal to 0.04 in specimen A1, 0.027 in A2, and 0.017 in A3. Where ρ is defined as the ratio of the volume of steel in a single ISSSB divided by the volume of the concrete in the specimen per spacing of ISSSB.

3.4 Laboratory Work and Instrumentation

In this section, a preview of the laboratory work is provided and supported with photos. All work pertaining to specimen preparation and fabrication was done in the manufacturing and structural labs at the American University of Sharjah. The first step was determining the types and quantities of materials needed and purchasing them. Then, the formwork was made for all the specimens. Afterwards, the steel cages were assembled. Two strain gauges were installed in each specimen in the middle region on two diagonally opposite longitudinal steel bars. To eliminate concentration of stresses and premature failure at the ends, two large steel jackets in the form of tubes were provided at the ends of each specimen.

The steel cages were tight-fitted inside the formwork, and two steel threaded bars were inserted laterally in the formwork through the steel cages prior to casting. These bars were used to attach the LVDTs on two opposite sides to them using clamps at one end and specially fabricated aluminum brackets at the other. The threaded bars were placed at equal distance from each end of the specimen such that the LVDTs attached to them could capture the displacement of the middle region. The distance between the threaded bars is the gauge length; it was recorded and used later to calculate the strain in the column core from the LVDT readings as a function of the applied load. Finally, the concrete was mixed in seven different batches due to the limited size of the concrete mixer. The final construction step involved casting the specimens and curing them regularly for 20 days.

3.5 Materials

3.5.1 Concrete. ASTM type I Ordinary Portland cement was used for all specimens in this study. The concrete mixes included the following constituents: 20 mm and 10 mm as coarse aggregates, crushed sand and dune sand as fine aggregates, in addition to cement, and water. The material properties of the fine and coarse

aggregates are provided in Table 6 and Table 7, respectively. The mix proportions used for the three different concrete strengths considered are provided in Table 8 per 100 kg of concrete produced. Note that the terms “weak,” “moderate,” and “strong” are relative terms used to identify the relative strengths of the different concrete used in the study.

Table 6: Material properties of fine aggregates

Parameter	Crushed sand	Dune sand
Fineness Modulus	3.51	0.74

Table 7: Material properties of coarse aggregates

Size (mm)	Apparent S.G.	Bulk S.G.	Moisture	Absorption	Crushing value	LA abrasion
10	2.70	2.84	1.18	3.99	19.1	24
20	2.73	2.64	0.78	1.16	19.8	18.6

Table 8: Mix proportions for the considered concrete mixes

Concrete strength	Coarse aggregate (kg)		Fine aggregate (kg)		Cement (kg)	Water (kg)
	20mm	10mm	Crushed	Dune		
Weak	28.49	15.37	20.97	13.95	11.28	9.94
Moderate	26.69	14.34	23.11	15.54	12.95	7.37
Strong	28.82	15.52	16.50	11.08	20.20	7.88

Due to drum size limitation of the concrete mixer, the concrete was mixed in seven different batches. The weak concrete was prepared in 3 batches, while the medium and strong concretes were prepared in 2 batches each. Several 150 mm by 300 mm cylinders were casted from each batch and tested at the same date as that on which the corresponding specimens were tested. Figure 18 shows a typical example of testing of standard concrete cylinder.



Figure 18: Testing of typical concrete cylinder

Testing of the cylinder and specimens was conducted on the same machine using the same conditions and loading rate to allow for comparison of the results later in the study. On average, the testing indicated $f'_c = 16$ MPa for the weak mix, $f'_c = 24$ MPa for the medium strength concrete mix, and $f'_c = 41$ MPa for the strong concrete mix. Figure 19, Figure 20, and Figure 21 show typical stress-strain diagrams for the three considered concrete mixes. These diagrams are used later on to obtain the different characteristics of the unconfined concrete, namely, strength, stiffness, and ductility.

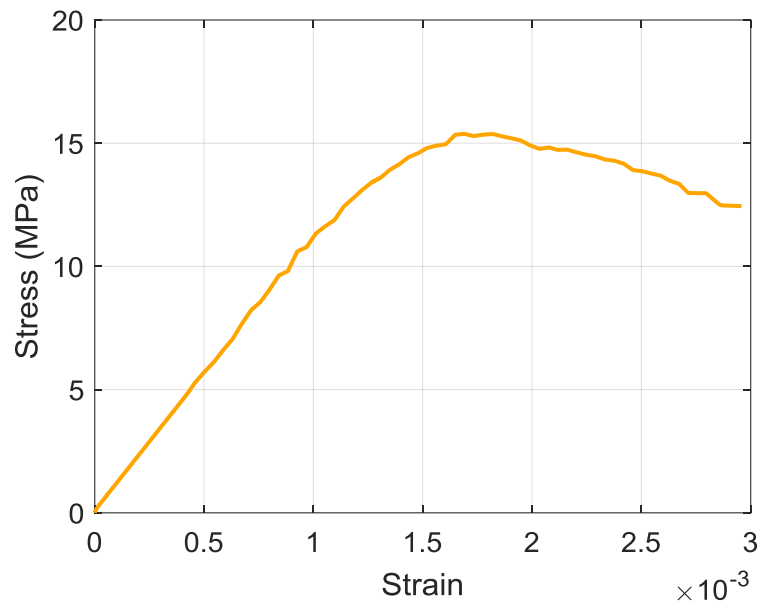


Figure 19: Stress-strain for the weak strength concrete

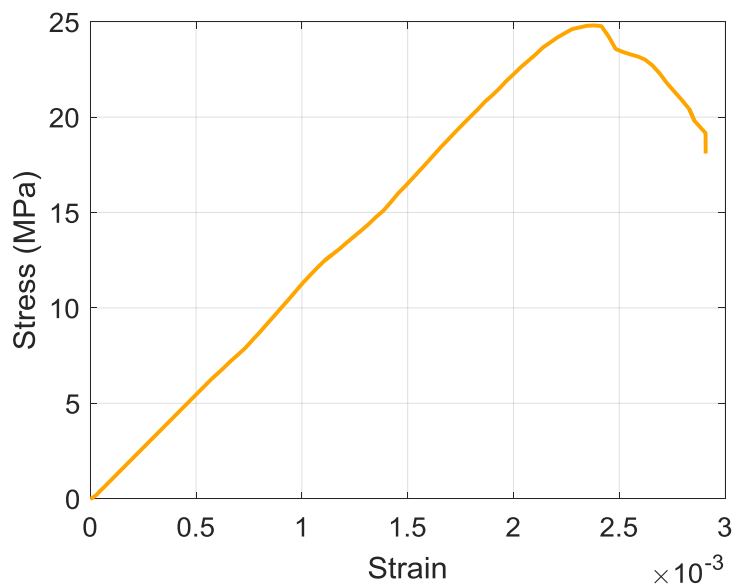


Figure 20: Stress-strain for the medium strength concrete

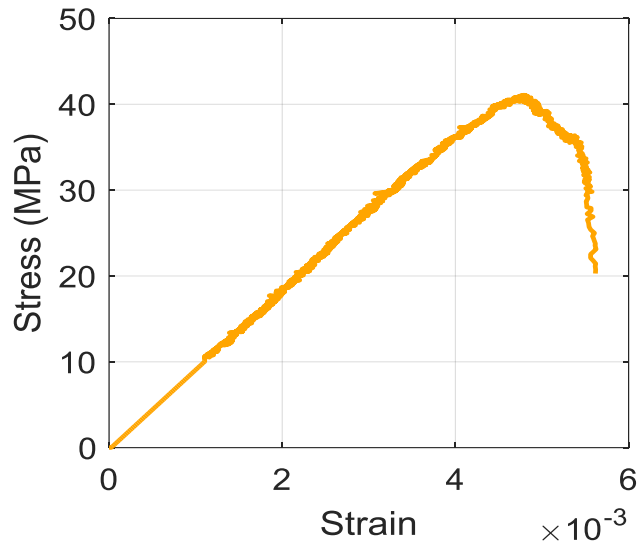
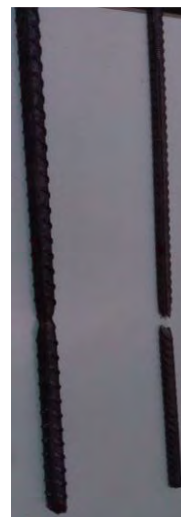


Figure 21: Stress-strain for cylinder for the strong concrete

3.5.2 Steel reinforcing bars. Steel bars with different diameters were used as ties. They include No. 6 non-deformed bars, and No. 8 and No. 10 deformed bars. The longitudinal reinforcement consisted of No. 12 deformed bars. Tensile testing was conducted on these steel bars to find their stress-strain relationships using a UTM. Figure 22 shows a typical tensile test of a steel bar, as well as fractured rebars at the end of the test. Tensile testing showed that all the deformed bars have well-defined yield point. In the case of the No. 6 non-deformed bar, there was no well-defined point of yielding, so the 0.2% method was used to approximate the yield strength of the steel.



(a) Tensile test



(b) Fractured bars

Figure 22: Testing of steel bars

Typical stress-strain diagrams for the different steel bars are presented in Figure 23 through Figure 26 below. The results demonstrated that the yield strength for the deformed bars varied within a narrow range, 540-560 MPa, and the corresponding yield strength for the non-deformed bar was much lower than those of the deformed bars because it has different specification. Moreover, all rebar tests exhibited a Young's Modulus of about 200 GPa, represented by the slope of the initial portion of the stress-strain diagram. Table 9 summarizes the results obtained from tensile testing of steel bars.

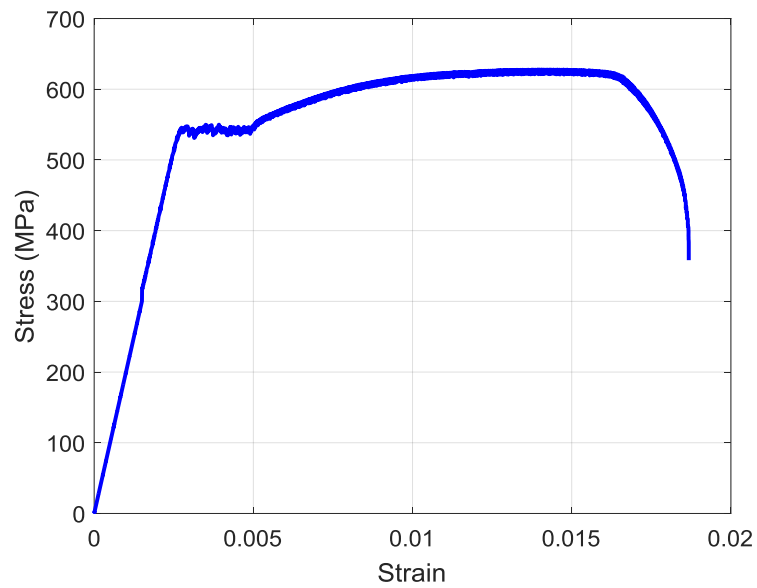


Figure 23: Stress-strain for 12 mm deformed bar

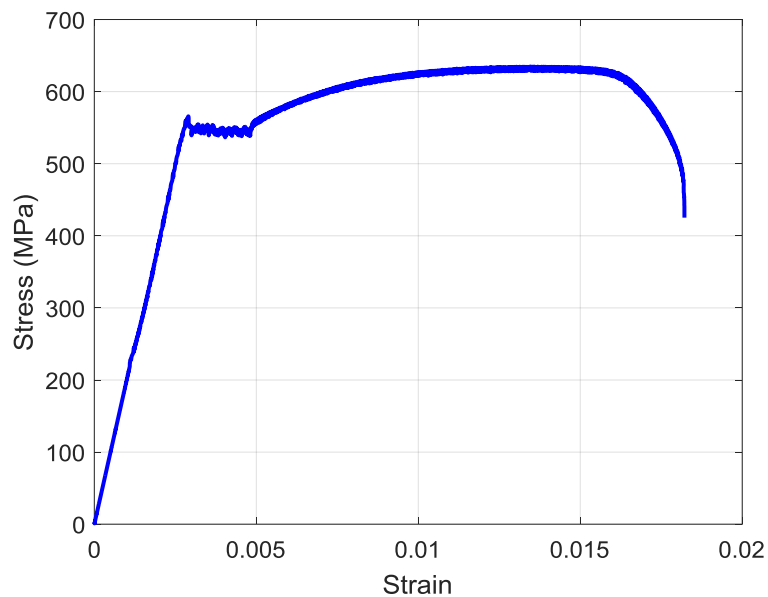


Figure 24: Stress-strain for 10 mm deformed bar

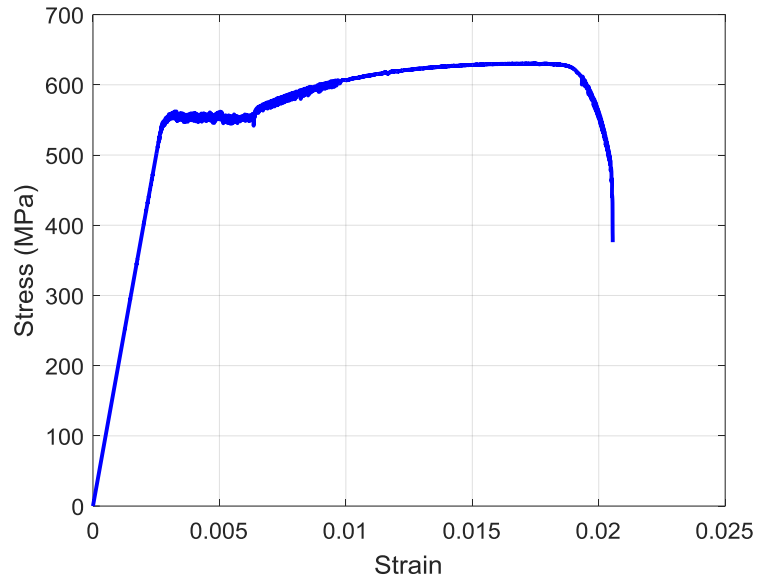


Figure 25: Stress-strain for 8 mm deformed bar

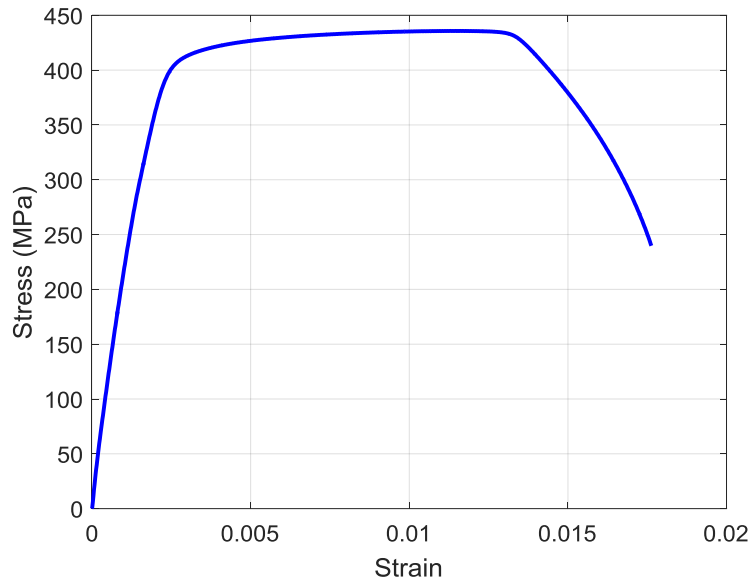


Figure 26: Stress-strain for 6 mm non-deformed bar

Table 9: Yield strength of the different steel bars

Bar diameter (mm)	Surface	F_y (MPa)
12	Deformed	540
10	Deformed	550
8	Deformed	560
6	Non-deformed	425

3.5.3 Structural steel tubes. The ISSSBs were cut from structural steel tubes. These tubes were purchased in four different configurations to satisfy the requirements of the experimental program presented in section 3.2. The dimensions of the tubes and wall thickness are shown in Table 10.

Table 10: Dimensions of steel tubes used

Tube	Shape	Cross-section dimensions		Wall thickness (mm)
		Width (mm)	Length (mm)	
1	Square	150	150	4
2	Square	150	150	3
3	Rectangular	75	150	3
4	Square	200	200	4

The strip bands that were used as transverse reinforcement to enclose the longitudinal bars in the column specimens were cut from tubes, as shown in Figure 27. Additionally dog-bone coupons were machined from the four different tubes according to the ASTM E8/E8M Standard [19] as shown in Figure 28.



Figure 27: ISSSBs cut from steel tubes



Figure 28: Steel coupon machined from Tube 4

Table 11 summarizes the results of the tensile testing conducted on the coupons. It indicates that the yield strength for all tubes varied between 310-370 MPa. Moreover, the stress-strain diagrams for the four steel tubes used for ISSSBs are produced in Figure 29.

Table 11: Yield strength of the steel tubes used as ISSSBs

Tube	f_y (MPa)
1	310
2	365
3	340
4	370

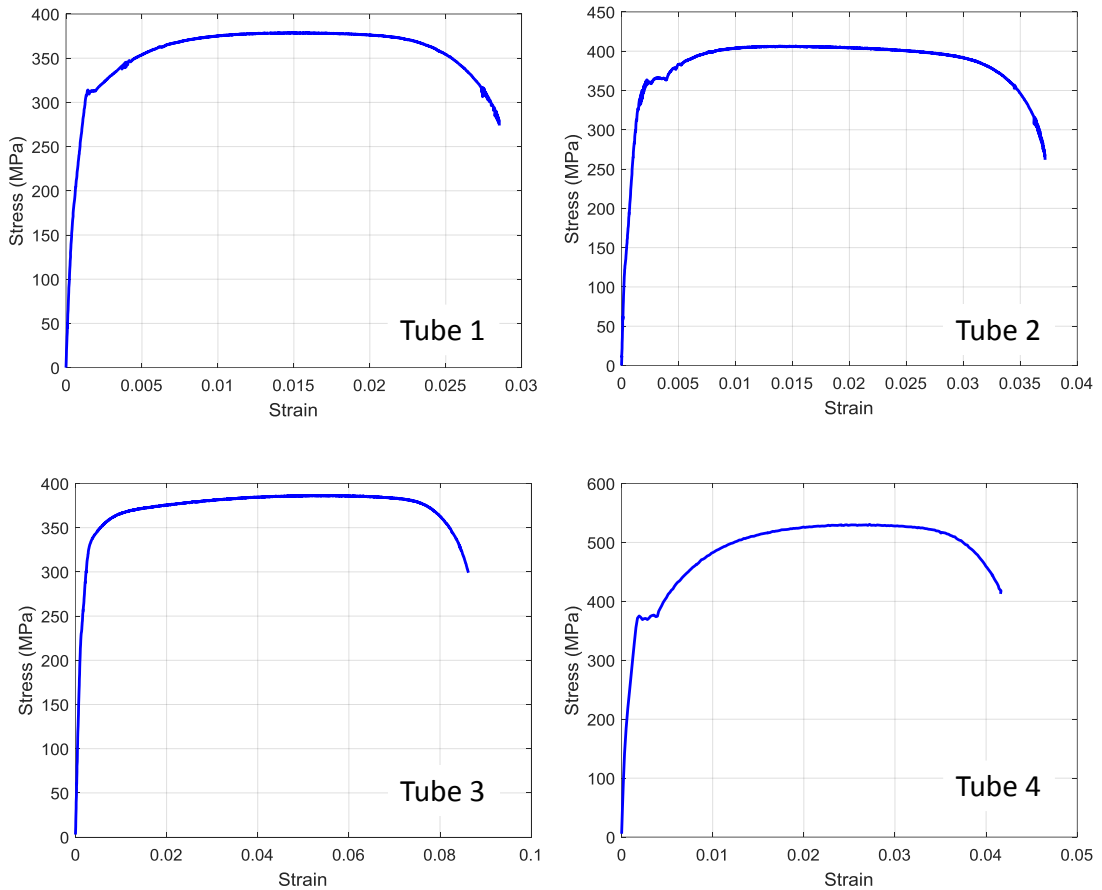


Figure 29: Stress-strain from tensile testing of Tube 1

3.6 Specimen Fabrication

Figure 30 through Figure 39 demonstrate the process of fabrication of the specimens. This process involves cutting steel to desired dimensions, welding, making end hooks, assembling the steel cage, placing end jackets, constructing the formwork, placing steel cage inside formwork, installing strain gauges on rebar, installing threaded bars through steel cage, preparing concrete constituents, mixing concrete, slump testing fresh concrete, casting concrete, and curing.



Figure 30: Making formwork in the manufacturing lab



Figure 31: Example of completed wood formwork



Figure 32: Making end hooks on ties using the steel bender



Figure 33: Cutting ISSSBs from hollow structural steel



Figure 34: Assembling and tack-welding the steel cage

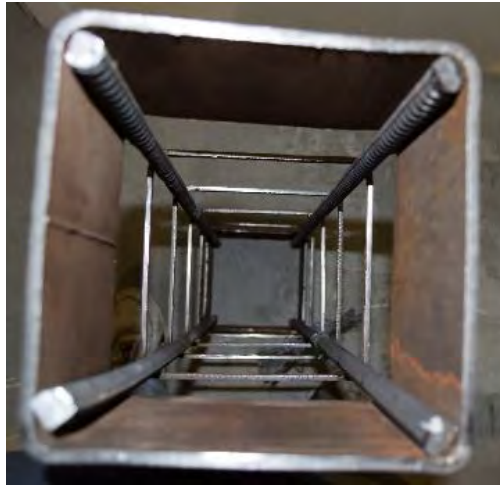


Figure 35: Top view of one ISSSB-confined specimen steel cage



Figure 36: Connecting strain gauges to longitudinal bars to a tied specimen



Figure 37: Placement of steel cages in formwork



Figure 38: Concrete mixing



Figure 39: Concrete curing



Figure 40: Painting specimens



Figure 41: Smoothing specimen ends by electric grinding

3.7 Data Acquisition

Pairs of specimens consisting of an ISSSB-confined column core and corresponding tied column core were tested on the same day. Results of the testing comprised of strain reading records from the two strain gauges fixed to the diagonally opposite longitudinal steel bars within the specimen, and displacement reading records from the two Linear Variable Differential Transformers (LVDTs) attached on two opposite sides of the specimen by means of the embedded threaded bars, as shown in Figure 42.



Figure 42: Connecting the LVDTs to the specimen

The strain gauge and LVDT measurements were recorded using a data

acquisition system synchronized with the test machine. Loading and displacement data from the actuator head were also obtained. Furthermore, a concrete cylinder from the same batch on the date of specimen testing was tested in compression by the same machine at the same loading rate. Cracking of the columns was closely monitored visually and photos of the specimens were taken during the testing at various stages of loading.

3.8 Test Setup

Before conducting the test, it was necessary to ensure that the column top and bottom surfaces were level to reduce any concentration of stresses and unintended eccentricity of the load on the specimen load which could result in premature failure. To achieve this end, care was taken to construct formwork to exact dimensions and minimum tolerances. When they were not parallel to each other, the column top and/or bottom surfaces were grinded with an electric grinder until they were horizontal and even, which was later ensured using a levelling device. All specimens were tested using the 2500 kN INSTRON Servo-hydraulic UTM Testing System in the AUS structural testing laboratory, as shown in Figure 43.

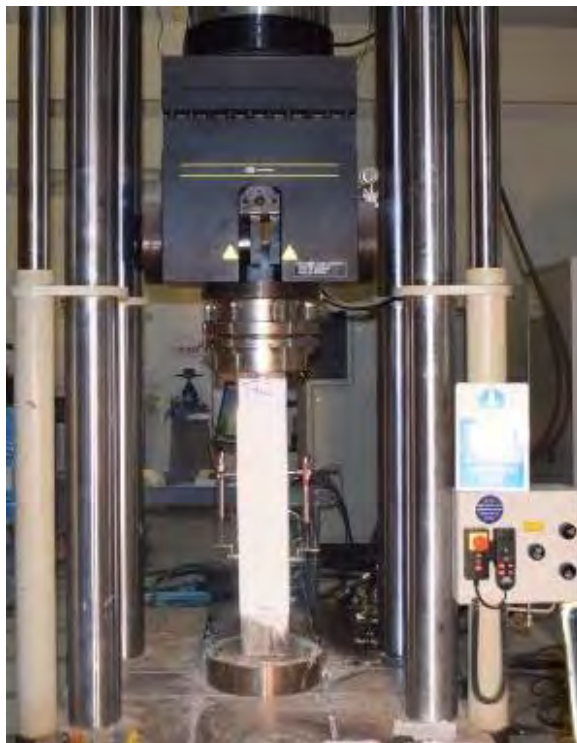


Figure 43: Test setup of specimen in the UTM

The testing was operated under displacement-controlled condition at a rate of

0.2 mm/min. This loading rate is in accordance with past studies on the subject [17, 18]. Application of the load on the specimens was continued beyond the peak on the load-displacement curve until the columns lost at least 35% of their capacity, at which point the structural condition of the specimen was deemed beyond repair. All specimens were preloaded in the elastic range up to 20% of the expected peak capacity and the LVDTs were checked to see if they had the same reading. If the displacements recorded by the LVDTs were significantly different, the specimen was horizontally moved within the test area to eliminate the unintended eccentricity imposed by the machine on the top of the column.

Chapter 4. Results

4.1 Introduction

This study investigates and compares the performance of unconfined concrete to that of concrete confined by ISSSBs or ties. The stress-strain diagram for the unconfined concrete can be obtained from the standard cylinder compression test results. The corresponding stress-strain diagram of confined concrete in the core of column specimens can be derived after filtering out the contribution of the longitudinal steel reinforcement, since in this study all column specimens were fabricated without the concrete cover. In this chapter, the process of obtaining these relationships for the concrete is explained in detail.

4.2 Stress-Strain Relationship for the Unconfined Concrete Cylinder

The specimens considered in this study were casted in seven different batches numbered I-VII. Standard concrete cylinders of height equal to 300 mm and diameter equal to 150 mm were casted from each batch and named cyl-I, cyl-II, cyl-III, cyl-IV, cyl-V, cyl-VI, and cyl-VII. Specimens and cylinders from the same batch were all tested on the same day at the same loading rate of 0.2 mm/min to later allow for meaningful comparisons. Table 12 shows the result of the concrete compressive strength of the cylinders from the seven batches. These values are obtained the average of the strength of two cylinders.

Table 12: f'_c from cylinder testing of the seven concrete batches

Batch No.	Actual f'_c (MPa)	Concrete Strength
I	15.5	weak
II	16.3	weak
III	15.9	weak
IV	40.3	strong
V	41.4	strong
VI	24.5	moderate
VII	24.8	moderate

4.3 Specimens Load-Deflection Relationships

The total applied load and the displacement as obtained from the testing machine are provided for each pair of specimens in addition to the three extra ISSSB reinforced specimens that did not have a tied counterpart. These plots allow for initial assessment of the performance of the concrete core confined by the two systems

investigated in this study.

The displacement readings of the actuator were not used in the analysis since they represent the response of the entire specimen, which include two disturbed regions at their ends. Instead, two LVDTs were installed in the middle region of each specimen at a specified gauge length to more accurately depict the behavior of the middle instrumented region away from the column jacketed ends. More detailed analysis of the behavior of the confined concrete cores is presented later in the following sections. Figure 44 through Figure 47 show the load-deflection relationships from the actuator head readings for the 25 tested column specimens. They indicate that the maximum load on the specimens generally ranged between 400 kN and 1300 kN, and the maximum displacement varied from 5 mm to 11 mm. They also show a pattern of load versus displacement behavior that is expected in reinforced concrete columns under concentric compressive loads. All columns had a clear ascending curve, a peak, and a descending curve, as none of the tests was stopped prematurely.

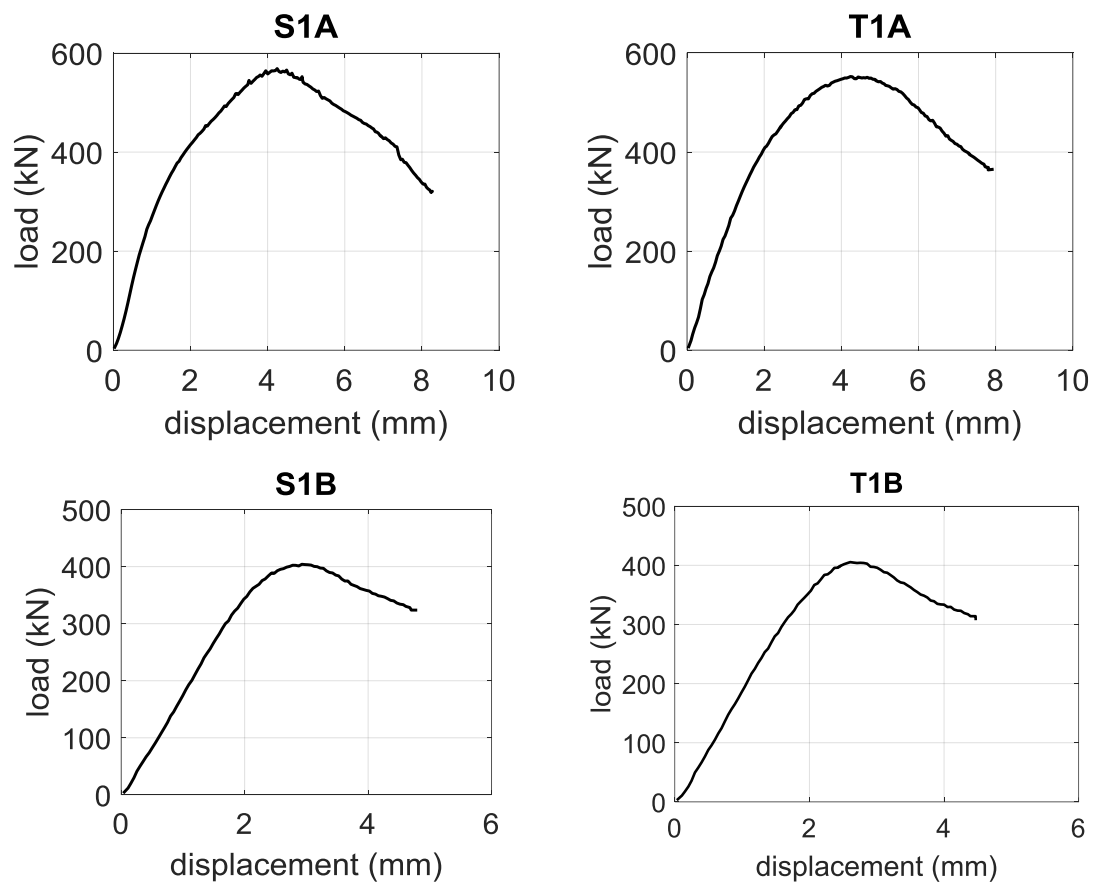


Figure 44: Load-displacement relationships for specimens 1 to 4

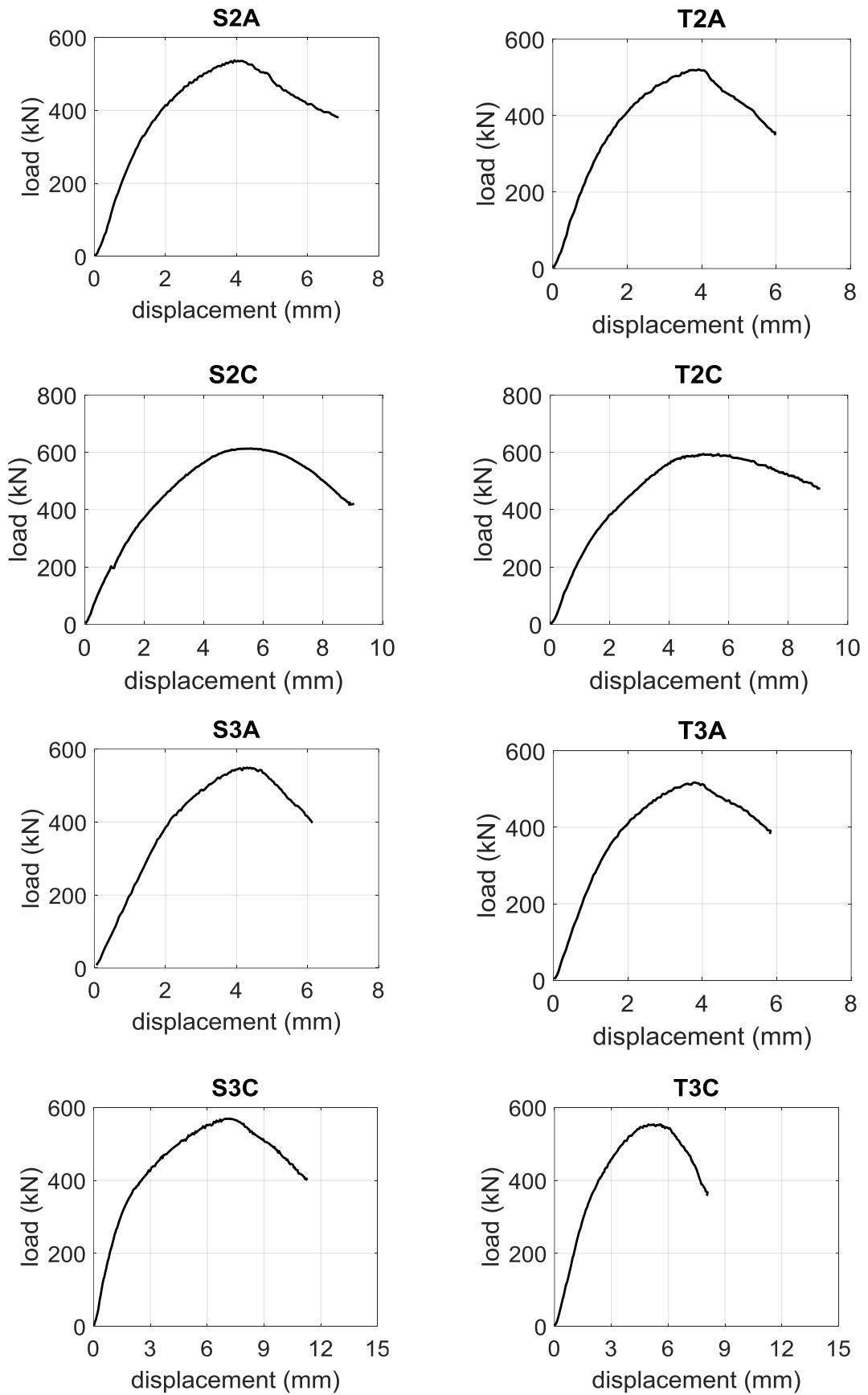


Figure 45: Load-displacement relationships for specimens 5 to 12

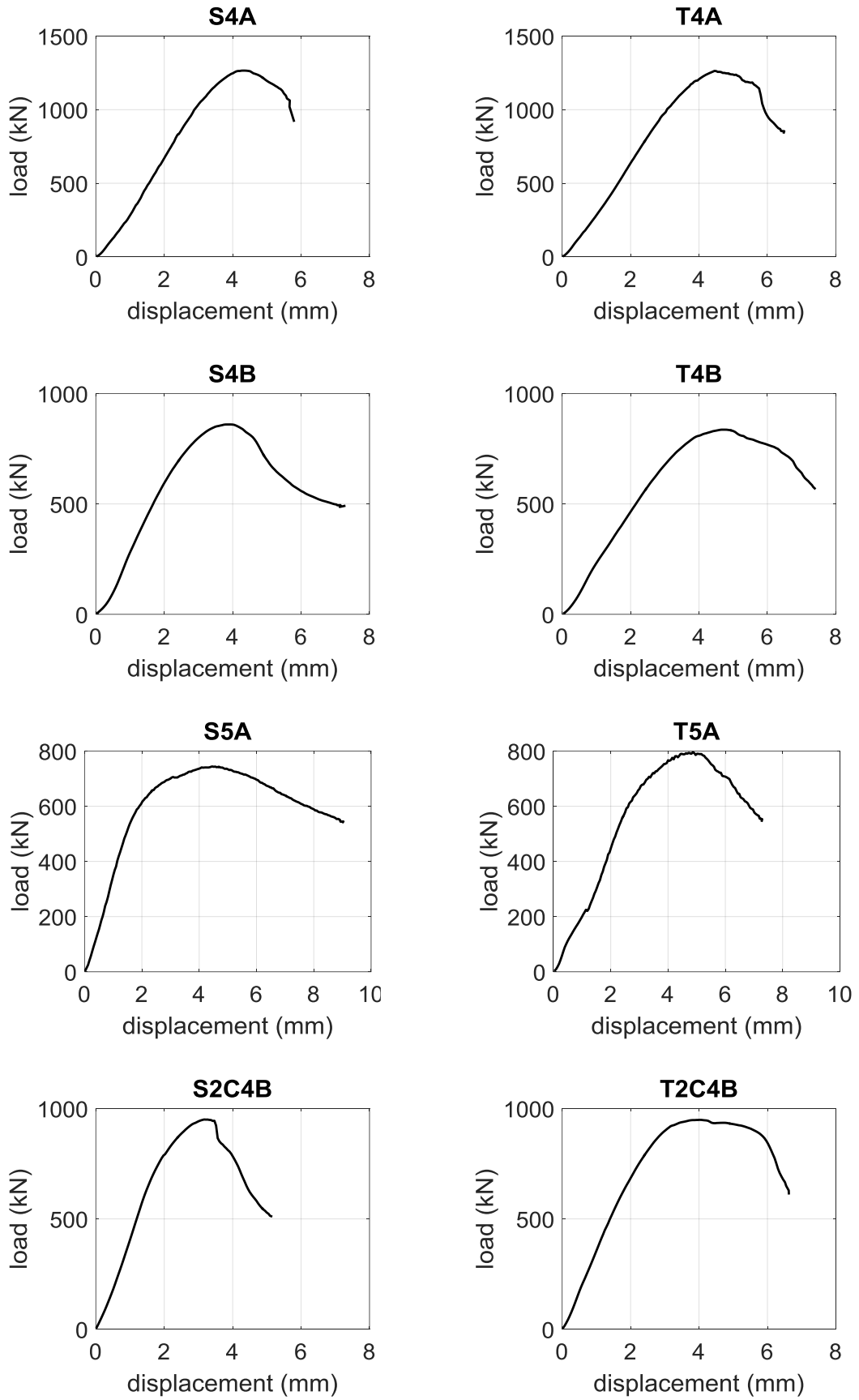


Figure 46: Load-displacement relationships for specimens 13 to 21

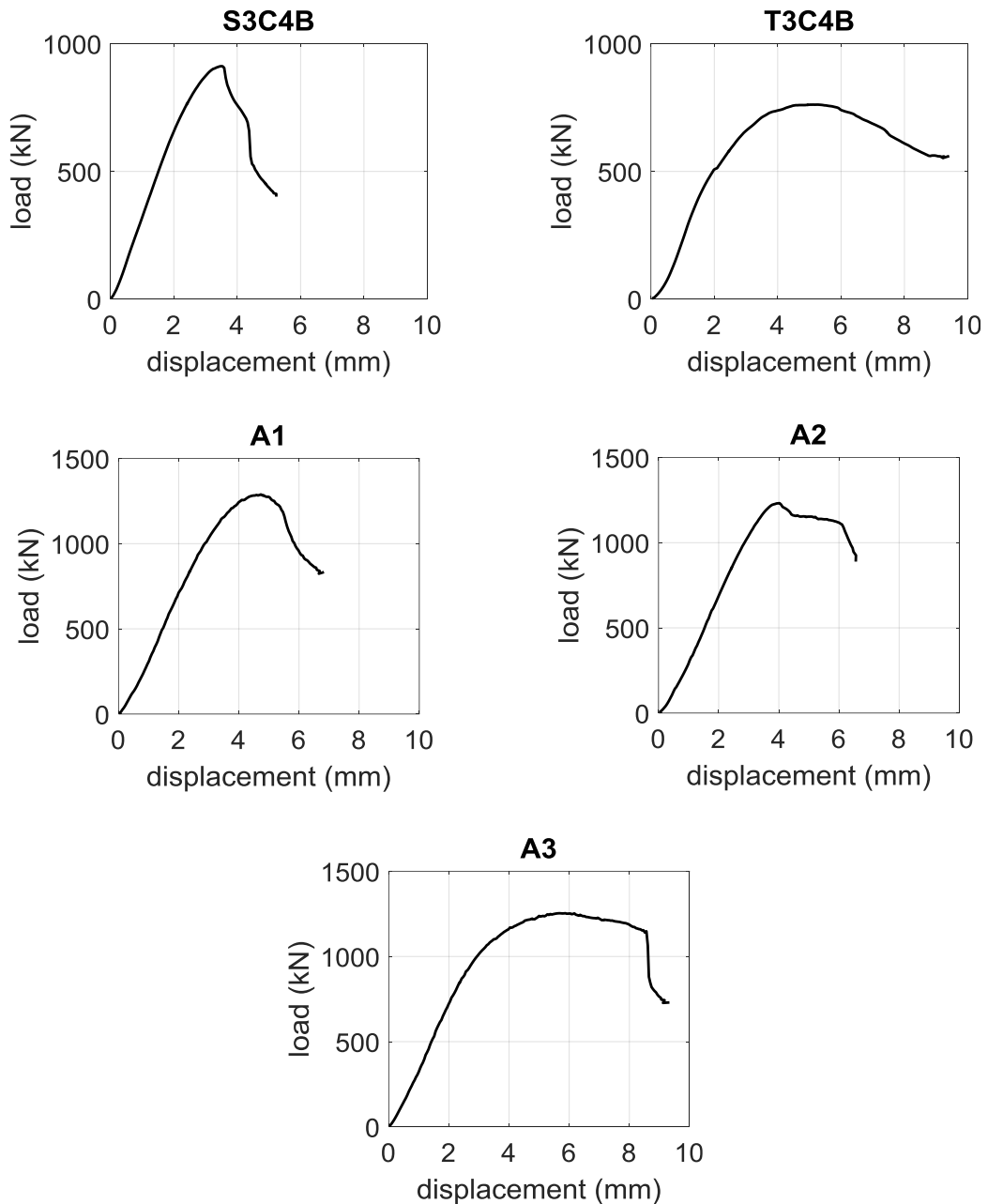


Figure 47: Load-displacement relationships for specimens 21 to 25

4.4 Strain in the Confined Concrete Core

The displacements obtained by the two LVDTs were converted to strains by means of division by the applicable gauge length. The strains from the two LVDTs were then averaged, in order to reduce any errors and minimize the effect of any bending moment resulting from imperfections in the specimens. Likewise, readings from the two strain gauges that are fixed to two longitudinal steel bars were also averaged. For illustration, Figure 48 shows a plot of the individual strains obtained

from the LVDTs and strain gauges versus the number of time steps for specimen S2C. Additionally, Figure 49 presents the corresponding averages as a function of the number of time steps for the same specimen.

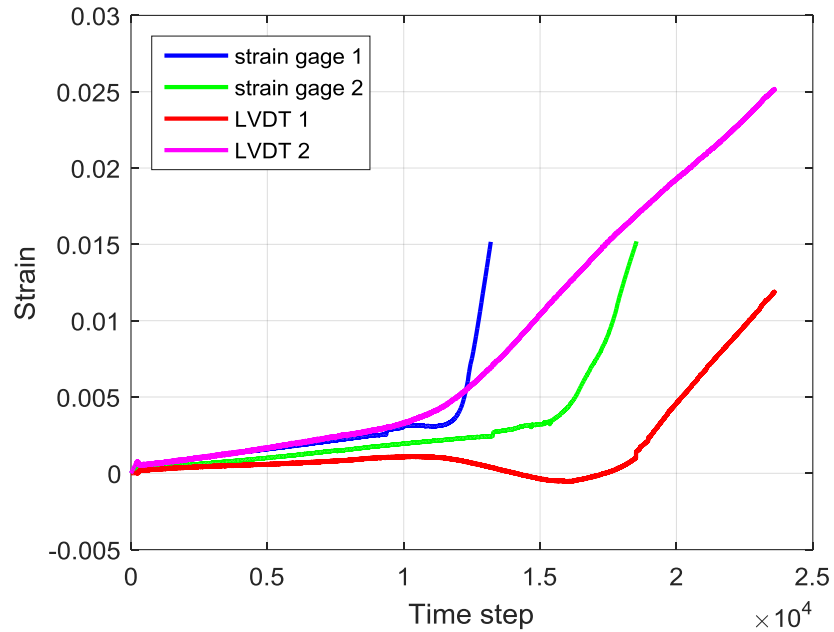


Figure 48: Individual strains against the number of time steps for S2C

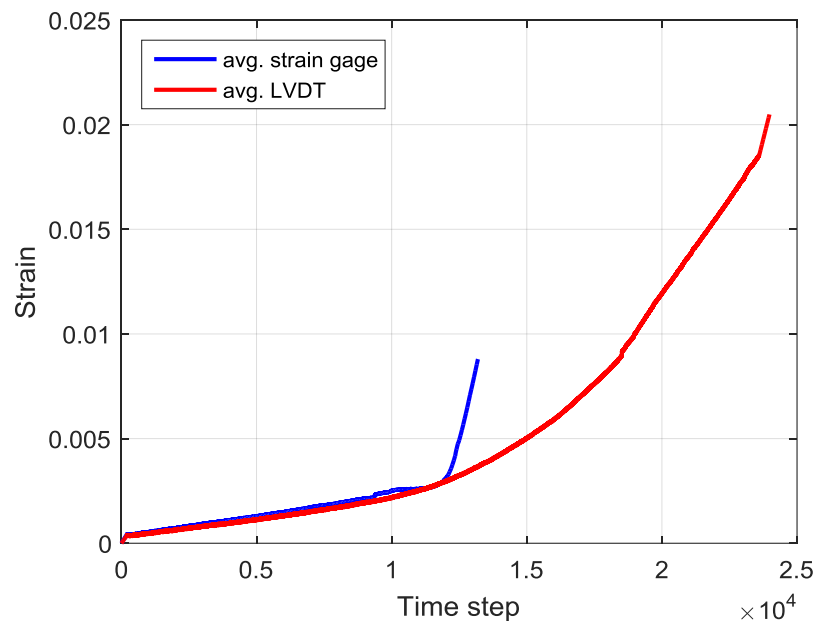


Figure 49: Average strains against the number of time steps for S2C

The same process was performed for all tested specimens and the plots of average strains against time step were produced as shown in Figure 50 to Figure 53. These plots are used to determine the onset of rebar buckling during the tests, as will be demonstrated later.

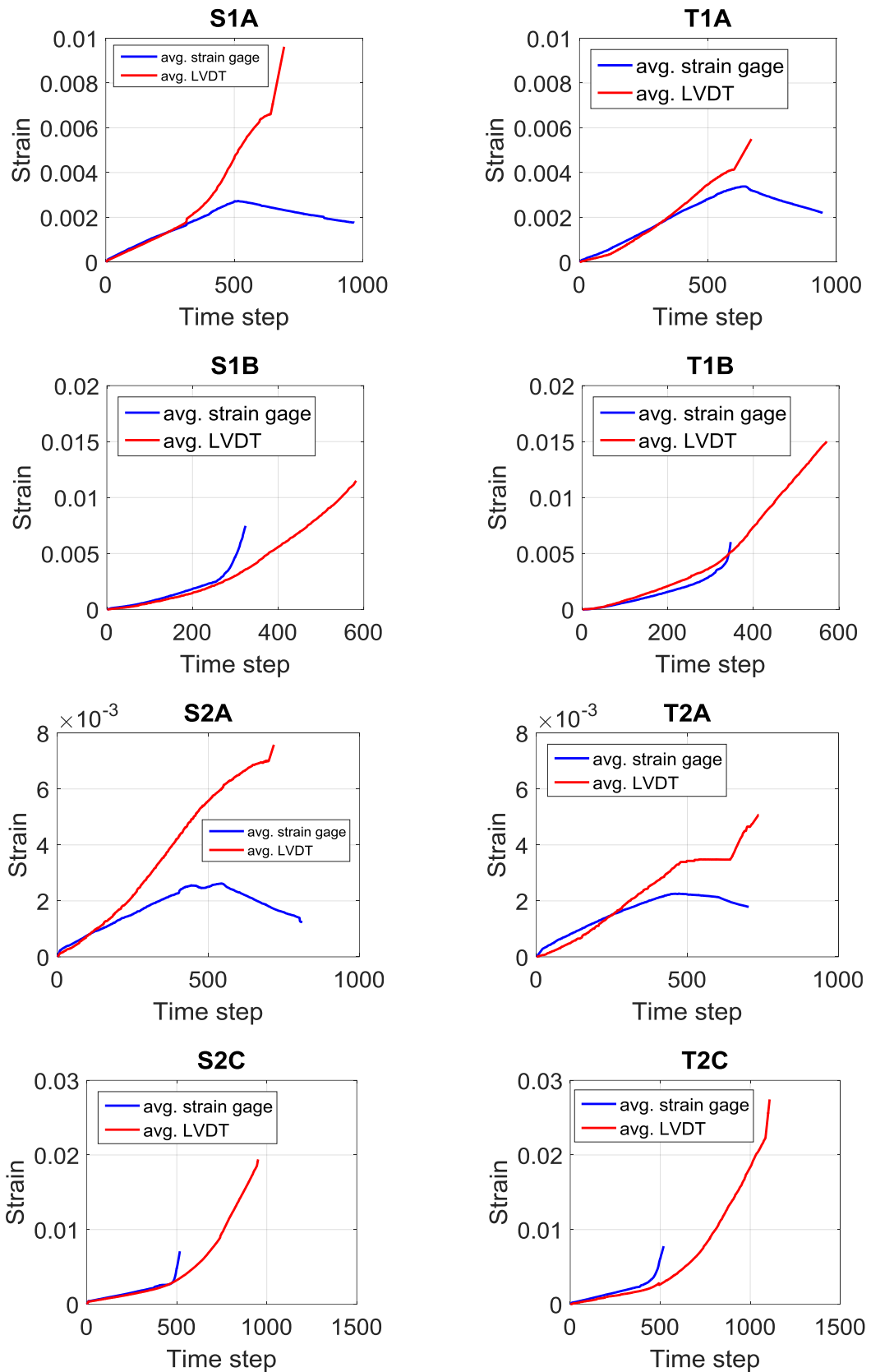


Figure 50: Average strains for specimens 1 to 8

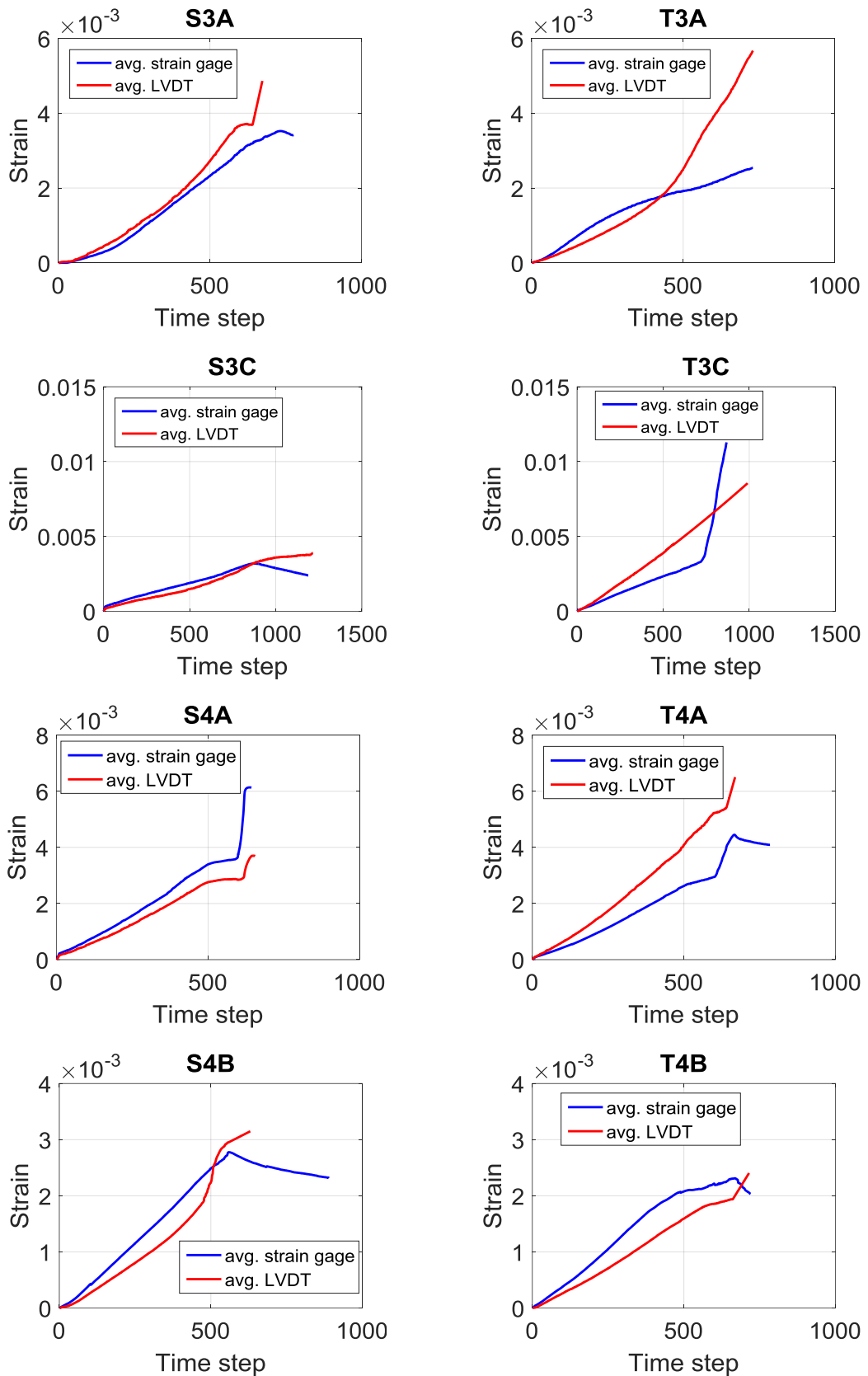


Figure 51: Average strains for specimens 9 to 16

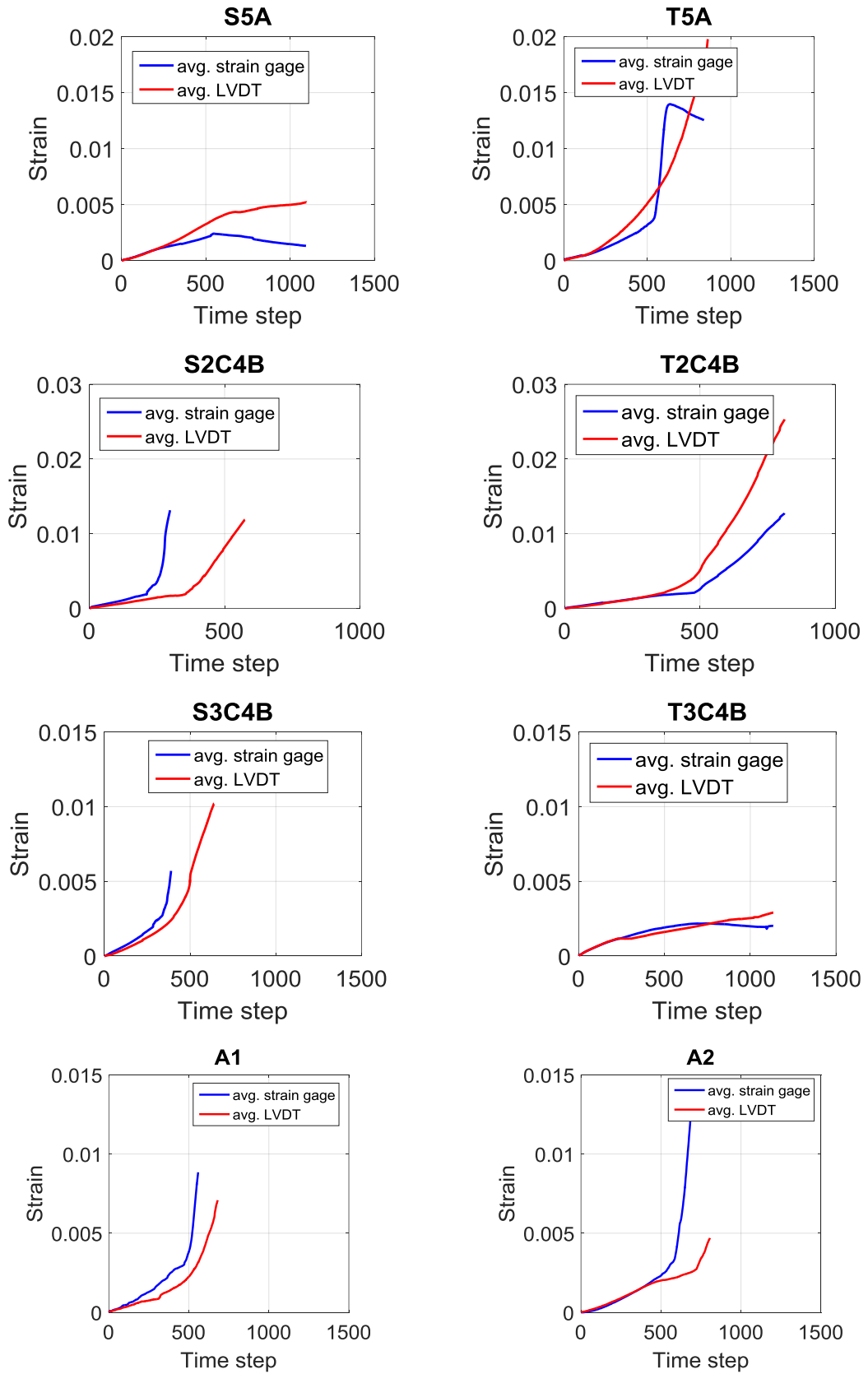


Figure 52: Average strains for specimens 17 to 24

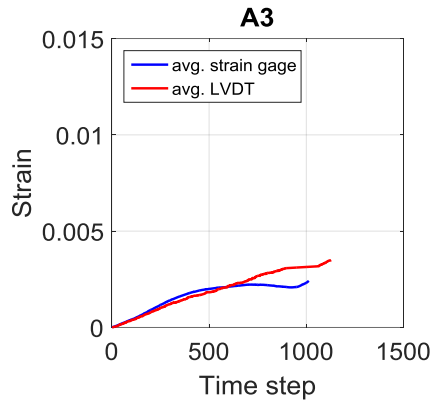


Figure 53: Average strains for specimen 25

All the results presented in Figure 50 to Figure 53 show about the same strain in the middle instrumented region depicted by the LVDTs and strain gauges; thus, confirming that there is no significant slippage between the concrete and steel. As the load was increased, some of the specimens experienced a sudden change in the strain gauge reading relative to the LVDTs. This separation between the two curves marked buckling of the longitudinal rebars. If the strain gauges were attached to the inside surface of the rebars in contact with the concrete, buckling of the rebars would cause a sudden increase in compression on that surface; thus, the strain gauge reading would sharply increase at that instant. The opposite is true if the strain gauges were attached to the outside surface of the rebars. Accounting for rebar on the performance of the concrete core within the columns is presented later. The observed strains in the concrete within the instrumented region at the onset of longitudinal rebar buckling are presented in Table 13 and Table 14 for all the tested specimens.

Table 13: Strain at buckling for the ISSSB and tied reinforced specimens

Specimen	Strain at buckling	Specimen	Strain at buckling
S1A	0.002717	T1A	0.003342
S1B	0.003169	T1B	0.003661
S2A	0.002624	T2A	0.00224
S2C	0.002992	T2C	0.003265
S3A	0.003513	T3A	NA
S3C	0.003231	T3C	0.004135
S4A	0.003475	T4A	0.00297
S4B	0.002676	T4B	0.002314
S5A	0.002387	T5A	0.004073
S2C4B	0.001997	T2C4B	0.003336
S3C4B	0.002736	T3C4B	0.002182

Table 14: Strain at buckling for the 3 extra ISSSB reinforced specimens

Specimen	Strain at buckling
A1	0.004059
A2	0.003043
A3	0.002221

The longitudinal reinforcement in all specimens consisted of No. 12 mm rebars having $f_y = 540$ MPa with a corresponding strain at yield equal 0.00270, based on a modulus of elasticity E_s equal to 200 GPa. Hence, the values found in Table 13 and Table 14 can be viewed in contrast to the strain at yield to discern whether the rebars buckled before, at, or after reaching the yield point.

With regard to the post-buckling behavior of longitudinal rebars in columns, there has been published research on the subject [20, 21]. The model developed by Dhakal et al. [22] is utilized in this study to obtain the stress-strain relationship of longitudinal rebars that buckle under compression. This model assumes that buckling always occurs at the yield point, which is not the case in this study. Thus the model had to be modified to take into account the actual point of buckling in the rebar as observed from the strain gauge readings. The modified model is shown in Figure 54.

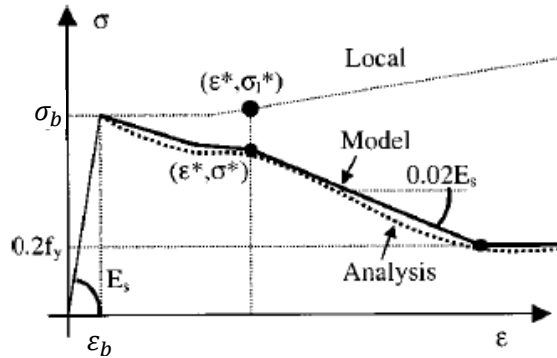


Figure 54: Modified Stress-strain model for rebars prone to buckling [22]

The modified model consists of four unique regions. The first one is the elastic region and it extends from zero to the point of buckling (ϵ_b, σ_b) . The second region extends from the point of buckling to the intermediate point (ϵ^*, σ^*) , showing a stage of moderate decay in stress. The third region has a constant negative slope equal to $0.02 E_s$ and extends until the stress is equal to $0.2 f_y$ (Where E_s is the modulus of elasticity of the steel rebar). Finally, in the last region the stress remains constant with increasing strain. The equations used to find the key point (ϵ^*, σ_l^*) shown in Figure 54 are presented following:

$$\frac{\varepsilon^*}{\varepsilon_b} = 55 - 2.3 \sqrt{\frac{f_y}{100} \frac{kL}{D}}, \varepsilon^*/\varepsilon_b \geq 7 \quad (15)$$

where ε_b is the strain at which buckling occurs, f_y is the yield strength of the rebar, k is the effective length factor, L the length of the rebar between the ISSSBs or ties, and D is the diameter of the rebar.

$$\frac{\sigma^*}{\sigma_l^*} = \alpha \left(1.1 - 0.016 \sqrt{\frac{f_y}{100} \frac{kL}{D}} \right), \sigma^* \geq 0.2 f_y \quad (16)$$

where σ_l^* is the stress corresponding to ε^* based on material model without considering buckling effect, which could be within or outside of the elastic region. Finally the stress, σ , can be found at a given strain, ε , using the expressions:

$$\frac{\sigma}{\sigma_l^*} = 1 - \left(1 - \frac{\sigma^*}{\sigma_l^*} \right) \left(\frac{\varepsilon - \varepsilon_b}{\varepsilon^* - \varepsilon_b} \right) \text{ for } \varepsilon_b < \varepsilon \leq \varepsilon^* \quad (17)$$

$$\sigma = \sigma^* - 0.02 E_s (\varepsilon - \varepsilon^*) \text{ for } \varepsilon > \varepsilon^* \text{ and } \sigma \geq 0.2 f_y \quad (18)$$

where σ_l is the stress based on material model without considering buckling effect.

When comparing the observed strain values in the longitudinal bars at buckling with $\varepsilon_y = 0.00270$, it is found that there are three possible scenarios for the stress-strain behavior of the longitudinal reinforcement. The first scenario is when the longitudinal bars buckle before reaching the yield point. The second scenario is when the rebars reach yield and then buckle. The final scenario is when the longitudinal steel rebars do not buckle throughout the entire test. Figure 55, Figure 56, and Figure 57 show the stress-strain behavior for the three stated scenarios. Note that the measured strains on the unbuckled longitudinal steel reinforcement showed that strain-hardening was not reached in all cases.

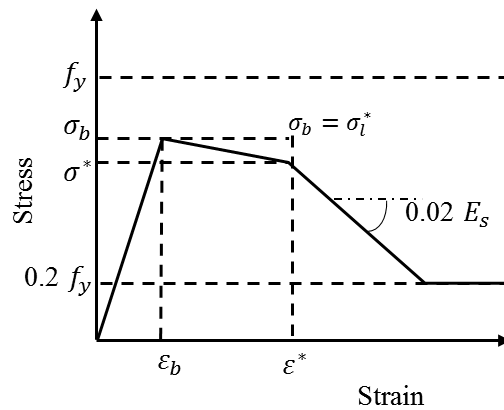


Figure 55: Steel rebar that buckles before reaching yield

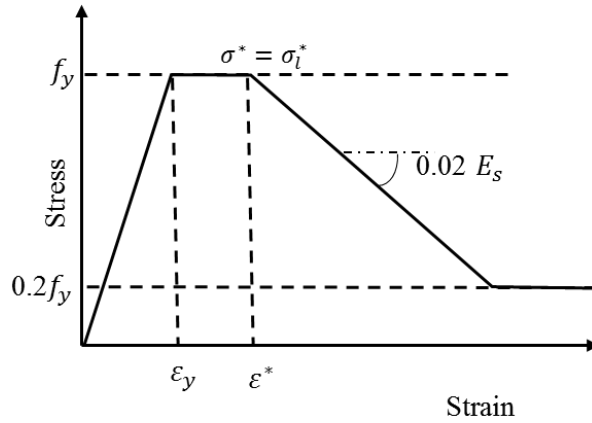


Figure 56: Steel rebar that buckles after reaching yield

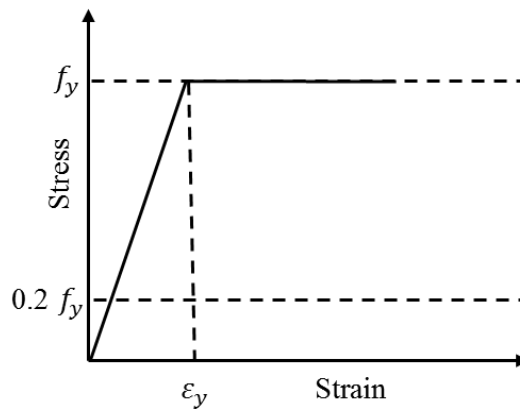


Figure 57: Steel rebar that does not buckle

4.5 Stress-Strain Relationship of the Confined Concrete Core

In this section, the stress-strain relationships for confined concrete in the column core are developed for ISSSB and tied specimens. To do so, the contribution of the longitudinal rebars in carrying a fraction of the load on the specimen must be filtered out. Several calculations had to be made in order to obtain the stress-strain relationship for the concrete core. First of all, the force in the longitudinal steel had to be determined. This was achieved in two steps. For the elastic range, Hooke's Law was utilized:

$$\sigma_s = E \varepsilon \quad (19)$$

where E is Young's Modulus (200 GPa), and ε is the strain.

Beyond the elastic range, the model discussed in Section 4.4 was used to obtain the stress in the longitudinal steel rebars as they could yield, buckle, or go through both phases. Here, stress-strain diagrams for the bars were constructed based

on the status of each bar with regard to buckling. Then the force taken by the steel bars at a given instant during the test was obtained by multiplying the computed stress by the area of the bars. All the specimens in this study had four deformed No. 12 bars with a total area equal to 452 mm².

Figure 58 shows the force taken by the longitudinal steel reinforcement versus the recorded strain for specimen S4A. Note that the longitudinal rebars in this specimen experienced buckling shortly after they started yielding. This is indicated on the diagram by the flat top of the curve between the yield strain of 0.0027 and the buckling strain of 0.003475.

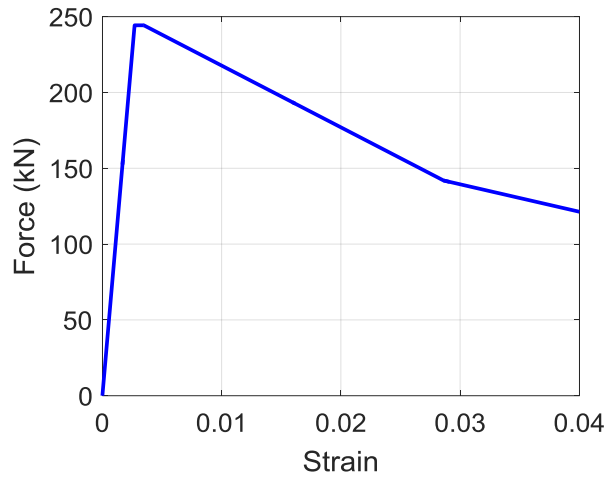


Figure 58: Force against strain in longitudinal rebar in S4A

Next, the force in the steel was filtered out from the total applied load on the specimen to give the load that is resisted by the concrete in the core. This filtering was done by subtracting the force in the steel from the total applied load by the machine:

$$P_{cc} = P_{tot} - P_{steel} \quad (20)$$

where P_{cc} is the load applied on the concrete in the core, P_{tot} is the total load applied by the machine's actuator, and P_{steel} is the load borne by the longitudinal steel reinforcement bars. Finally, the load P_{cc} was converted into stress by division over the area of concrete in the core. The area of the concrete in the core (A_{cc}), is given by:

$$A_{cc} = A_{tot} - A_{steel} \quad (21)$$

where A_{tot} is the gross area of the column core, and A_{steel} is the total area of longitudinal steel which is equal to 416 mm² in this study.

The stress-strain diagrams for the concrete in the column core were constructed for all the tested specimens. It is these final diagrams that are to be assessed and analyzed to evaluate the performance of the two confinement systems under consideration. As an example, one such stress-strain diagram of the concrete in the core is presented in Figure 59 for specimen S4A.

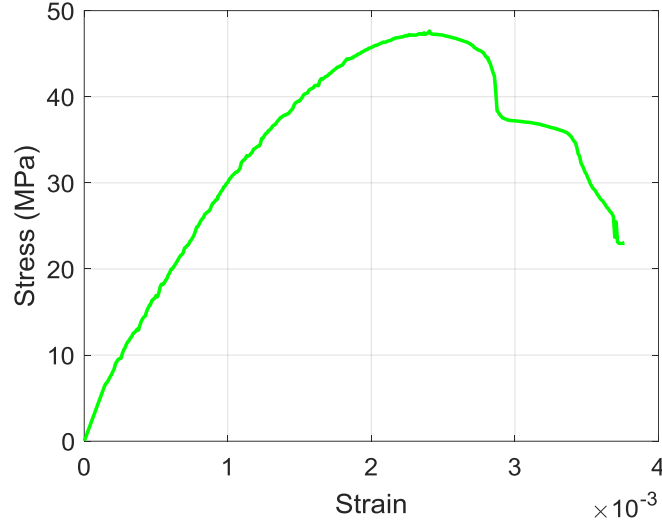


Figure 59: Stress in the concrete core vs. strain for specimen S4A

4.6 Concrete Performance Criteria

Three key properties were designated as criteria for the evaluation of the performance of the confined concrete in the column cores. These are strength, stiffness, and ductility. Strength is defined as the highest stress level reached by the concrete core during testing. The strength enhancement factor, S , is introduced to judge the effectiveness of the confinement method in enhancing the concrete strength, relative to unconfined concrete:

$$S = \frac{f'_{cc}}{f'_c} \quad (22)$$

where f'_{cc} is the peak stress of the confined concrete core and f'_c is the peak stress of the unconfined standard concrete cylinder.

Stiffness is defined as the slope of the initial straight segment of the stress-strain diagram, which is equal to Young's Modulus of Elasticity. The stiffness enhancement factor, K , is defined as the ratio of the modulus of elasticity of confined concrete to that of unconfined concrete:

$$K = \frac{E_{cc}}{E_c} \quad (23)$$

where E_{cc} and E_c are the Young's Moduli for the transversely confined concrete and the unconfined standard concrete cylinder, respectively.

Ductility of a specimen indicates its ability to sustain some resistance beyond the peak stress and can be measured in different ways. In this study, the ductility, μ , of a type of concrete is defined as follows:

$$\mu = \frac{\varepsilon_{0.85_post}}{\varepsilon_{0.85_pre}} \quad (24)$$

where $\varepsilon_{0.85_post}$ is the strain at 85% of the peak stress on the descending branch of the stress-strain curve and $\varepsilon_{0.85_pre}$ is the strain at 85% of the peak stress on the ascending branch. The ductility enhancement factor, D , is then defined as the ratio of the ductility of the specimen to the ductility of the corresponding cylinder as follows:

$$D = \frac{\mu_{cc}}{\mu_c} \quad (25)$$

where μ_{cc} is the ductility of the ISSSB or tie confined concrete and μ_c is the ductility of the unconfined concrete obtained from the cylinder test.

To calculate the three concrete performance factors S , K , and D for the concrete core in the specimens confined with ISSSBs and ties, the software packages Excel and Matlab were utilized. The strength of a specimen was found by fitting the nearby region within the crest of the stress-strain diagram with a parabola and then finding its maximum value. This was necessary because some specimens did not exhibit a smooth relationship between the stress and strain near the peak. The modulus of elasticity was found by fitting the stress-strain diagram of the concrete with a line from the points at 15% of peak stress to 55% of the peak stress along the vertical axis and then finding the slope of that line. The strains required for the calculation of D were also found with the help of the software.

4.7 Results

Photos of all the specimens during the conducted experimental tests are

included in Table 15 to Table 25. The photos show the status of the specimens roughly at 90% of the peak load on the ascending branch of the load-deflection relationship, at the peak load, and also at about 90% of the peak load in the descending stage. They are intended to demonstrate the crack formation patterns and the mode of failure occurring in the specimens in the vicinity of the maximum load.

The resulting stress-strain diagrams for the concrete in the core of each pair of specimens are shown in Figure 60 through Figure 70 consisting of one ISSSB-confined column (shown in green) and the corresponding tied column (shown in pink). The pertinent cylinder is also included in these plots (shown in orange). The stress-strain results of the ISSSB confined concrete, tie confined concrete and unconfined concrete cylinder are presented in one graph to facilitate comparisons among them. Additionally, individual stress-strain diagrams are provided. Note that pair S1A-T1A is equivalent to pairs S2B-T2B, S3B-T3B, S4C-T4C, and S5B-T5B, as explained earlier in Section 3.3.1 on the discussion of repeated specimens. Results of repeated pairs are not reproduced below as they are deemed redundant; however, they are discussed and analyzed in the Chapter 5.

Table 15: Condition of specimen pair S1A-T1A during testing

At 90% of peak load ↑	At peak load	At 90% of peak load ↓
		
		

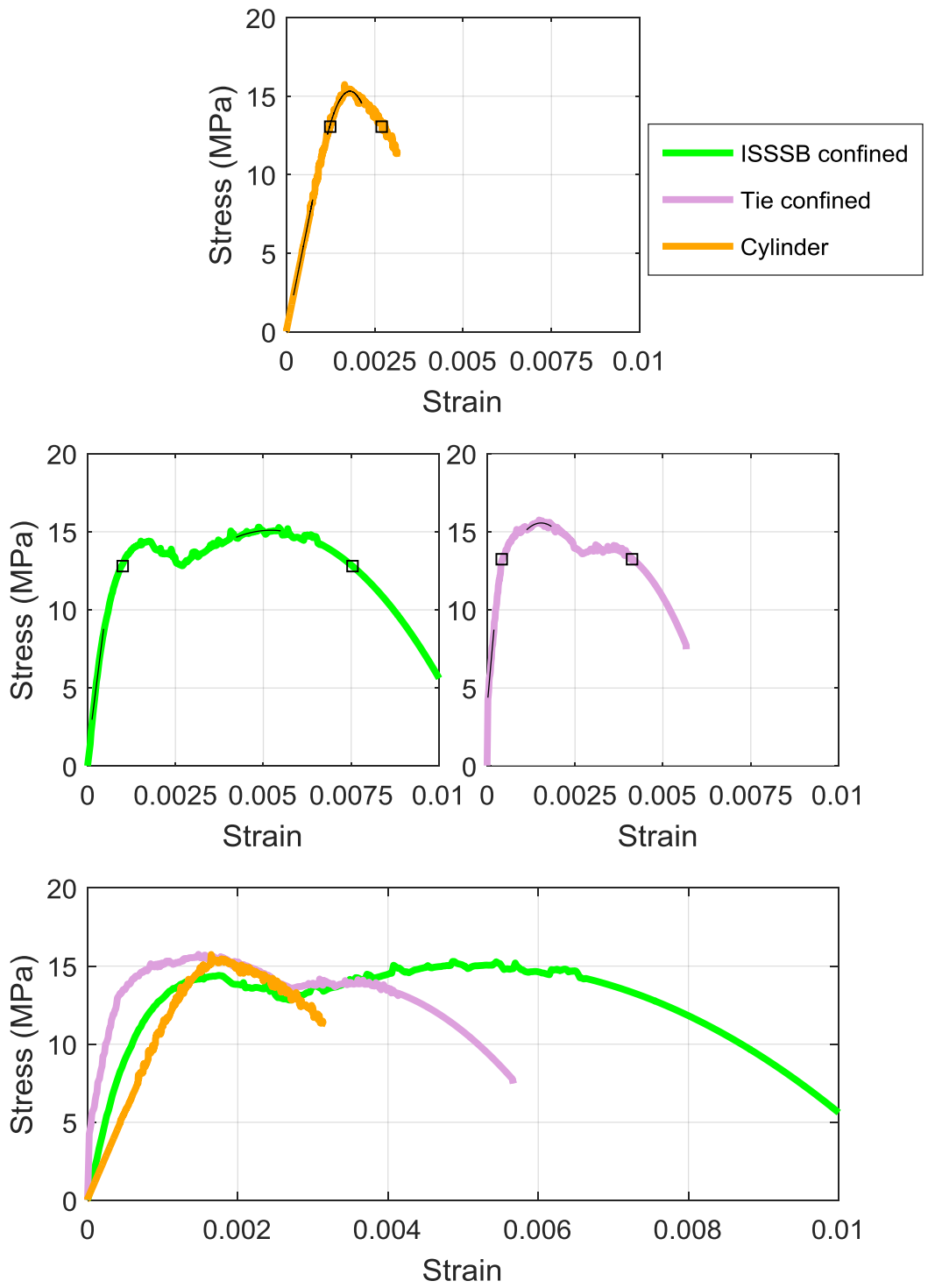


Figure 60: Stress-strain for S1A-T1A and the corresponding cylinder

Table 16: Condition of specimen pair S1B-T1B during testing

At 90% of peak load ↑	At peak load	At 90% of peak load ↓
		
		

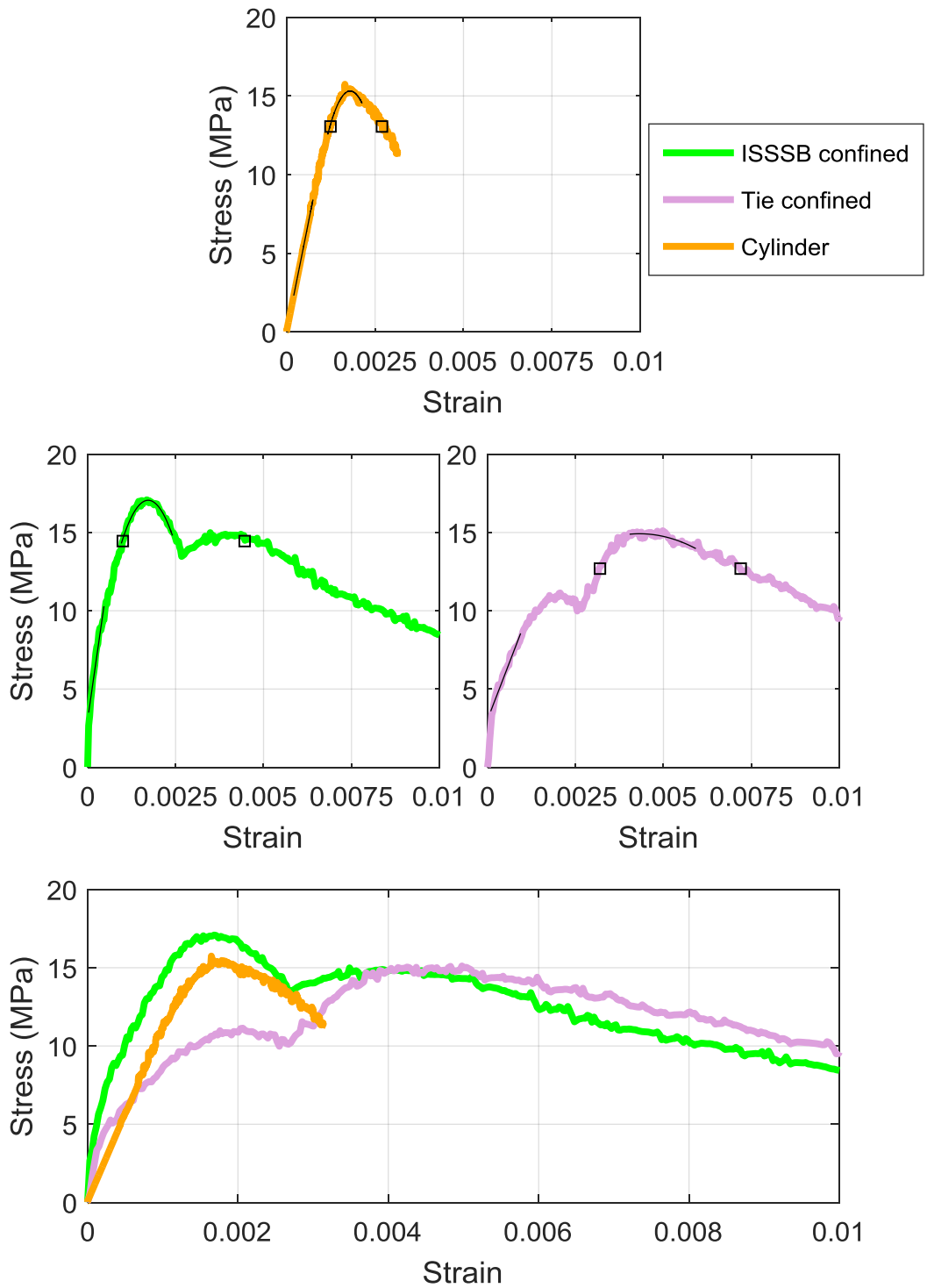


Figure 61: Stress-strain for S1B-T1B and the corresponding cylinder

Table 17: Condition of specimen pair S2A-T2A during testing

At 90% of peak load ↑	At peak load	At 90% of peak load ↓
<p>Photograph of specimen S2A during testing at 90% of peak load with an upward load. The specimen is a vertical concrete column with a steel reinforcement cage. A label at the bottom indicates a load of 500 kN with an upward arrow. The specimen is marked with 'S2A' and 'S2A I'.</p>	<p>Photograph of specimen S2A during testing at peak load with an upward load. A label at the bottom indicates a load of 540 kN with an upward arrow. The specimen is marked with 'S2A' and 'S2A I'.</p>	<p>Photograph of specimen S2A during testing at 90% of peak load with a downward load. A label at the bottom indicates a load of 500 kN with a downward arrow. The specimen is marked with 'S2A' and 'S2A I'.</p>
<p>Photograph of specimen T2A during testing at 90% of peak load with an upward load. A label at the bottom indicates a load of 500 kN with an upward arrow. The specimen is marked with 'T2A' and 'T2A I'.</p>	<p>Photograph of specimen T2A during testing at peak load with an upward load. A label at the top indicates a load of 520 kN with an upward arrow. The specimen is marked with 'T2A' and 'T2A I'.</p>	<p>Photograph of specimen T2A during testing at 90% of peak load with a downward load. A label at the top indicates a load of 450 kN with a downward arrow. The specimen is marked with 'T2A' and 'T2A I'.</p>

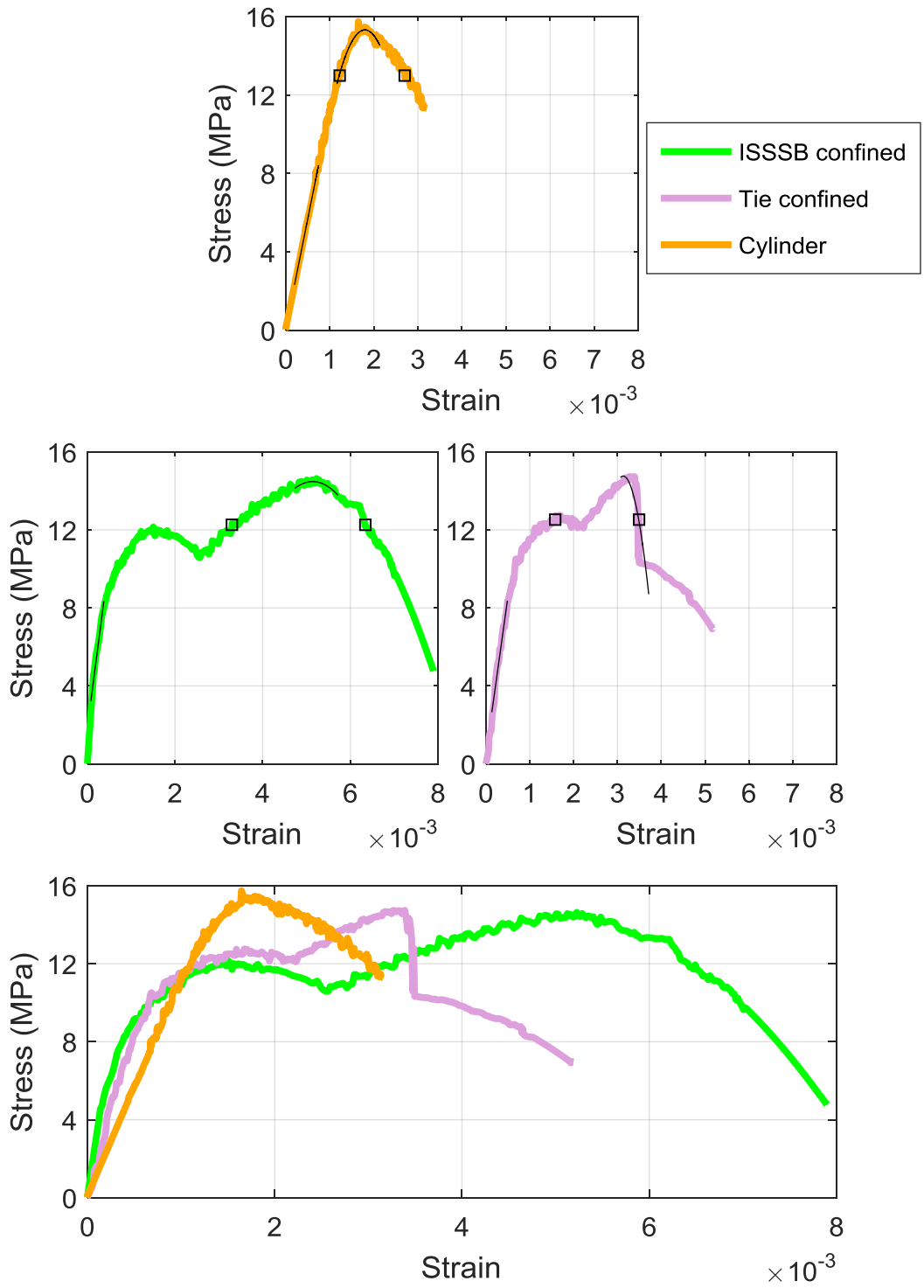


Figure 62: Stress-strain for S2A-T2A and the corresponding cylinder

Table 18: Condition of specimen pair S2C-T2C during testing

At 90% of peak load ↑	At peak load	At 90% of peak load ↓
<p>Specimen S2C at 90% of peak load (upward). The specimen is a vertical cylindrical concrete column with a white paper label at the bottom indicating 550 kN and an upward arrow. Red markings 'H' and 'S2C' are visible on the concrete surface.</p>	<p>Specimen S2C at peak load. The specimen shows significant concrete spalling and damage. A white paper label at the bottom indicates 615 kN and an upward arrow. Red markings 'H' and 'S2C' are visible.</p>	<p>Specimen S2C at 90% of peak load (downward). The specimen shows concrete damage. A white paper label at the bottom indicates 550 kN and a downward arrow. Red markings 'H' and 'S2C' are visible.</p>
<p>Specimen T2C at 90% of peak load (upward). The specimen is a vertical cylindrical concrete column with a white paper label at the bottom indicating 550 kN and an upward arrow. Red markings 'H' and 'T2C' are visible.</p>	<p>Specimen T2C at peak load. The specimen shows significant concrete spalling and damage. A white paper label at the bottom indicates 595 kN and an upward arrow. Red markings 'H' and 'T2C' are visible.</p>	<p>Specimen T2C at 90% of peak load (downward). The specimen shows concrete damage. A white paper label at the bottom indicates 540 kN and a downward arrow. Red markings 'H' and 'T2C' are visible.</p>

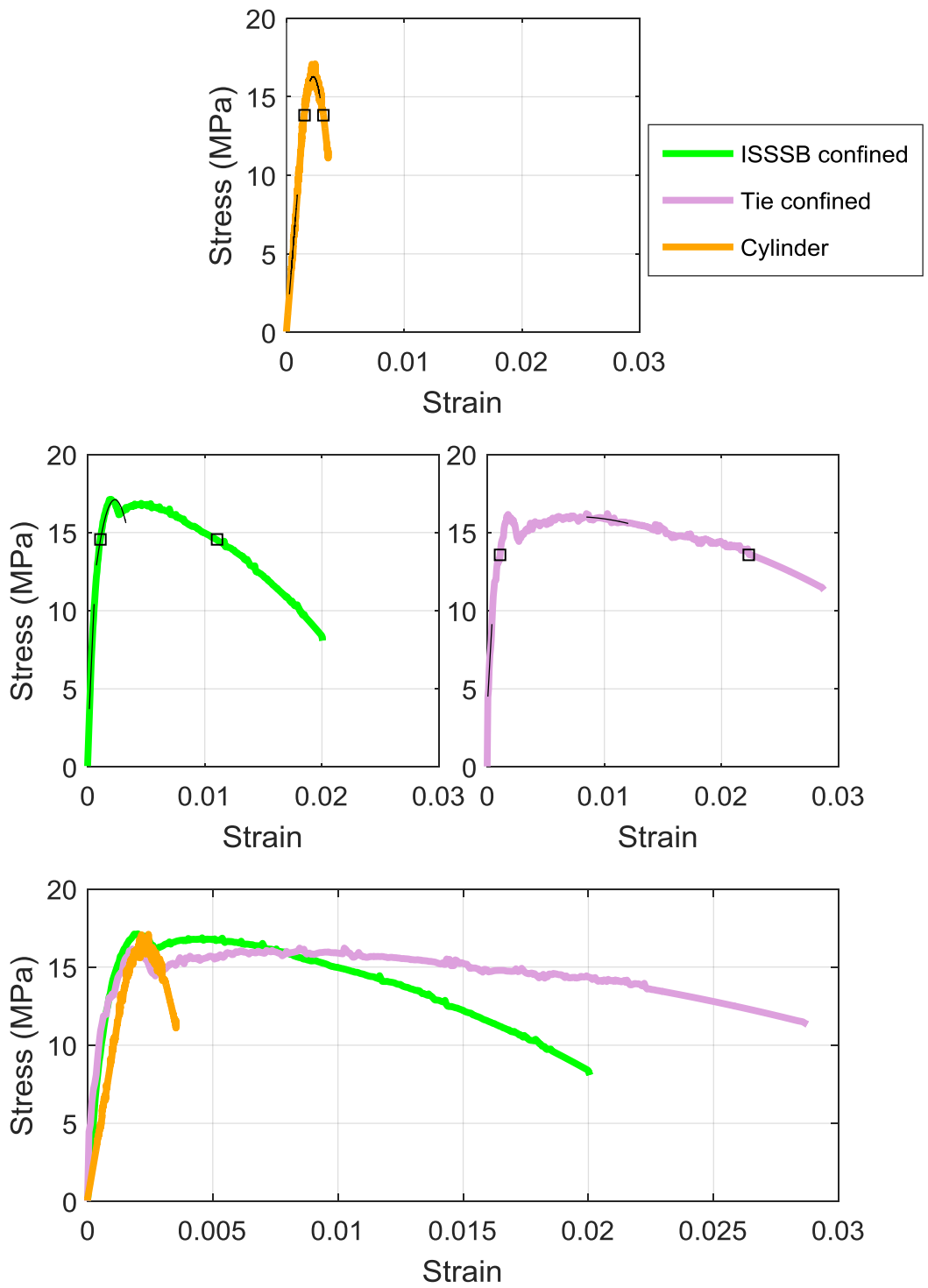


Figure 63: Stress-strain for S2C-T2C and the corresponding cylinder

Table 19: Condition of specimen pair S3A-T3A during testing

At 90% of peak load ↑	At peak load	At 90% of peak load ↓
		
		

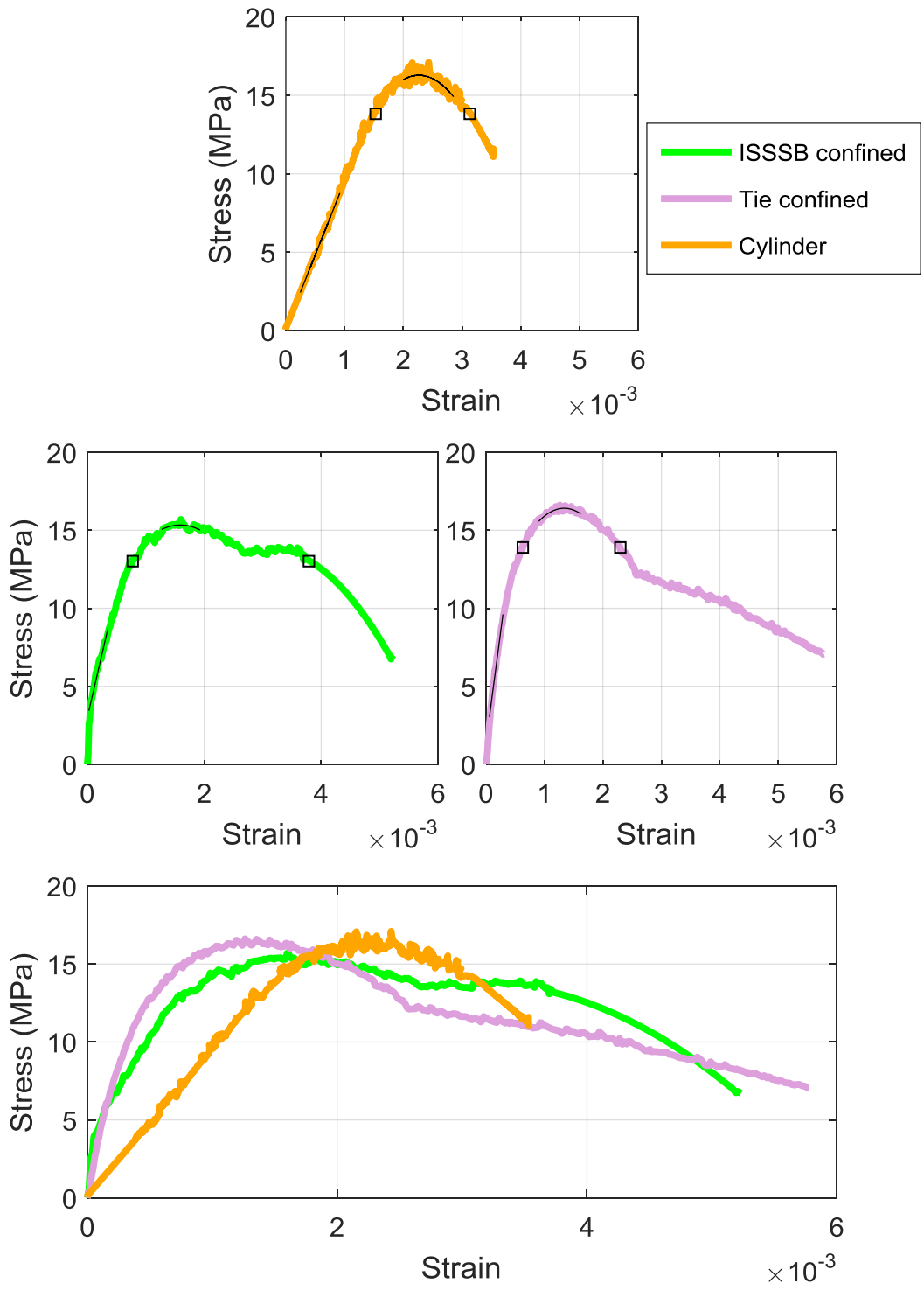




Figure 64: Stress-strain for S3A-T3A and the corresponding cylinder

Table 20: Condition of specimen pair S3C-T3C during testing

At 90% of peak load ↑	At peak load	At 90% of peak load ↓
		
		

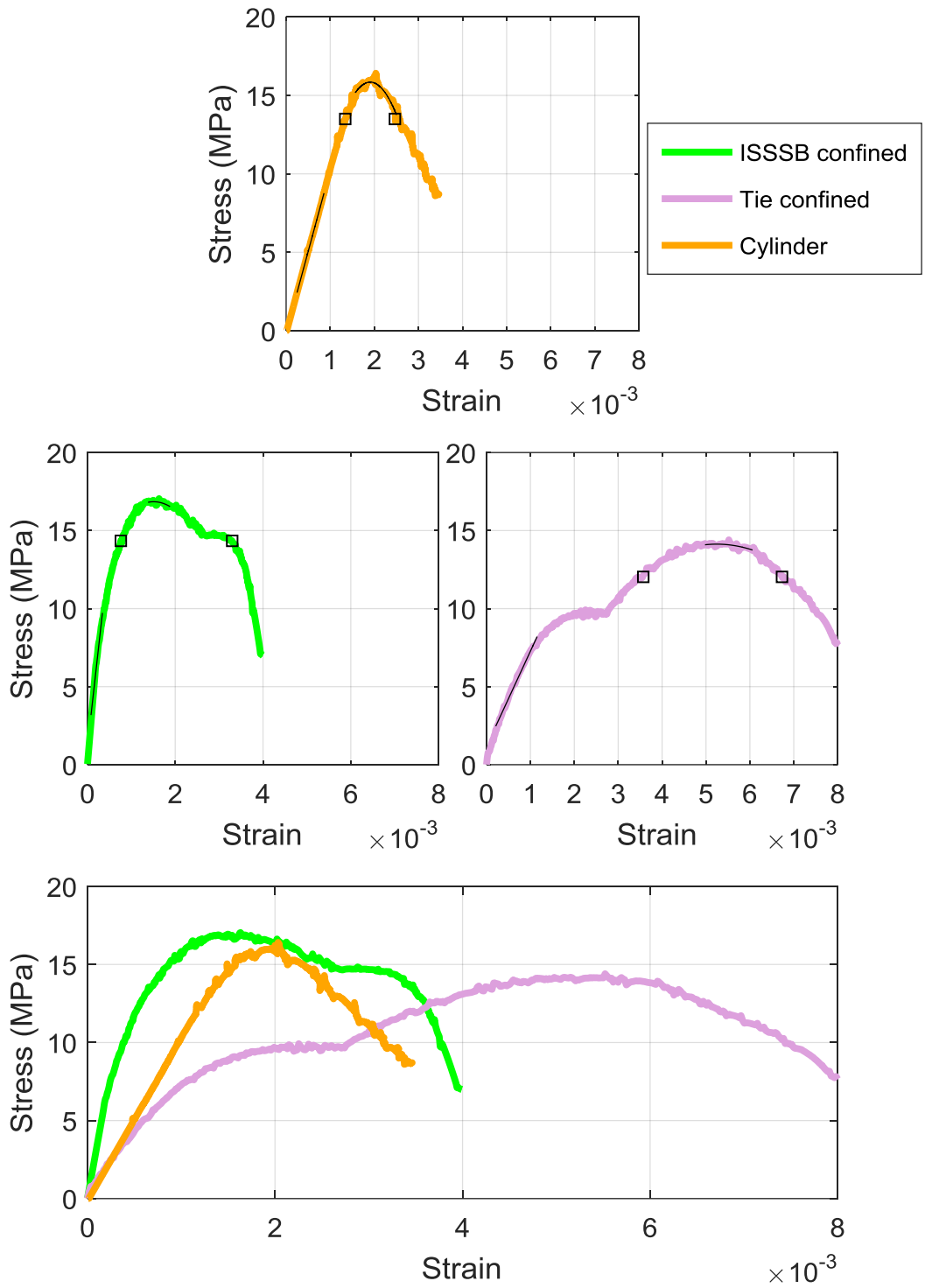






Figure 65: Stress-strain for S3C-T3C and the corresponding cylinder

Table 21: Condition of specimen pair S4A-T4A during testing

At 90% of peak load ↑	At peak load	At 90% of peak load ↓
		
		

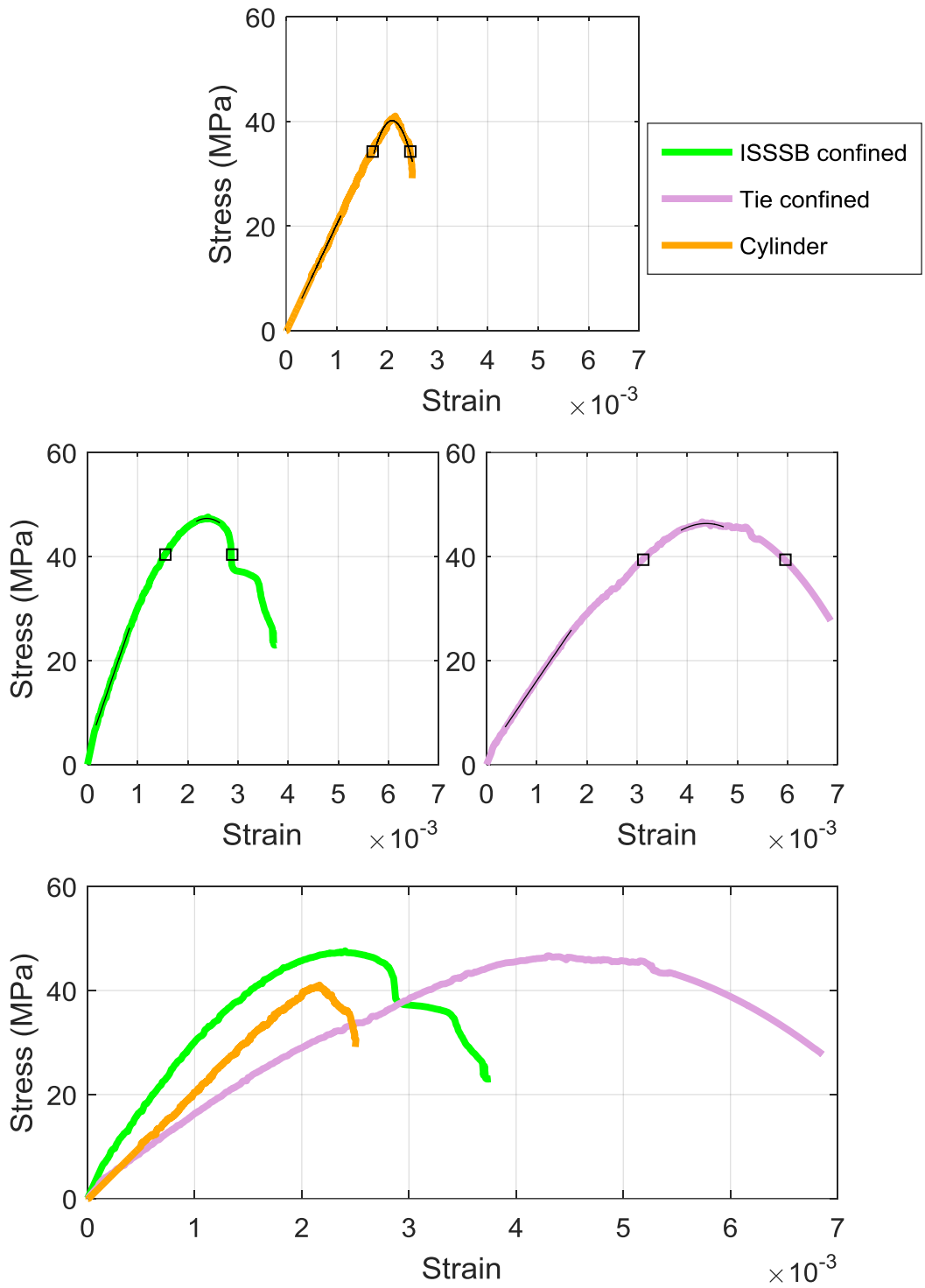


Figure 66: Stress-strain for S4A-T4A and the corresponding cylinder

Table 22: Condition of specimen pair S4B-T4B during testing

At 90% of peak load ↑	At peak load	At 90% of peak load ↓
 <p>S4B</p>	 <p>S4B</p>	 <p>S4B</p>
 <p>T4B</p>	 <p>T4B</p>	 <p>T4B</p>

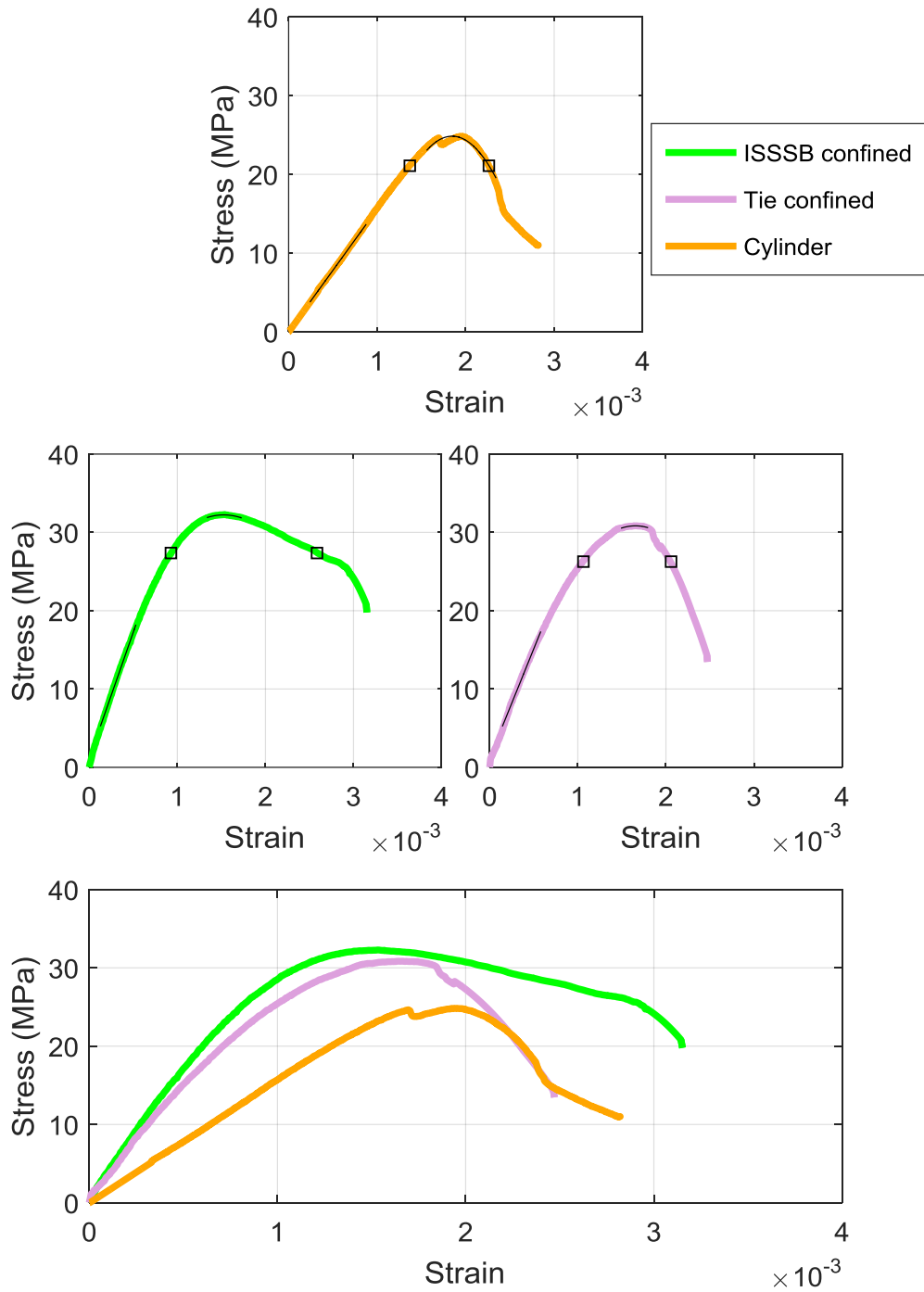


Figure 67: Stress-strain for S4B-T4B and the corresponding cylinder

Table 23: Condition of specimen pair S5A-T5A during testing

At 90% of peak load ↑	At peak load	At 90% of peak load ↓
		
		

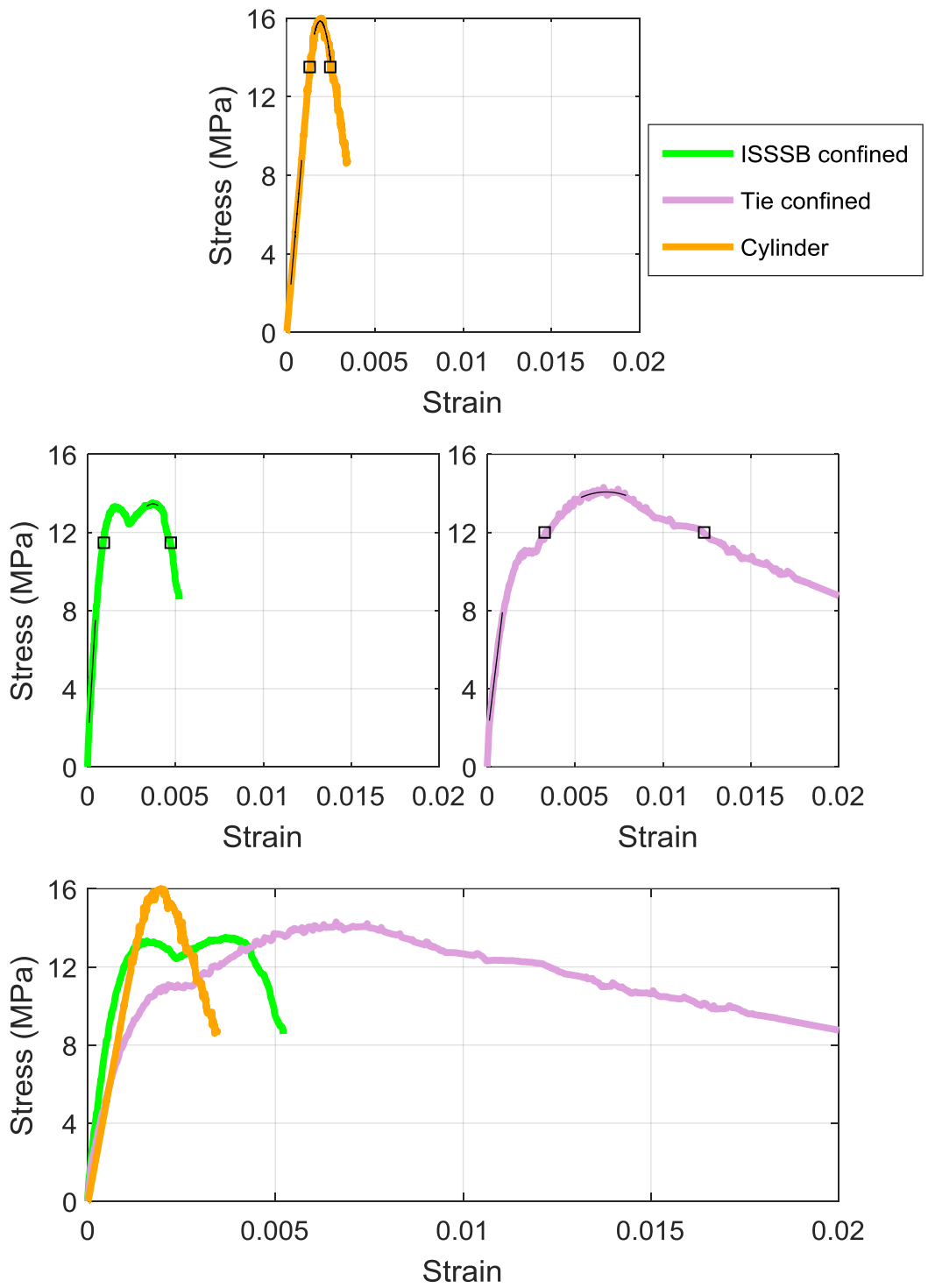


Figure 68: Stress-strain for S5A-T5A and the corresponding cylinder

Table 24: Condition of specimen pair S2C4B-T2C4B during testing

At 90% of peak load ↑	At peak load	At 90% of peak load ↓
		
		

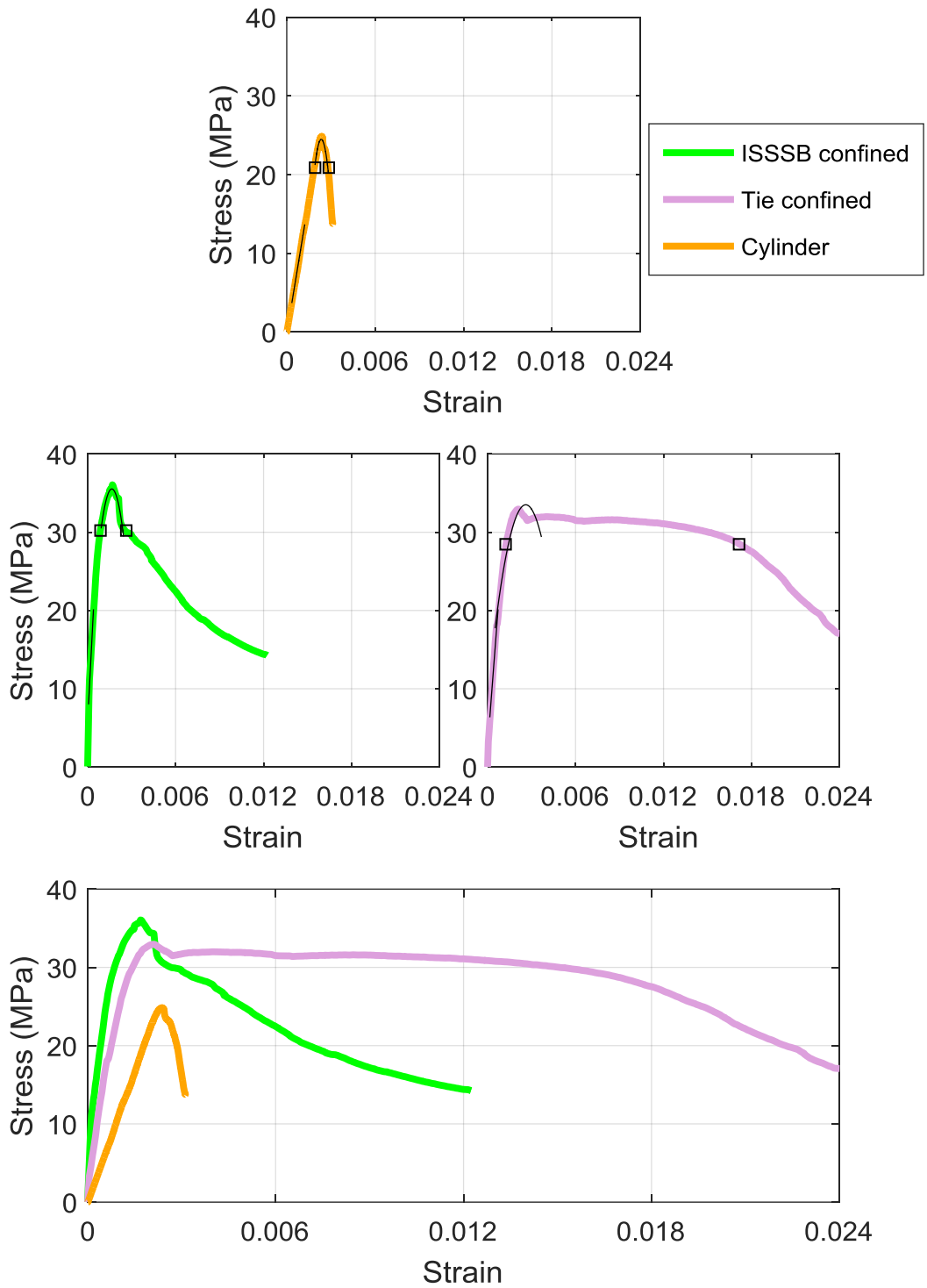








Figure 69: Stress-strain for S2C4B-T2C4B and the corresponding cylinder

Table 25: Condition of specimen pair S3C4B-T3C4B during testing

At 90% of peak load ↑	At peak load	At 90% of peak load ↓
		
		

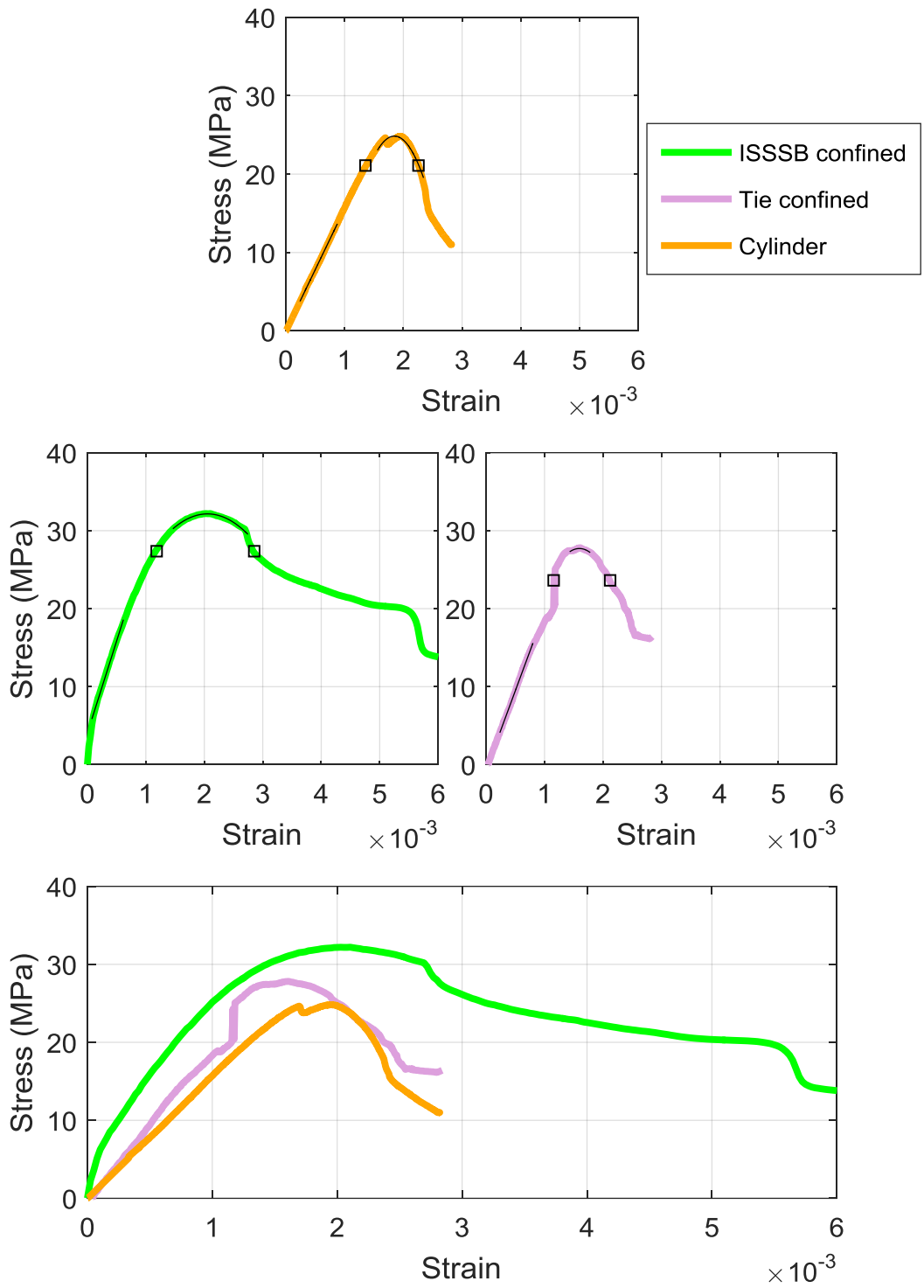


Figure 70: Stress-strain for S3C4B-T3C4B and the corresponding cylinder

Table 26: Condition of specimen A1 during testing

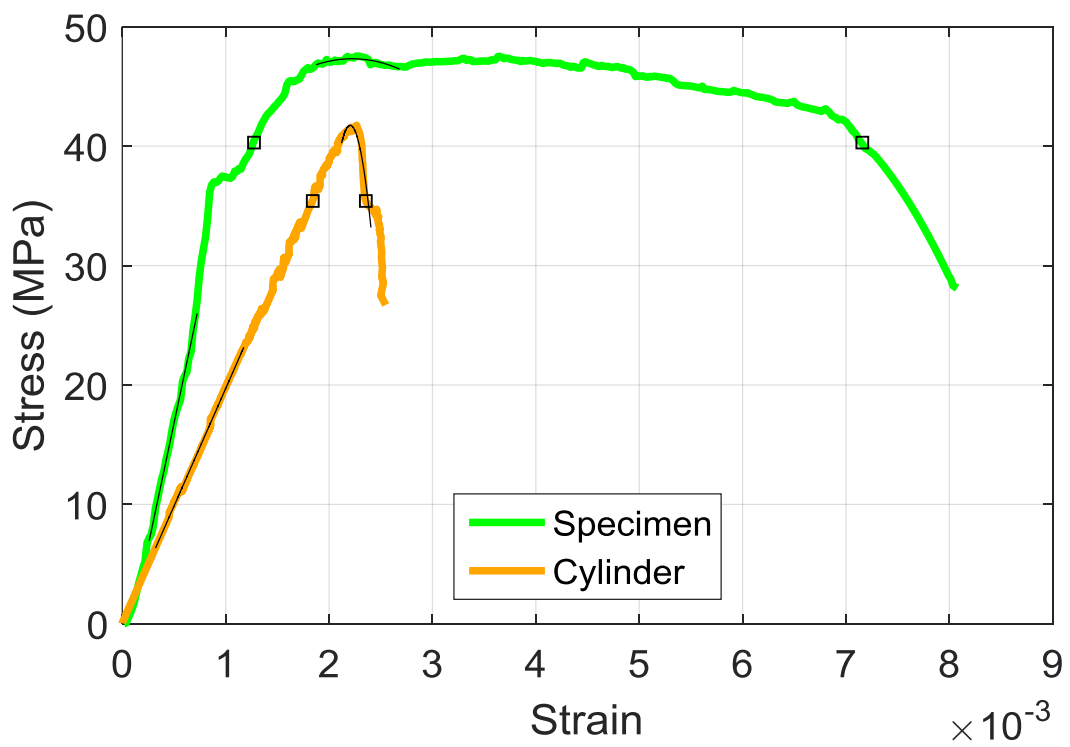
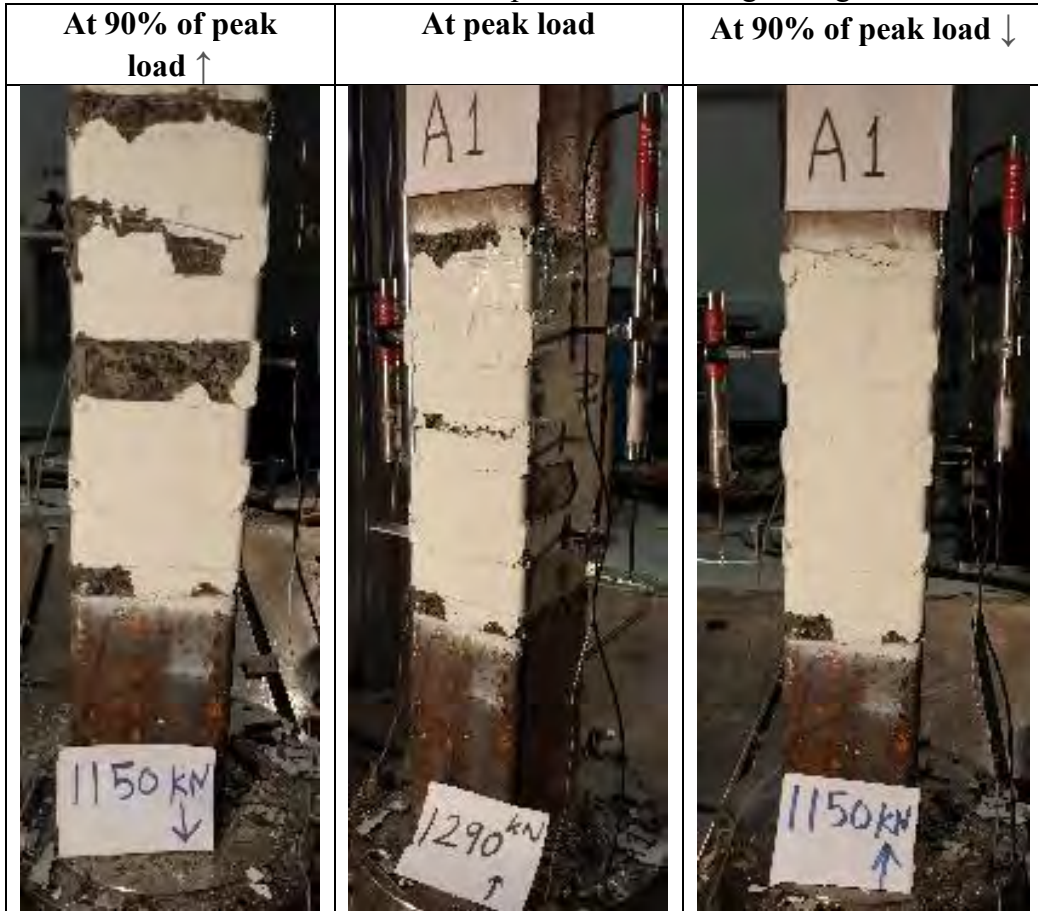


Figure 71: Stress-strain for A1 concrete core and the corresponding cylinder

Table 27: Condition of specimen A2 during testing

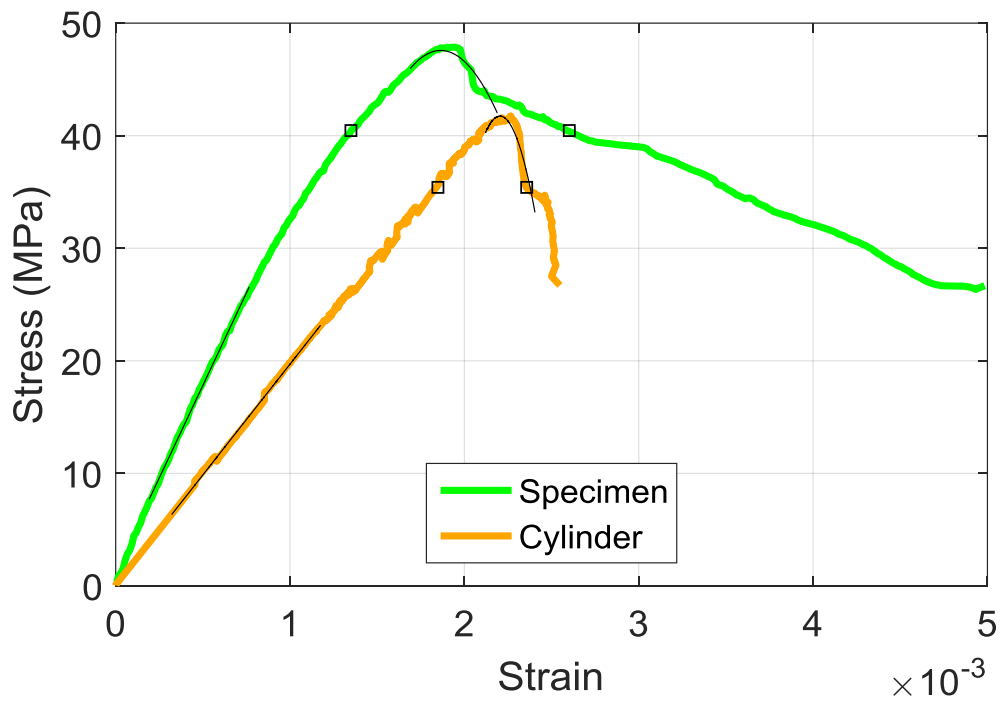
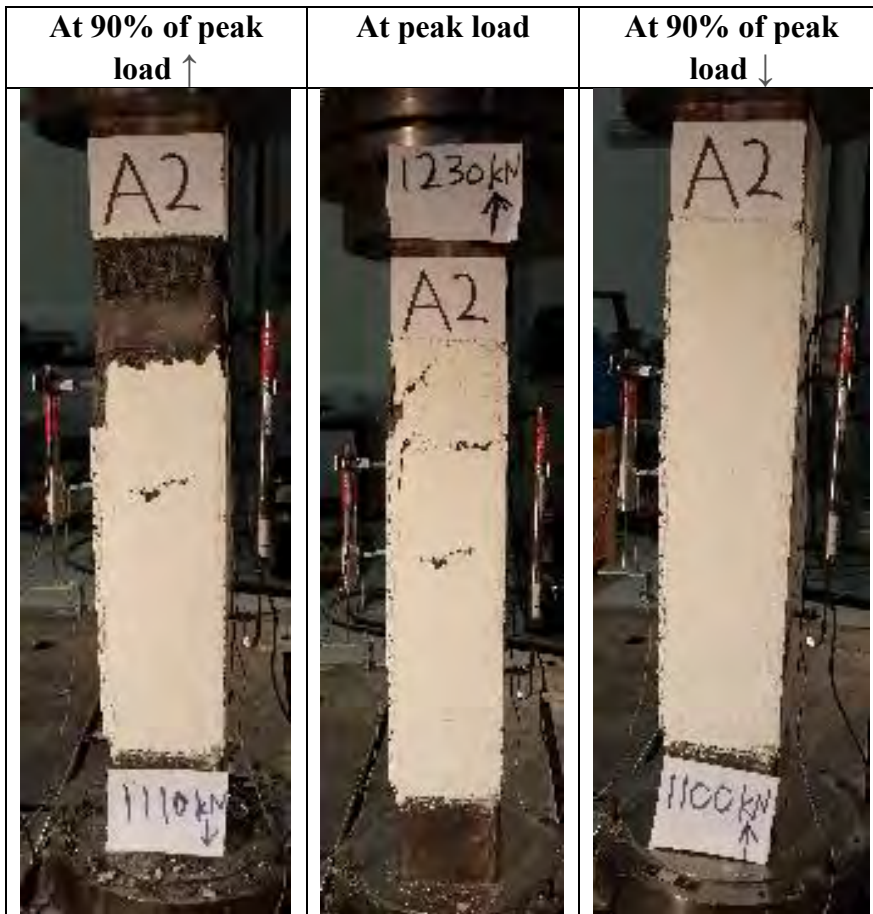


Figure 72: Stress-strain for A2 concrete core and the corresponding cylinder

Table 28: Condition of specimen A3 during testing

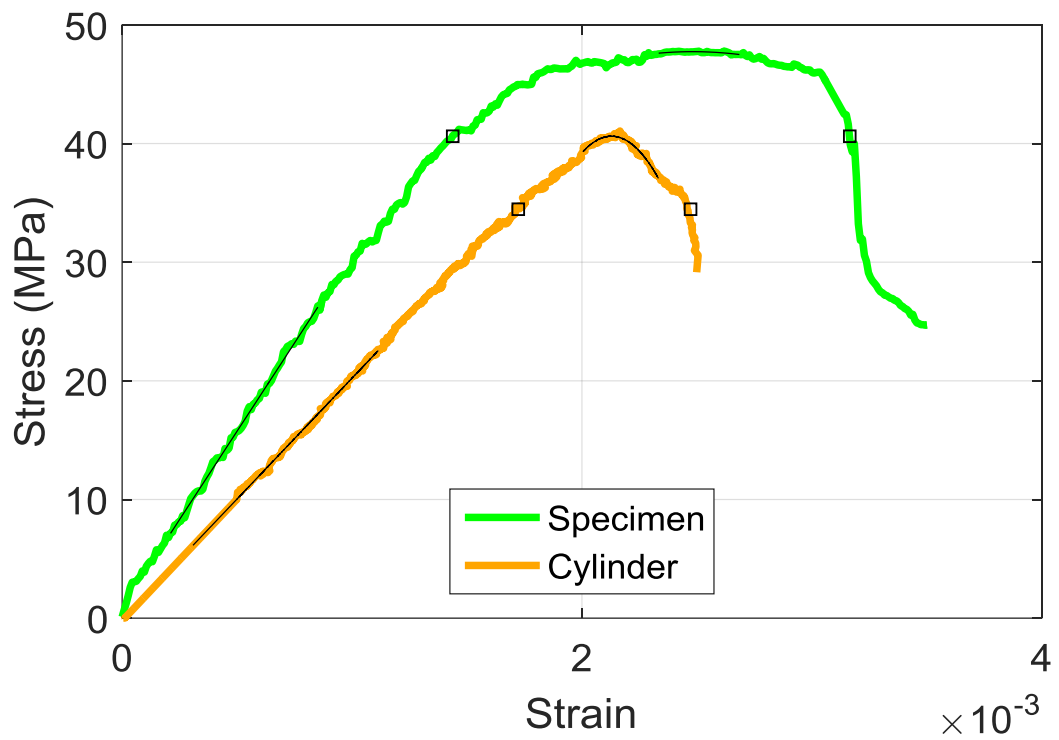
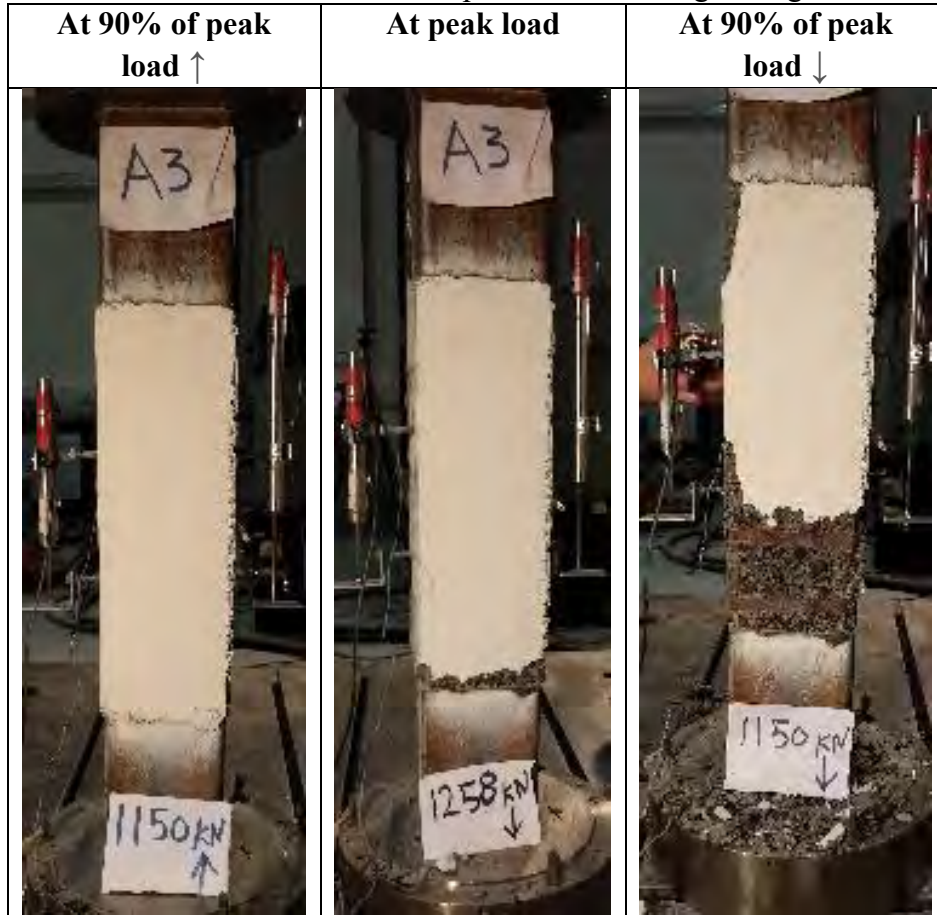


Figure 73: Stress-strain for A3 concrete core and the corresponding cylinder

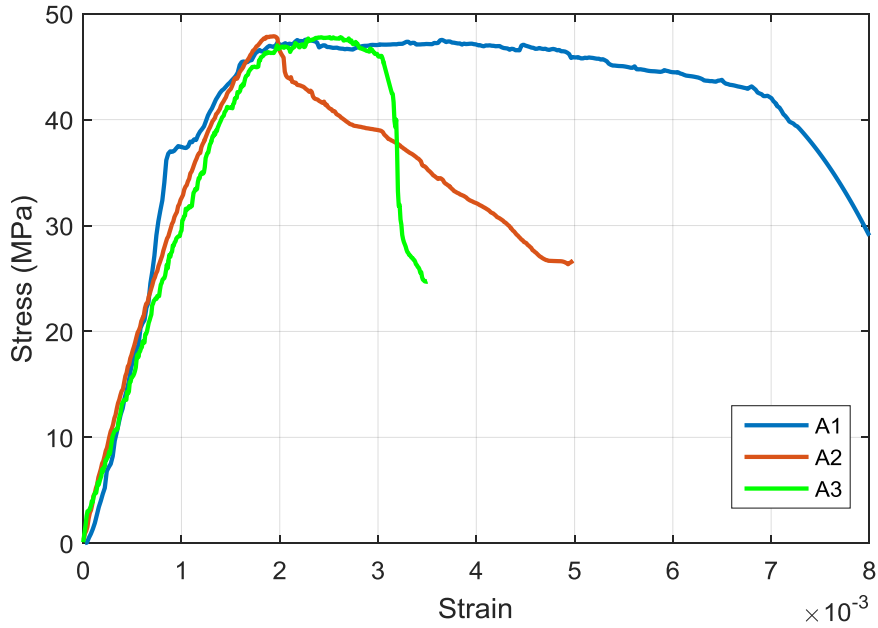


Figure 74: Stress-strain in the concrete core of A1, A2, and A3

Key information related to the results presented in Figure 60 through Figure 73 are extracted. Corresponding calculations are carried out on each specimen to find the three key performance indicators, namely, the strength enhancement factor, S , stiffness enhancement factor, K , and ductility enhancement factor, D . These parameters, as well as the information needed to calculate them, are shown in Table 29 to Table 34 for ISSSB and tie confined concrete cores. The enhancement factors of the 3 extra ISSSB confined specimens that do not have a matching tied counterpart are included in Table 35 to Table 37. Analysis and discussion of these results is provided in the next chapter.

Table 29: Strength results for ISSSB specimens

Specimen	f'_{cc}	f'_c	S
S1A	15.1	15.4	0.98
S1B	17.0	15.4	1.11
S2A	14.5	15.4	0.94
S2C	17.0	16.3	1.05
S3A	15.3	16.3	0.94
S3C	16.8	16.0	1.05
S4A	47.3	40.6	1.17
S4B	32.2	24.8	1.30
S5A	13.5	16.0	0.84
S2C4B	35.7	24.8	1.44
S3C4B	32.1	24.8	1.30

Table 30: Strength results for tied specimens

Specimen	f'_{cc}	f'_c	S
T1A	15.6	15.4	1.01
T1B	14.9	15.4	0.97
T2A	14.8	15.4	0.96
T2C	15.9	16.3	0.98
T3A	16.4	16.3	1.01
T3C	14.1	16.0	0.88
T4A	46.4	40.6	1.14
T4B	30.8	24.8	1.24
T5A	14.1	16.0	0.88
T2C4B	33.1	24.8	1.34
T3C4B	27.7	24.8	1.12

Table 31: Stiffness results for ISSSB specimens

Specimen	E_{cc}	E_c	K
S1A	17.7	11.2	1.58
S1B	15.6	11.2	1.39
S2A	17.3	11.2	1.54
S2C	17.4	9.4	1.85
S3A	16.2	9.4	1.72
S3C	25.2	10.4	2.43
S4A	28.0	20.4	1.38
S4B	32.2	15.6	2.07
S5A	15.0	10.4	1.44
S2C4B	36.0	11.4	3.17
S3C4B	23.6	15.6	1.52

Table 32: Stiffness results for tied specimens

Specimen	E_{cc}	E_c	K
T1A	25.5	11.2	2.28
T1B	5.9	11.2	0.52
T2A	16.2	11.2	1.44
T2C	13.4	9.4	1.43
T3A	28.4	9.4	3.02
T3C	6.1	10.4	0.59
T4A	14.1	20.4	0.69
T4B	27.8	15.6	1.79
T5A	7.4	10.4	0.72
T2C4B	25.7	11.4	2.26
T3C4B	20.3	15.6	1.31

Table 33: Ductility enhancement factor for ISSSB specimens

Specimen	$\epsilon_{0.85_pre}$	$\epsilon_{0.85_post}$	D
S1A	0.00099	0.00754	7.62
S1B	0.00102	0.00447	4.38
S2A	0.00331	0.00633	1.91
S2C	0.00111	0.01116	10.05
S3A	0.00077	0.00382	4.96
S3C	0.00076	0.0033	4.34
S4A	0.00154	0.00288	1.87
S4B	0.00093	0.00259	2.78
S5A	0.00089	0.00473	5.31
S2C4B	0.00089	0.00252	2.83
S3C4B	0.00118	0.00285	2.42

Table 34: Ductility enhancement factor for tied specimens

Specimen	$\epsilon_{0.85_pre}$	$\epsilon_{0.85_post}$	D
T1A	0.00045	0.00411	9.13
T1B	0.00319	0.0072	2.26
T2A	0.00159	0.00347	2.18
T2C	0.00115	0.02269	19.73
T3A	0.00064	0.00229	3.58
T3C	0.00344	0.00674	1.96
T4A	0.00312	0.00595	1.91
T4B	0.00106	0.00206	1.94
T5A	0.00331	0.01237	3.74
T2C4B	0.00128	0.0175	13.67
T3C4B	0.00116	0.00212	1.83

Table 35: Strength enhancement factor for 3 extra ISSSB specimens

Specimen	f'_{cc}	f'_c	S
A1	47.3	41.7	1.13
A2	47.6	41.7	1.14
A3	47.7	40.6	1.18

Table 36: Stiffness enhancement factor for 3 extra ISSSB specimens

Specimen	E_{cc}	E_c	K
A1	41.0	19.7	2.08
A2	32.9	19.7	1.67
A3	29.8	20.4	1.46

Table 37: Ductility enhancement factor for 3 extra ISSSB specimens

Specimen	$\epsilon_{0.85_pre}$	$\epsilon_{0.85_post}$	D
A1	0.00127	0.00717	5.65
A2	0.00135	0.0026	1.93
A3	0.00144	0.00317	2.20

The presented results in the previous tables will be analyzed in the next chapter. The behavior of the concrete cylinder will be compared with corresponding concrete cores laterally confined with ties and ISSSB. The effects of the various design parameters on the stress-strain relationships in terms of strength, stiffness and ductility will be discussed.

Chapter 5. Discussion and Analysis of Results

5.1 Introduction

This chapter provides discussion and analysis of the results obtained from the experimental testing. First, there is a general description of the condition of the specimens during loading, with details about the observed mode of failure. This is followed by an explanation about the differences between the stress-strain curve of confined concrete and unconfined concrete. Finally, the effect of the considered variables in the experimental program on the behavior of confined concrete laterally reinforced with ISSSB and ties is discussed.

5.2 Failure of Specimens

In general, experimental testing showed less intensive crack formation, concrete spalling and crack opening on the ISSSB reinforced specimens compared with equivalent tied specimens when the level of load was just about the same. Figure 75 through Figure 77 show crack formation on three typical ISSSB and corresponding tie reinforced columns made with weak, moderate and strong concrete. For the columns with two different types of lateral reinforcement, there was no observable damage or intensive crack formation until the specimens reached their peak capacity, as shown in the previous chapter in Table 15 to Table 25. Even then, most specimens remained intact and only few developed small cracks causing insignificant damage to the specimens.

It is only at the onset of the descending phase of loading that large longitudinal and diagonal cracks were formed. These cracks were soon followed by small fragments of concrete breaking off from the core, followed by longitudinal steel buckling. Some of the specimens failed in regions closer to the top and bottom ends despite steel jackets at the column ends, were provided to preclude failure in these regions. At high axial deformation levels a failure plane formed across the cross-section of the columns, accompanied with clear rebar buckling of the longitudinal reinforced and concrete crushing. Also, there was no slippage of the ties from the concrete and no fracture in either the ties or ISSSB due to the Poisson effect, even at 40% reduction in the peak load on the descending part of the load-deflection curve. Careful examination of the specimens after testing revealed no signs of yielding in the

transverse steel.

Furthermore it was observed during testing that specimens confined by ISSSBs suffered less damage at a certain level of loading compared to the corresponding tied column. This was recorded for specimens at the three levels of concrete compressive strengths: weak, moderate and high, as seen in Figure 75, Figure 76, and Figure 77.



Figure 75: Observed damage of ISSSB and tied specimen (weak concrete)



Figure 76: Observed damage of ISSSB and tied specimen (medium concrete)



Figure 77: Observed damage of ISSSB and tied specimens (strong concrete)

5.3 Stress-Strain Relationships of Confined Concrete

Whether confined by ISSSB or ties, the stress-strain relationship of confined concrete has different characteristics and shape than that of unconfined concrete, as was observed in the Chapter 4 in Figure 60 to Figure 72 and Figure 71 to Figure 73. This is because the lateral steel often enhances the strength and ductility of the concrete; thus stretching the stress-strain curve of the relevant cylinder vertically and horizontally. The initial stiffness of the confined concrete is usually higher than for unconfined concrete. Moreover, buckling of the longitudinal reinforcement sometimes causes the stress-strain relation to experience a double-peak phenomenon due to the change in the longitudinal steel contribution in resisting the applied load before and after buckling. A typical stress-strain relationship for confined concrete experiencing a double-peak and equivalent unconfined concrete cylinder is shown in Figure 78.

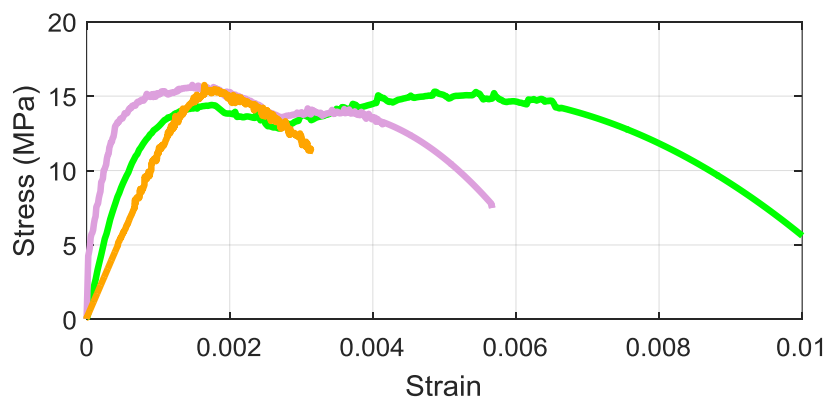


Figure 78: Typical stress-strain for confined vs. unconfined concrete

5.4 Effect of Variables on Confined Concrete

This section discusses the general effect of the considered variables in section 3.2 on the performance of the tested specimens as measured by the 3 key performance indicators; namely, *S*, *K* and *D*. Specifically, the effects of the concrete compressive strength, spacing of lateral steel reinforcement, concrete core size, the ISSSB's thickness-to-width ratio, and aspect ratio of the concrete core. In all the cases, all variables are taken at their standard value and only the parameter under consideration is varied. In the discussion, two approaches are followed, one in which the effect of concrete confinement is judged against the unconfined concrete; the other involves comparison between the effectiveness of ISSSB against tie reinforcement.

5.4.1 Effect of concrete strength. In this section, three ISSSB reinforced and another three tied specimens made with different concrete compressive strengths are studied. In addition, the three corresponding concrete cylinders are included in the analysis in order to be able to compute the 3 key performance indicators. The three considered concrete strengths are labeled as weak, moderate and strong. The standard cylinder compressive strengths of the considered concrete are 16 MPa, 24 MPa and 41 MPa. All column specimens are 150 mm x 150 mm in cross-section and reinforced longitudinally with 4 No. 12 bars. The cross-sectional area of the transverse reinforcement is 50.3 mm² (No. 8 for the ties) and the ISSSB has a thickness of 3 mm and width of 16.8 mm. Figure 79 presents the results for the enhancement factors for the ISSSB and tie paired columns for the three different considered concrete strengths.

Results of the strength enhancement factor showed that the impact of lateral confinement on the concrete is insignificant when the concrete strength is low because it crumbles prematurely under compression before large deformations take place due to the Poisson's effect. Therefore, the low strength concrete is incapable of taking advantage of the lateral steel confinement system and exhibits a behavior similar to plain concrete. However, confinement clearly improves the strength of plain concrete for moderate strength concrete and above. The results show strength increase for the confined concrete in the order of 14-30% above the cylinder strength.

It is observed that the initial stiffness of confined concrete along the ascending

branch of the stress-strain relationship is generally higher than that of unconfined concrete. This is consistent with past studies, as the higher strength causes the slope of the stress-strain curve to become steeper.

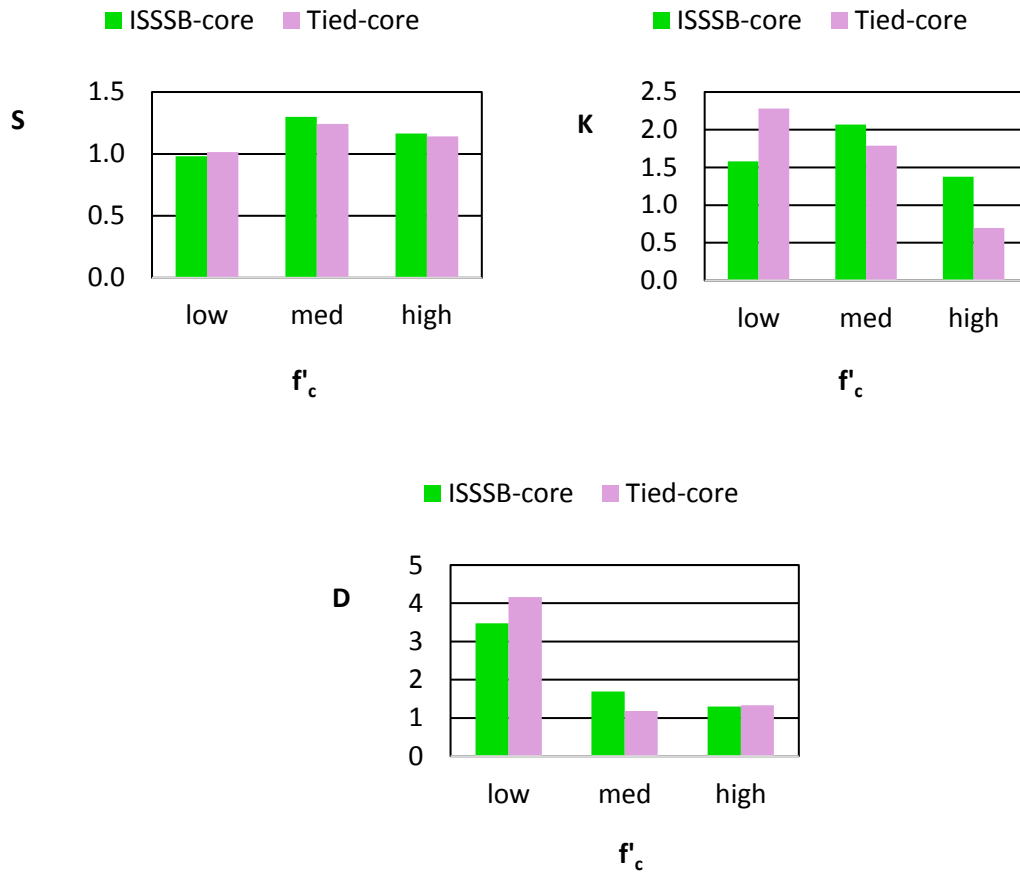


Figure 79: Effect of concrete compressive strength

Improvement in stiffness due to confinement is more pronounced in low strength concrete than in moderate or high strength concrete. Also, it can be observed that ties are more effective in enhancing the stiffness of low strength concrete than ISSSBs. The opposite is true for moderate and high strength concrete. Unexpectedly, the tied specimen made with strong concrete had a lower stiffness than the cylinder. Upon further review of the stress-strain curve of this specimen, it was noticed that the strain at peak stress for this specimen was much larger than that of the cylinder, so even with higher strength the slope of the ascending branch was mild.

With respect to ductility, it is seen that lateral confinement improves the ductility of low strength concrete more than moderate or high strength concrete. Ties seem to be more effective in confining low strength concrete than moderate or high. However, ISSSBs are more effective than ties in improving the ductility of moderate

and high strength concrete.

5.4.2 Effect of lateral reinforcement spacing. The effect of spacing of ISSSB and ties on the strength, stiffness and ductility of confined concrete is presented in Figure 82. Three different spacings of lateral reinforcement are considered: 100 mm (denoted by low), 150 mm (denoted by med) and 200 mm (denoted by high). All specimens are 150 mm x 150 mm in cross-section and made from weak concrete having a 16 MPa compressive strength. They are reinforced laterally with either No. 8 ties or ISSSBs having width-to-thickness ratio equal to 0.18.

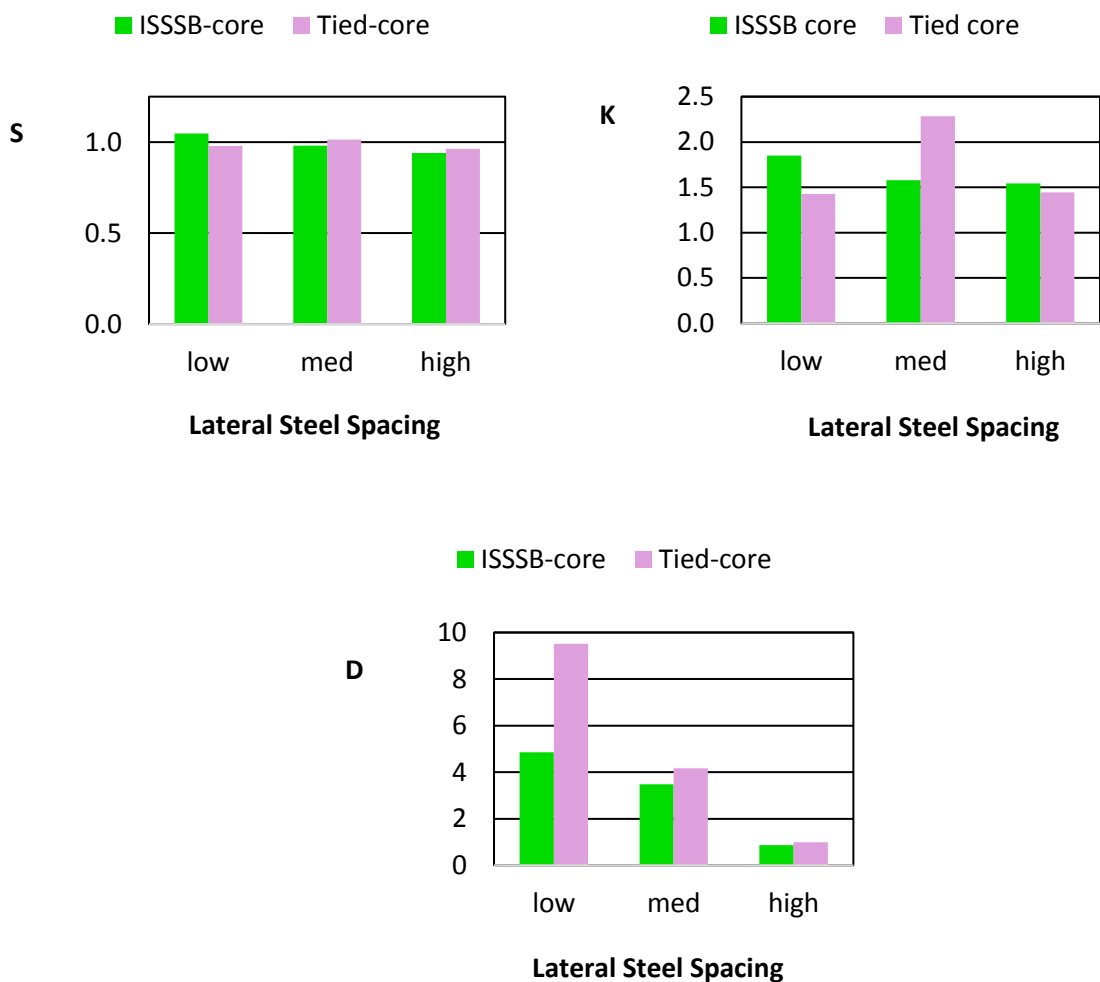


Figure 80: Effect of spacing of lateral reinforcement.

As expected, the results indicate that effect of lateral confinement on the strength of the concrete core of the specimens is minimal due to the low strength concrete as explained in the previous section. Hence, the lateral steel reinforcement did not increase the strength beyond the cylinder strength regardless of the spacing.

However, the impact of the confining steel on the stiffness enhancement factor is clear. Both ISSSBs and ties were able to increase the modulus of elasticity of the concrete in the core by at least 43%, with ISSSBs being more effective than ties when the spacing was low. As expected, when the lateral steel spacing increases the ductility decreases. This is clearly illustrated by the findings of the tests. When the lateral steel spacing is so high that it does not follow the ACI 318 code (as in the case of 200 mm, which is larger than the column dimension), the ductility enhancement factor is close to 1.0.

5.4.3 Effect of core size. To investigate the effect of the size of the concrete core, two square cross-sections with different sizes are considered, such that one area is about 78% larger than the other. Figure 81 below shows the calculated enhancement factors for both the ISSSB and the tie confined cores with respect to the concrete core area.

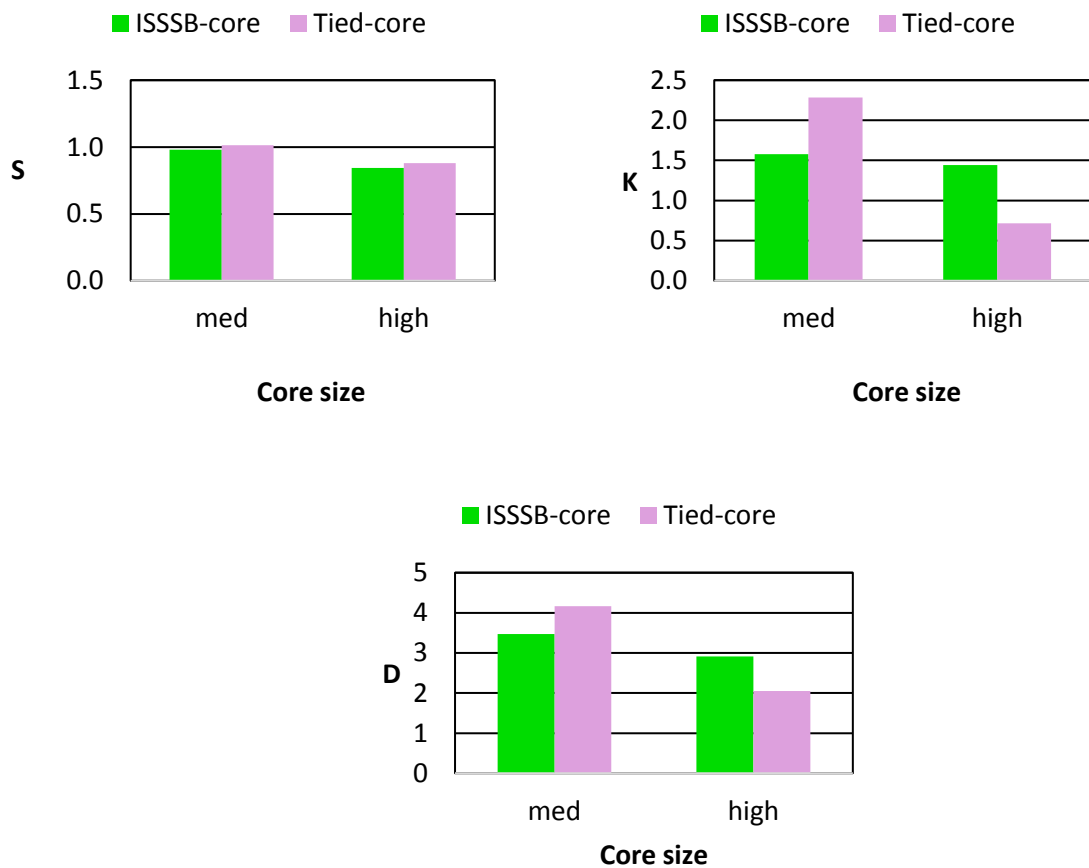


Figure 81: Effect of core size.

The results are presented for specimen pairs S5B-T5B with a cross section that is 150 mm x 150 mm (labeled med), and S5A-T5A with a cross section that is 200 mm x 200 mm (labeled high). All specimens in this group have the same longitudinal reinforcement (4 No. 12 rebars), the same spacing of transverse reinforcement (150 mm), and the same concrete strength ($f'_c = 16$ MPa).

The tests showed that increasing the core size from medium to high results in a drop in all three enhancement factors for both ISSSB and tied specimens. Specifically, the strength enhancement factor dropped by about 15% for both types of lateral confinement when the core size increased. The stiffness enhancement factor is reduced by 9% for ISSSB confined specimens and by 68% for tied specimens. The ductility enhancement factor decreased by 16% and 51% for the ISSSB and tie confinement systems, respectively. The reason for this drop can be explained in two stages. In a previous section, it was found that the 150 mm x 150 mm weak concrete specimens did not benefit much from lateral steel confinement due to concrete crushing prior to activation of lateral confinement. Increasing the size of the core in this case does not help since the number of longitudinal rebars and spacing of the transverse steel is the same. Further, the large size of the column is associated with high strain energy in the specimen that, once released, causes localized cracks in the concrete to grow at a faster rate; thus, reducing the overall strength of the concrete [23]. The same trend holds for the stiffness and ductility enhancement factors, although in the case of ductility the decreased value was still adequate. When comparing ISSSB confined and tied specimens, the ISSSB confined concrete performed better with the large size than the tied concrete as far as stiffness and ductility are concerned.

5.4.4 Effect of core aspect ratio. Effect of core aspect ratio. The effect of the aspect ratio of the concrete core cross-section is studied based on square and rectangular cross-sections. Note that the cross-sectional area of the square section is not equal to that of the rectangular section; thus, both the aspect ratio and core size are reflected in the performance. Specimens of cross sections with aspect ratio equal to 1.0 (150 mm x 150 mm) and 2.0 (150 mm x 75 mm) were experimentally tested. The effects of increasing the aspect ratio from 1 to 2 can be seen in Figure 82. It is observed that confinement has minimal effect on the strength performance of the

concrete core with strength enhancement factors approximately equal to one, regardless of the aspect ratio of the core.

On the other hand, a large aspect ratio has a strong influence on the stiffness and ductility enhancement factors K and D , respectively. Both factors drop significantly when using a rectangular cross section when compared to using the square cross-section, even though the rectangular section has a smaller area. Furthermore, the ISSSB specimen retains more stiffness and ductility than the equivalent tied one. At an aspect ratio equal to 2, the K and D factors of the ISSSB reinforced specimen were about 3 and 2 times the corresponding factors of the tied specimen, respectively.

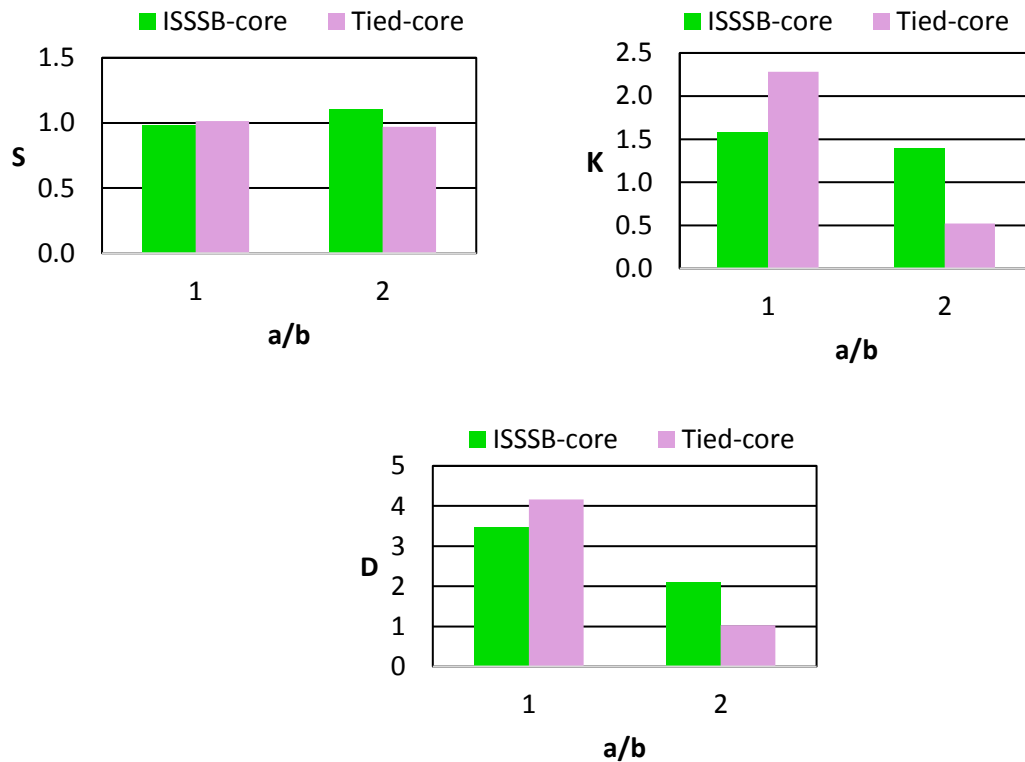


Figure 82: Effect of aspect ratio, a/b

5.4.5 Effect of thickness to width ratio of ISSSB. In this section, the effect of aspect ratio of the cross-section of the ISSSB on the structural performance is investigated. The thickness-to-width ratio of the cross-section of the ISSSB, t/w , is not applicable to ties since they have a circular cross-section. However, counterpart tied specimens are included in this discussion for the purpose of comparison with the

ISSSB. The smallest tie is No. 6, the moderate is No. 8 and the largest is No. 10. The corresponding ISSSB cross-sections are 3 mm x 9.4 mm, 3 mm x 16.8 mm, and 3 mm x 26.2 mm. The effect of t/w on the performance of specimens is shown in Figure 83. The results reveal that the impact on strength is minimal as the strength factors remained almost constant regardless of the value of t/w . With regard to stiffness, it is observed that the ISSSB columns performed best at the lower t/w ratio. With regard to ductility, the results suggest an optimum value of t/w at which the ISSSB specimen exhibited the highest ductility factor being larger than 3.

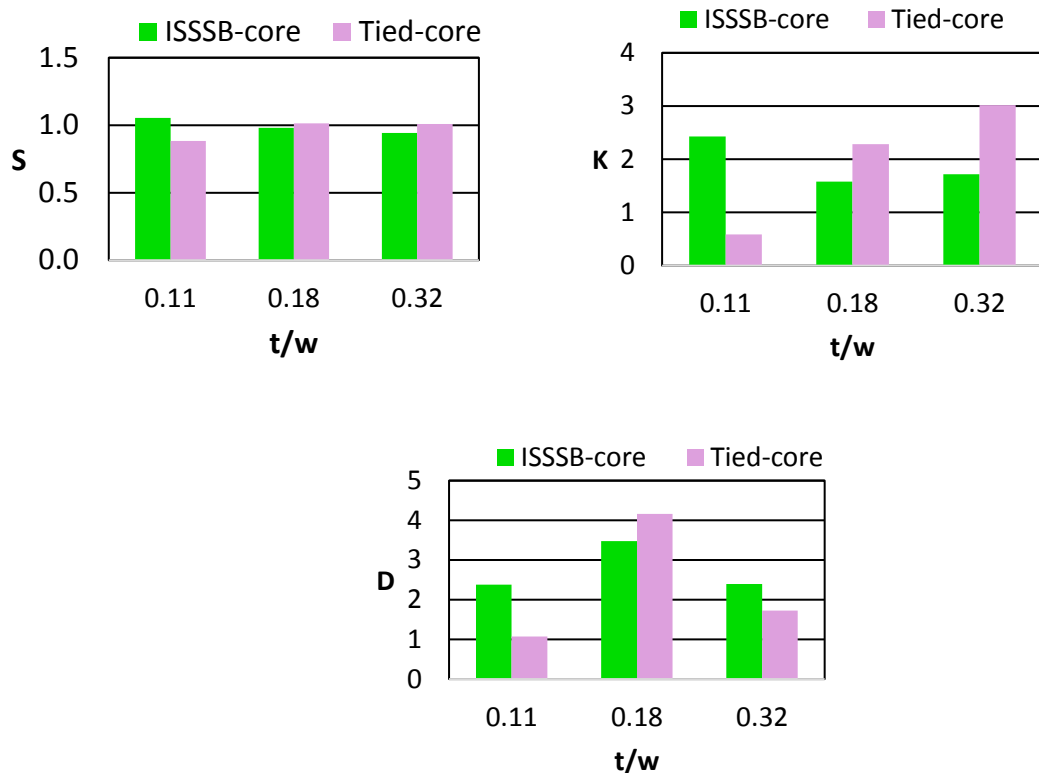


Figure 83: Effect of thickness to width ratio, t/w

5.5 Overall Comparison of ISSSB and Tie Confinement

This section analyzes the effect of the five considered variables on the performance of the ISSSB confinement system relative to the tie confinement system. In other words, it is desired to compare the performance of the two confinement systems at the different levels of the variable under consideration. To achieve this goal, Relative Enhancement Factors for strength, stiffness and ductility, denoted respectively by S_r , K_r , and D_r were introduced as shown in the Equations (26-28).

$$S_r = \frac{S_{ISSSB}}{S_{tie}} \quad (26)$$

$$K_r = \frac{K_{ISSSB}}{K_{tie}} \quad (27)$$

$$D_r = \frac{D_{ISSSB}}{D_{tie}} \quad (28)$$

Figure 84 through Figure 86 show plots for each of the Relative Enhancement Factors against the 11 different ISSSB-tie specimen pairs tested in this study. The goal from these figures is to assess the overall performance of the ISSSB confinement system and evaluate the general appropriateness of ISSSBs as an alternative to ties. With regard to strength, it is observed that for most specimens the relative strength enhancement factor is just about unity, indicating equal performance of ISSSB to tie systems. Statistical analyses of S_r indicates a mean value equal to 1.05 with a coefficient of variation of 8.5%.

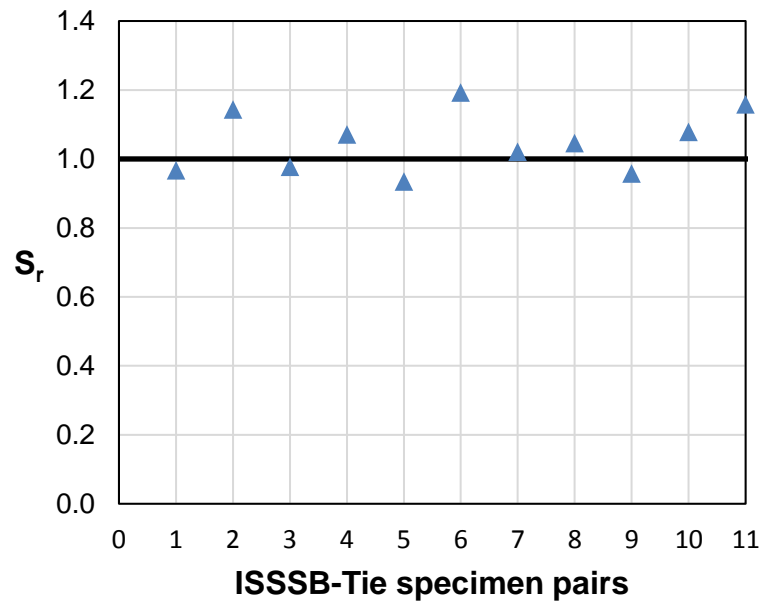


Figure 84: S_r values for all ISSSB-tie specimen pairs

Results show that K_r is more responsive to the type of confinement compared to S_r , with few K_r values appreciably higher than the horizontal line at 1.0 as observed in Figure 85. In general, the ISSSB reinforced specimens have exhibited higher stiffness as indicated by the mean value of 1.65; however, the fluctuation in the

results has caused the coefficient of variation to reach 59%.

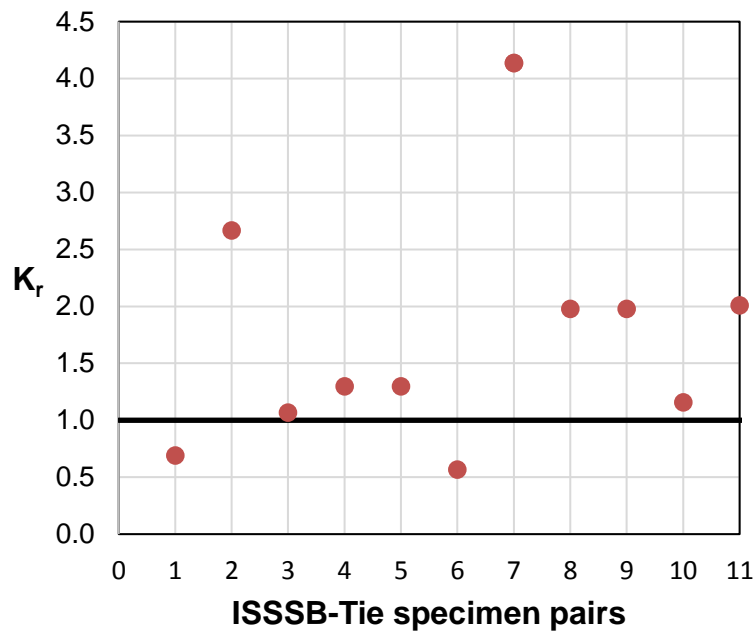


Figure 85: K_r values for all ISSSB-tie specimen pairs

The plot for relative ductility enhancement shown in Figure 86 seems to follow roughly the same trend observed in the relative stiffness enhancement plot in Figure 85. Statistical analysis of D_r gives a mean of 1.2 and coefficient of variation equal to 50%.

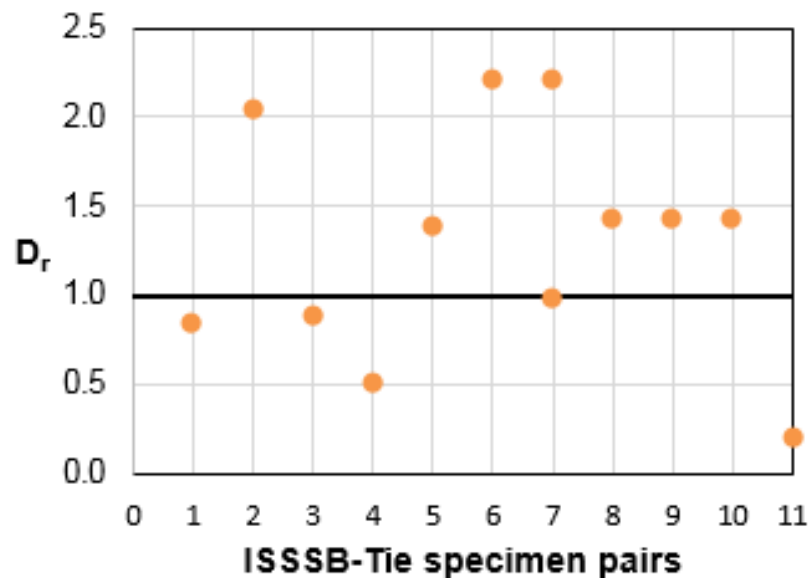


Figure 86: D_r values for all ISSSB-tie specimen pairs

5.6 Test Results versus ACI 318

In this section, the experimental strength is compared with the theoretical

strength based on the ACI 318M-14 code for all of the specimens constituting the 11 specimen pairs considered in the study. The experimental strength was taken as the maximum load exerted by the testing machine during the test. The nominal strength for each specimen, P_n , was calculated using Equation (1) and Equation (2) from the ACI 318M-14. These equations are used to predict the capacity of RC columns under axial load taking in account the accidental eccentricity. Since the specimens of this study represent a one-third scale model, 13.3 mm concrete cover was assumed in the calculation of the gross area, A_g , which is one third of the concrete cover of full scale columns typically equal to 40 mm.

Table 38 shows the experimental strength and theoretical strength for the 11 specimen pairs considered. It must be noted that the ACI equations depend only on the area of the column and the area and yield strength of the longitudinal steel. Thus, a single strength value is predicted regardless of the lateral steel reinforcement system used.

Table 38: Experimental and theoretical strengths for all specimen pairs

Specimen Pair	Experimental Strength (kN)		ACI Predicted Strength (kN)
	ISSSB	tie	
S1A- T1A	569	554	530
S1B- T1B	404	406	386
S2A- T2A	539	523	530
S2C- T2C	614	595	530
S3A- T3A	550	518	530
S3C- T3C	570	555	530
S4A- T4A	1266	1265	1053
S4B- T4B	860	837	697
S5A- T5A	745	799	749
S2C4B- T2C4B	950	949	697
S3C4B- T3C4B	912	761	697

The experimental strength was divided by the theoretical strength for all specimens and the results are tabulated in Table 39 and presented in graphical format in Figure 87. It can be seen from Figure 87 that all data points for both confinement systems are equal to or slightly larger than unity. This observation verifies the testing results obtained. Additionally it is concluded that the strength of the ISSSB confined columns could be predicted well by the ACI equations originally developed for tied columns.

Table 39: Experimental/ theoretical strength for specimen pairs

Specimen	P_{exp}/P_{ACI}	Specimen	P_{exp}/P_{ACI}
S1A	1.07	T1A	1.05
S1B	1.05	T1B	1.05
S2A	1.02	T2A	0.99
S2C	1.16	T2C	1.12
S3A	1.04	T3A	0.98
S3C	1.08	T3C	1.05
S4A	1.20	T4A	1.20
S4B	1.23	T4B	1.20
S5A	0.99	T5A	1.07
S2C4B	1.36	T2C4B	1.36
S3C4B	1.31	T3C4B	1.09

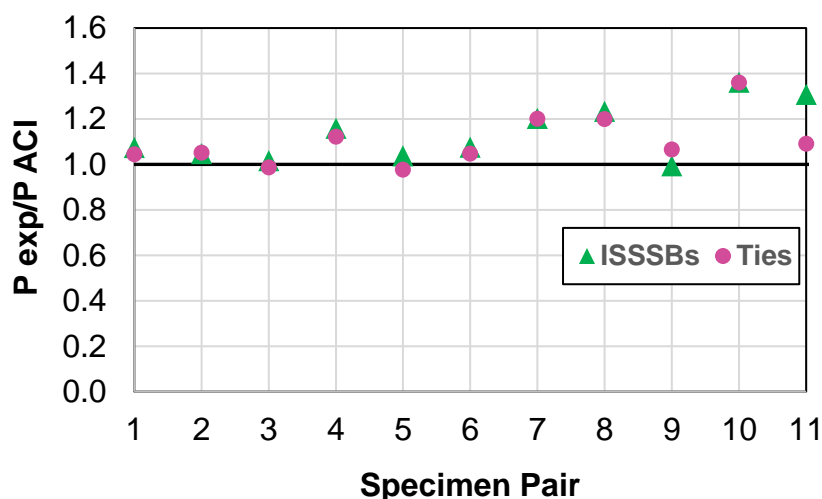


Figure 87: Experimental/ theoretical strength for specimen pairs

5.7 Effect of lateral steel volumetric ratio

The effect of the lateral steel volumetric ratio, ρ , on the performance of the three additional ISSSB columns is discussed hereby. The value of ρ was calculated by dividing the volume of the ISSSB provided over the volume of the concrete within the specimen per spacing of ISSSB. The 3 additional ISSSB column specimens have a cross-sectional area of 150 mm by 150 mm and concrete compressive strength of 41 MPa, and are longitudinally reinforced with 4 No. 12 bars. One specimen was laterally reinforced with ISSSBs having cross-sectional dimensions of 3 mm x 50 mm at 100 mm spacing, another with 3 mm x 50 mm at 150 mm spacing, and the last with 3 mm x 16.8 mm at 80 mm spacing resulting in three different steel volumetric ratios

namely: 0.017, 0.027, and 0.04. It is observed from Figure 88 that while changing ρ does not affect the strength enhancement factor in a significant manner, it does affect the stiffness and ductility to a great extent. Increasing ρ from 0.017 to 0.04, causes an increase in the stiffness enhancement factor by 50% and the ductility enhancement factor by 200%.

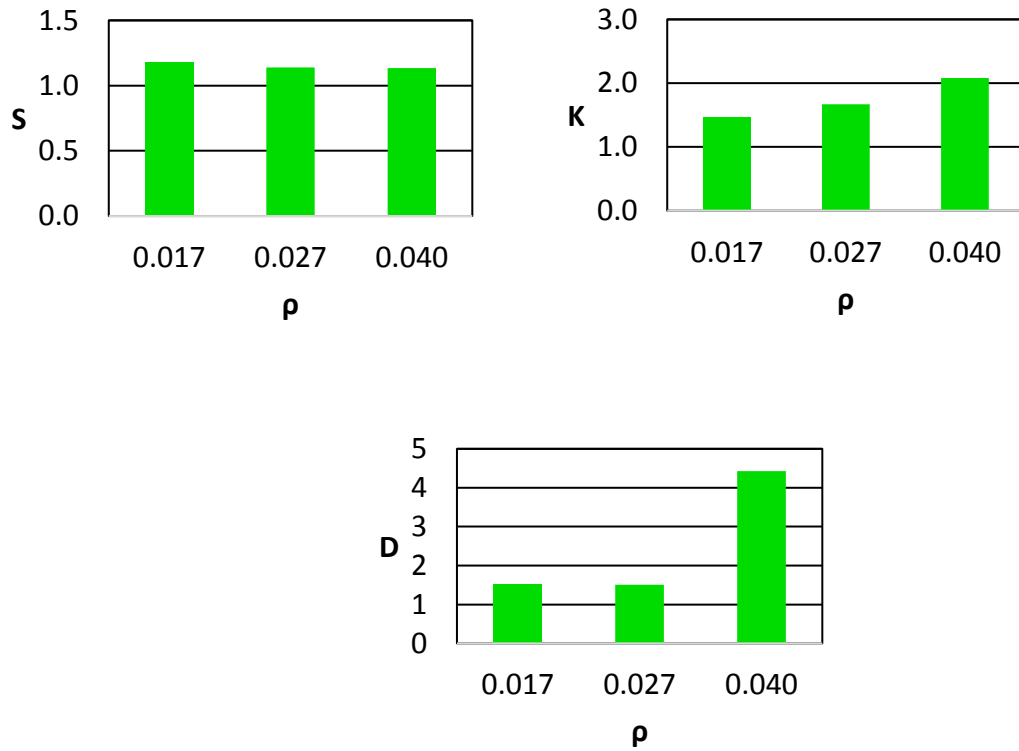


Figure 88: Effect of volumetric steel ratio, ρ

Chapter 6. Summary and Conclusions

6.1 Summary

Transverse reinforcement in reinforced concrete columns is mainly responsible for preventing premature buckling of the longitudinal reinforcement after cover spalling and enhancing the ductility of the structural member under increasing loads. The most common type of lateral reinforcement is rectilinear ties. A close examination of the use of ties in RC column reveals some shortcomings of this type of lateral reinforcement. Tied columns retain very little post-peak strength since they cannot effectively resist lateral bulging of the concrete beyond the peak stress point. Also, previous studies have showed that the stress level in the ties at maximum capacity is significantly less than the yield stress, which highlights inefficient use of the material. Moreover, the potential for buckling of the longitudinal steel bars is high in a typical tied RC column having large tie spacing. The weak confinement associated with rectilinear ties cannot be solved merely by increasing the amount of lateral steel reinforcement since increasing the amount of lateral reinforcement comes at a large cost and could lead to congestion in the steel cage. This study investigates the use of internal structural steel strip bands (ISSSB) for RC column core confinement as an alternative to ties. The steel strip bands are cut from square or rectangular structural steel tubes, depending on the cross-section of the column, and subsequently used to contribute to the RC column steel cage.

The ISSSBs can be attached by wires or spot-welded into place (without changing the material properties). The basic idea here is not to use more transverse steel than what is normally used in a tied column. Instead, the proposed concept of ISSSB reinforced column is to rearrange the material within the circular cross-section of the tie into a rectangular thin plate with more width; thus, providing more confinement influence area at the location of the lateral reinforcement along the column's length compared to the tie. Although structural steel is about 30% more expensive than rebars, it is expected that the decrease in labor associated with ISSSB reinforced columns will more than offset the slight increase in material, especially that the ISSSBs have reduced weight compared to the ties since they do not have end hooks.

The main objectives of this study are to: (1) investigate the behavior of RC

columns confined by ISSSBs under pure axial compression using experimental testing of small-scale models, (2) compare the performance of ISSSB confined columns with that of corresponding tied columns, (3) determine the effect of the relevant design parameters on the performance of RC columns confined by ISSSBs relative to that of traditional ties, and (4) develop design recommendations regarding the use of ISSSB confinement system in RC columns as an alternative to the tie confinement system. To achieve the stated objectives, five variables are considered: (1) aspect ratio of the cross section, (2) spacing of ISSSBs, (3) thickness to width ratio of the ISSSBs, (4) compressive strength of concrete, and (5) area of the column's cross-section.

The experimental work involved the construction of 25 short reinforced concrete specimens with different configurations and testing them under concentric axial compression. All specimens were instrumented with strain gauges and LVDTs to monitor the strain in the steel reinforcement and shortening of the specimens under increased loading. The behavior of the concrete core in ISSSB reinforced and tied columns is studied and compared to the unconfined concrete cylinder.

6.2 Conclusions

The main conclusions of this study are summarized below:

1. Longitudinal reinforcement in laterally confined concrete columns may either yield before buckling or may buckle before reaching yield. The effect of buckling of rebars on the shape of the stress-strain relationship of confined concrete in the core of columns causes formation of double peak, occurring at the instant of rebar buckling.
2. Performance of confined concrete relative to unconfined concrete can be reasonably measured in terms of the strength enhancement factor, stiffness enhancement factor, and the ductility enhancement factor enhancement factors. These three factors measure the key indicators applied to the core concrete with respect to the corresponding concrete cylinder.
3. Lateral confinement in columns made with weak concrete has a minor effect on strength even at high lateral steel volumetric ratios. This is because the concrete crumbles too early before it experiences large lateral deformations (Poisson effect), which are necessary for the activation of the lateral steel confinement system.

4. In general, the strength enhancement factor for columns that are laterally confined with either ISSSBs or ties increases with an increase in the concrete strength utilized in the columns.
5. In terms of strength, the ISSSBs reinforced columns exhibited slightly improved performance than the tied counterpart in the medium and high strength concrete specimens.
6. There is no clear trend of the effect of spacing of lateral steel reinforcement on the elastic stiffness of the concrete core. However, increasing the spacing of lateral reinforcement leads to significant decrease in the ductility enhancement factor. For instance, increasing the spacing from 100 mm to 150 mm leads to approximately 30% and 55% drop in the ductility relative enhancement factor in the ISSSB and tied specimens, respectively.
7. Increasing the size of the core area leads to general degradation of the performance of confined concrete due to the size effect. For example, increasing the core area from 150 mm x 150 mm to 200 mm x 200 mm in ISSSB confined concrete resulted in about 15% drop in the strength and ductility enhancement factors, and 9% decrease in the stiffness enhancement factor.
8. Columns with square cross-section exhibited much higher enhancement in stiffness and ductility compared to columns having rectangular cross-section. A 75% drop was observed in stiffness relative enhancement factor and ductility relative enhancement factor in rectangular tied specimens as compared to square ones. A similar trend was noticed in the ISSSB-confined specimens.
9. For the weak concrete, the stiffness enhancement factors of ISSSB reinforced and tied columns were generally the same. However, the ISSSB confinement was superior to the tie confinement with stiffness relative enhancement factor being 15% and 100% higher than the corresponding value for tied specimens when medium and high strength concretes were utilized, respectively.
10. On average, the use of ISSSBs resulted in 5% increase in the strength, 65% increase in initial stiffness, and 20% increase in ductility of the concrete core compared to the use of ties in all the considered specimens.
11. Increasing the lateral steel volumetric ratio in specimens with high strength

concrete resulted in no change in the strength enhancement factor but appreciable improvement in both stiffness and ductility. Enhancements of 40% in stiffness and 190% in ductility were realized when increasing lateral steel volumetric ratio from 0.017 to 0.040.

It should be noted that more studies on the subject need to be conducted in order to support the above findings. Since this study investigated the effect of the design variables on the performance of confined concrete having low strength, future work should be expanded to studying the effects of the design variables with specimens having medium and high strength concrete as well. It is recommended that two or more copies of each specimen be constructed and tested as opposed to having only one sample. Having multiple copies (repetitions) of each specimen helps to confirm the validity and the reproducibility of the test results.

Additionally, it is advised that future work in this subject utilizes Internal Structural Steel Strip Bands and ties having the same yield strength to ensure that the yield strength property of the materials does not affect the results of the comparisons of the pairs of specimens. Furthermore, it would be a better approach for future studies to incorporate the lateral steel volumetric steel ratio as one the considered design variables rather than studying it separately using extra specimens.

References

- [1] A. Shafqat and A. Ali, "Lateral Confinement of RC Short Column," *Science International*, vol. 24, no. 4, pp. 371-379, 2012.
- [2] J. C. McCormac and R. H. Brown, *Design of Reinforced Concrete*. Hoboken, NJ: Wiley, 2014.
- [3] I. American Concrete, A. C. I. Committee, and S. International Organization for, *Building Code Requirements for Structural Concrete (ACI 318M-14) and Commentary (ACI 318RM-14)*. Farmington Hills, Mich: American Concrete Institute, 2014.
- [4] V. Badalamenti, G. Campione, and M. L. Mangiavillano, "Simplified Model for Compressive Behavior of Concrete Columns Strengthened by Steel Angles and Strips," *Journal of Engineering Mechanics-Asce*, vol. 136, no. 2, pp. 230-238, 2010.
- [5] A. M. El-Kholy and H. A. Dahish, "Improved Confinement of Reinforced Concrete Columns," *Ain Shams Engineering Journal*, vol. 7, no. 2, pp. 717-728, 2016.
- [6] M. F. Tahir, Q. U. Z. Khan, M. Rizwan, M. Ashraf, and M. Yaqub, "Experimental Behavior of RC Columns, Confined with Stirrup and Strips, Under Cyclic Axial Load," *Arabian Journal for Science and Engineering*, Article vol. 39, no. 5, pp. 3449-3460, 2014.
- [7] K. H. Yang and A. F. Ashour, "Tests of Reinforced Concrete Short Columns Laterally Strengthened With Wire Rope Units and Steel Elements," *Magazine of Concrete Research*, vol. 59, no. 8, 2007.
- [8] K. H. Yang, A. F. Ashour, and E. T. Lee, "Axial Behaviour of Reinforced Concrete Short Columns Strengthened with Wire Rope and T-shaped Steel Plate Units," *Magazine of Concrete Research*, vol. 61, no. 2, 2009.
- [9] M. A. Hussain and R. G. Driver, *Seismic Rehabilitation of Reinforced Concrete Columns through Confinement by Steel Collars* (Structural engineering report ; no. 259). Edmonton: Dept. of Civil and Environmental Engineering, University of Alberta, 2005.
- [10] M. Saatcioglu and S. R. Razvi, "Strength and Ductility of Confined Concrete," *Journal of Structural Engineering-ASCE*, vol. 118, no. 6, pp. 1590-1607, Jun 1992.
- [11] J. B. Mander, M. J. N. Priestley, and R. Park, "Theoretical Stress-Strain Model for Confined Concrete," *Journal of Structural Engineering-ASCE*, vol. 114, no. 8, pp. 1804-1826, Aug 1988.
- [12] S. A. Sheikh and S. M. Uzumeri, "Strength and Ductility of Tied Concrete Columns," *Journal of the Structural Division-ASCE*, vol. 106, no. 5, pp. 1079-1102, 1980 1980.
- [13] S. W. Tabsh, "Stress-Strain Model for High-Strength Concrete Confined by Welded Wire Fabric," *Journal of Materials in Civil Engineering*, vol. 19, no. 4, 2007.
- [14] S. Popovics, "A Numerical Approach to the Complete Stress-Strain Curve of Concrete," *Cement and Concrete Research*, vol. 3, no. 5, pp. 583-599, 1973.
- [15] J. Hoshikuma, K. Kawashima, K. Nagaya, and A. W. Taylor, "Stress-Strain Model for Confined Reinforced Concrete in Bridge Piers," *Journal of Structural Engineering -New York*, vol. 124, no. 10, p. 1227, 1998.

- [16] R. Montuori and V. Piluso, "Reinforced Concrete Columns Strengthened with Angles and Battens Subjected to Eccentric Load," *Engineering Structures*, vol. 31, no. 2, pp. 539-550, Feb 2009.
- [17] E. Gimenez, J. M. Adam, S. Ivorra, and P. A. Calderon, "Influence of Strips Configuration on the Behaviour of Axially Loaded RC Columns Strengthened by Steel Angles and Strips," *Materials & Design*, vol. 30, no. 10, pp. 4103-4111, 2009.
- [18] N. Lambert-Aikhionbare and S. W. Tabsh, "Confinement of High-Strength Concrete with Welded Wire Reinforcement," *ACI Structural Journal*, vol. 98, no. 5, pp. 677-685, 2001.
- [19] *ASTM E8 / E8M-16a, Standard Test Methods for Tension Testing of Metallic Materials*, 2016.
- [20] Z. Zong, S. Kunnath, and G. Monti, "Material Model Incorporating Buckling of Reinforcing Bars in RC Columns," *ASCE Journal of Structural Engineering*, vol. 140, no. 1, art. no. 04013032, 2014.
- [21] S. Bae, A. M. Miseses, and O. Bayrak, "Inelastic Buckling of Reinforcing Bars," *Journal of Structural Engineering*, vol. 131, no. 2, pp. 314-321, 2005.
- [22] R. P. Dhakal and K. Maekawa, "Modeling for Postyield Buckling of Reinforcement," *Journal of Structural Engineering*, vol. 128, no. 9, pp. 1139-1147, 2002.
- [23] Z. P. Bazant and Y. W. Kwon, "Failure of Slender and Stocky Reinforced Concrete Columns: Tests of Size Effect," *Materials and Structures*, vol. 27, no. 166, pp. 79-90, 1994.

Vita

Ahmad Towaiq is from Arramtha, Jordan. Ahmad holds the International Baccalaureate from RCNUWC in Norway and he has earned a Bachelor of Science degree in civil engineering from Bucknell University in May, 2012. Ahmad has joined the Master of civil engineering program at the American University of Sharjah in the Fall of 2013.